PREDICTING THE POSITION OF FAULT STRANDS THROUGH BOREHOLE CORRELATION OF THE TOP OF TERTIARY BEDROCK IN THE SEATTLE FAULT ZONE, SEATTLE, WASHINGTON

Devin A. Maloney

A report prepared in partial fulfillment of
The requirements for the degree of

Masters of Science
Earth and Space Sciences: Applied Geosciences

University of Washington
December, 2019

Project Mentor:
Kathy Troost, University of Washington

Internship Coordinator:
Kathy Troost

Reading Committee:
Kathy Troost
Steven Walters

MESSAGe Technical Report Number: [80]

EXECUTIVE SUMMARY

Only a few strands of the Seattle Fault Zone have been identified on land in Seattle, Washington due to heavy manipulation of the landscape by repeat glaciations, geomorphic reworking, and the interference of the growing metropolitan community concealing potentially dangerous active faults below the surface. Previous difficulty locating faults on the ground surface led to the idea of using geotechnical boring logs to "see into" the subsurface structure. Can the depth to the contact between Quaternary deposits and Tertiary bedrock, obtained from existing geotechnical boring logs, be used to predict the locations of fault strands in the Seattle Fault Zone in Seattle? The University of Washington Pacific Northwest Center for Geologic Mapping Studies (GeoMapNW) database contains thousands of geotechnical boring logs readily available. Over 18,000 boring logs were processed using the computer programming language Python to select boring logs containing bedrock-related terms describing Blakely Harbor Formation, Blakeley Formation, Tukwila Formation, and any other bedrock in Seattle. This process isolated 1700 boreholes that potentially intersected bedrock. Each of the 1700 boring logs were individually categorized to determine if the Python code was valid. This process reduced the queried boring logs to 809 boreholes containing bedrock within the Seattle Fault Zone. The boreholes containing bedrock were used to construct preliminary contours of the bedrock surface in AutoCAD Civil 3D. Both boreholes containing bedrock and boreholes not containing bedrock were used to generate 108 geologic cross sections using the geographic information system (GIS) Geologic Cross Section Toolbox developed in 2018. The variation in depth to the contact between Quaternary deposits and Tertiary bedrock was evaluated in the cross sections highlighting 66 anomalies in southeast Seattle. The anomalies were checked against the triangular irregular network (TIN) surface and contours generated in AutoCAD Civil 3D to better visualize the Seattle Fault Zone structure. The anomalies ranged from potential faults and geomorphic alterations to possible human alterations such as hillslope grading along Interstate 5. Fifty percent of the anomalies were identified as potential faults based on the continuation of offset patterns in neighboring cross sections. Published fault locations from multiple reliable sources supplied by the U.S. Geological Survey (USGS) and Washington State Department of Natural Resources (DNR) were checked to assess the connection of anomalies to mapped faults. Some of the anomalies found through borehole correlation suggest revisions and continuations of existing published fault locations through the City of Seattle. Identifying potential fault anomalies by correlating detailed boring logs proved successful and could be applied to complex fault zones worldwide. The next step is to investigate the anomalies identified as potential faults to determine if they are representations of faults strands within the Seattle Fault Zone.

ACKNOWLEDGEMENTS

I am grateful for the support, guidance, and knowledge provided by Kathy Troost, Steven Walters, and Juliet Crider. I also thank Jesse Schaefer, Drew Schwitters, and Martin Weiser for the development of their Geologic Cross Section Toolbox which made processing over one hundred cross sections possible during the duration of this work.

TABLE OF CONTENTS

1.0 INTRODUCTION

Can anomalies along the contact between Quaternary deposits and Tertiary bedrock, obtained from existing geotechnical boring logs, be used to locate fault strands in the Seattle Fault Zone in Seattle, Washington? The Seattle Fault Zone is an active 50-mile-long east to west trending reverse fault zone of multiple semi-parallel faults dipping to the south (Figure 1) (Johnson et al., 1999; Pratt et al., 2015). A Magnitude 7.0-7.5 earthquake 1100 years ago (A.D. 900-930) displaced the southern hanging wall by more than 20 feet, initiating landslides and a tsunami (Pratt et al., 2015, 1992; Blakely et al., 2002; Atwater and Moore, 1992). Knowing the location of strands of the Seattle Fault Zone can better prepare the Puget Sound community and emergency rescue personnel for when the next high magnitude earthquake hits the region. Locating strands can also improve the scientific understanding of the relationship between Puget Lowland faults and the Cascadia Subduction Zone. More specifically, mapping faults can reveal how fault zones accommodate strain between earthquakes. Three fault strands have been mapped crossing Seattle. Other previously mapped fault strands were identified in waterways such as Puget Sound, Lake Washington, and Lake Sammamish using high-resolution marine seismic reflection data, aeromagnetic data, and well logs (Yount et al., 1985; Johnson et al., 1994; Blakely et al., 2002; Johnson et al., 2016). Few faults have been identified on land in Seattle, partially due to the interference of the growing metropolitan community and infrastructure. However, with the availability of thousands of geotechnical boring logs within city limits and the Geologic Cross Section Toolbox developed in 2018 for geographic information system (GIS) data, the subsurface geologic structure beneath the heavily populated City of Seattle can now be examined using geospatial analytic methods (Schaefer et al., 2018). Processed boring logs were displayed using the Geologic Cross Section Toolbox to create cross sections where anomalies were identified along the contact between Quaternary deposits and Tertiary bedrock. Anomalies were identified as abrupt changes in elevation of the bedrock surface. These anomalies were inferred as potential fault strands, compressional features, erosion, or caused by human activity.

2.0 GEOLOGIC SETTING

2.1 TECTONICS

The subduction of the oceanic Juan de Fuca plate below the North American continental plate in an oblique clockwise rotation tectonically compresses the Pacific Northwest from the southwest at a rate of about 1.5 inches per year along the Cascadia Subduction Zone (Brocher et al., 2017). The accretionary wedge of the Olympic Peninsula and volcanic Cascade Mountain Range bound the Puget Lowland basin. The Puget Lowland experiences north-south crustal shortening, developing the east-west trending shallow (less than 20 miles deep) crustal faults such as the South Whidbey Island Fault Zone, Seattle Fault Zone,

and Tacoma Fault Zone (Figure 2) (Johnson et al., 1999; Nelson et al., 2014). The Seattle Fault Zone includes a series of south dipping parallel reverse faults approximately 50 miles long (east-west) and 5 miles wide (north-south) (Blakely et al., 2002; Pratt et al., 2015). Strands of the Seattle Fault Zone have been located west of Bremerton to east of Issaquah (Figure 1) (Johnson et al., 1999; Liberty and Pratt, 2008; Sherrod, 2002; Nelson et al., 2014). The Seattle Fault Zone is a fault-propagation fold where the southern hanging wall, known as the Seattle uplift, uplifts marine terraces and Tertiary bedrock as the north foot wall, the Seattle basin, moves down in elevation (Johnson et al., 1994; Pratt et al., 2015). The Seattle Fault Zone ruptured about 1100 years ago with a Magnitude 7.0-7.5 earthquake, which caused a localized tsunami in Puget Sound (Atwater and Moore, 1992; Pratt et al., 2015). Tsunami deposits were identified at West Point, Discovery Park, Seattle and in Cultus Bay on the south end of Whidbey Island (Atwater and Moore, 1992). Measurements taken at Restoration Point on Bainbridge Island estimated the hanging wall uplifted more than 20 feet during the rupture 1100 years ago (Bucknam et al., 1992). Winslow Marsh, located on Bainbridge Island, transitioned from a freshwater wetland to a tidal marsh indicating tectonic subsidence in the area (Bucknam et al., 1992). Similar subsidence was identified on the eastern shores of Puget Sound at West Point in Discovery Park where marsh subsided approximately 3 to 5 feet accumulating sand and tidal flat deposits (Atwood and Moore, 1992). Active strands of the Seattle Fault Zone have been identified on Bainbridge Island where the faults cut to the surface through Holocene deposits as seen in bare earth light detection and ranging (LiDAR) digital elevation models (DEMs) (Nelson et al., 2003). Nelson et al. (2003) took samples from five trenches across the fault scarp on Bainbridge Island. Based on carbon 14 dating methods, the most recent earthquake along this scarp occurred 1050-1020 calibrated years before present. The trenches also exposed deformed strata, signs of liquefaction, and landslide deposits (Nelson et al., 2003).

2.2 TERTIARY GEOLOGY

The Seattle uplift exposes Tertiary sedimentary and igneous bedrock. Blakely et al. (2002) identified three exposed north dipping planes of Tertiary bedrock in the Seattle uplift using high-resolution aeromagnetism and geologic surveying. The three strata from north to south were identified as Blakely Harbor Formation (Tbh), Blakeley Formation (Tb), and Tukwila Formation (Tpt) (Figure 3). The Miocene-age (23.0 – 5.3 Ma) Blakely Harbor Formation includes nonmarine fluvial deposits and basalt conglomerate. The Blakeley Formation (Tb) was deposited in the Eocene (56.0 – 33.9 Ma) to Oligocene (33.9 – 23.0 Ma) and consists of marine sedimentary rock (Blakely et al., 2002). The shallow marine sequencing of sandstone, siltstone, and claystone found in the Blakeley Formation is exposed at Alki Point, Seattle; it has minor inclusions of lahar-transported ash and wood from the proto-Cascade Mountain Range. During the Eocene, the early Cascade Mountain Range was actively extruding andesitic

rock forming the Tukwila Formation (Tpt) exposed in south Seattle along with another late Eocene Andesite (Tva) (Figure 4) (Blakely et al., 2002; Troost et al., 2005).

Exposed bedrock outcrops and seismic reflection surveys display multiple faults and folds within the Tertiary bedrock. Yount and Gower (1991) mapped exposed bedrock outcrops in the Puget Lowland from 1978-1982 (Figure 5). Alki Point shows a series of strikes in bedrock oriented northwest to southeast parallel to the shoreline with moderate dips from 30-53° east. At the farthest northwest tip of Alki Point, the bedding changes direction and strikes east-west with a dip of 80° south aligning with strikes measured on Bainbridge Island. The near vertical and overturned bedding at Alki Point exposes the sandstone, siltstone, and mudstone sequencing of the Blakeley Formation along an anticline that merges to the north (Troost and Booth, 2008). The anticline is suspected to merge with a strand of the Seattle Fault Zone. In southeast Seattle, the bedding shows anticlinal folding parallel to Interstate 5 to the east. Farther east, the bedding is oriented nearly east-west with dips to the north ranging from about 15-88° north with at least one measurement identifying vertical bedding (Yount and Gower, 1991). Seismic reflection profiles through Puget Sound and Lake Washington have exposed buried folds, faults, and drag fold features within the Quaternary deposits and Tertiary bedrock (Johnson et al., 1994; Pratt et al., 2015). The top of bedrock in Seattle is not flat as a result of folding, scouring, slope failure, and human alteration.

2.3 QUATERNARY GEOLOGY

The modern Seattle landscape was developed from a combination of tectonic, glacial, volcanic, fluvial, and hillslope processes along with human influences. A minimum of seven continental glaciations have advanced into the Puget Lowland over the last 2.4 million years (Troost and Booth, 2008). The most recent glacier occupied the Puget Lowland from 17,400 to 16,400 calibrated years before present (Porter and Swanson, 1998). Subglacial scour left deep troughs that later filled with water, becoming Puget Sound, Lake Washington, and the Duwamish valley (Troost and Booth, 2008). Smaller subglacial troughs filled with glacial and interglacial deposits, creating buttress unconformities with the preexisting surface. Surficial glacial units deposited by the Quaternary Vashon Stade of the Fraser Glaciation included Lawton Clay (Qvlc), advance outwash (Qva), subglacial till (Qvt), and recessional deposits (Qvr) (Figure 4). Lawton Clay deposited as the glacier advanced, filling low energy glacial lakes with laminated clay and silt. Vashon advance outwash formed as proglacial streams deposited sand and gravel when the glacier advanced southward from Canada. Vashon subglacial till included compact diamict silt, sand, and gravel. As the glacier melted retreating northward, streams deposited well sorted sand and gravel as recessional outwash and clay as recessional lacustrine deposits (Troost et al., 2005). The active volcanic

Cascade Mountain Range contributed lahar deposits to the Puget Lowland following alpine glacier rivers to Puget Sound. Multiple reworked Mount Rainier lahars have been documented reaching Seattle (Zehfuss et al., 2003). Waterways accumulate alluvium of rounded to subrounded silt, sand, gravel, and cobbles (Troost et al., 2005). Puget Lowland slope failure is common due to the steep topography, high amount of winter precipitation, geologic structure, groundwater, and human activity. Landslides often occur in the winter season on steep slopes where high-permeability deposits sit atop low-permeability deposits, eventually failing as water accumulates atop the low-permeability strata. As a result of slope failure, colluvium deposits at the base of the slope burying strata. Toe erosion of slopes also initiates slope failure from wave cut or human removal of material (Troost and Booth, 2008). Besides natural processes, humans have altered the Seattle topography by restricting the Duwamish waterway, grading hills, and filling shallow marine tidelands with artificial fill to support the city's development (Troost and Booth, 2008). Active faulting, repeat glaciations, geomorphic processes, and human alterations create many geologic unconformities, leaving behind a complex stratigraphic profile in the Seattle Fault Zone.

3.0 BACKGROUND

The Seattle Fault Zone is a collection of multiple parallel reverse faults extending east-west through the southern part of Seattle (Pratt et al., 2015). Previously mapped concealed faults have been located using high-resolution seismic reflection data in the Puget Lowland waterways. Three faults and the deformation front have been located on land crossing Seattle (Figure 4). The deformation front is located north of Yesler Way approximately below Spring Street in downtown Seattle (Pratt et al., 2015). Deformation in the Eocene sediment located in the Seattle basin suggests faulting within the Seattle Fault Zone began in the late Eocene (~40 Ma) (Johnson et al., 1994).

In 1985, Yount, Dembroff, and Barats mapped the depth to bedrock from Everett to south Seattle using water well logs, exploration oil or gas well logs, geotechnical well logs, and marine seismic reflection data available at the time. Their map also showed bedrock outcrops in southeast Seattle. To the north of these outcrops, the depth to bedrock increased from 0 to over 3600 feet below downtown Seattle. This drop in bedrock elevation aligned with the northern limits of the Seattle Fault Zone and southern boundary of the Seattle basin (Yount et al., 1985).

Johnson et al. (1999) identified the Seattle Fault as a zone consisting of three or more parallel east-trending faults through Seattle and two or more right lateral faults extending north-south in Puget Sound between Bainbridge Island and West Seattle. These strands of the Seattle Fault Zone were identified using

high-resolution seismic reflection data in Dyes Inlet, Puget Sound, and Lake Washington. The northernmost east-west strand divided the Seattle basin from the Seattle uplift (Johnson et al., 1999). Consultants for Sound Transit drilled along a miles-long transect and created a geological cross section through Seattle for the construction of the Seattle to SeaTac Link light rail (AMEC Earth and Environmental Inc., and PanGEO Inc., 2004). Their cross section utilized existing and new boreholes identifying subsurface contacts between Quaternary deposits and Tertiary bedrock along a linear path (Figure 4). They noted abrupt stratigraphic offsets in the Duwamish valley south of Boeing Field.

Cowell, a former University of Washington graduate student, conducted a geophysical investigation of the unconformity between Tertiary Blakeley Formation bedrock and Quaternary Vashon till in Seward Park, Seattle. Cowell suggested this unconformity was potentially caused by offset along a strand of the Seattle Fault Zone (Cowell, 2018) (Figure 4).

Booth, Troost, and Shimel (2003) identified several potential fault locations while completing geologic mapping for the City of Seattle. They identified potential faults in West Seattle based on stratigraphic anomalies in the subsurface and associated geomorphic features. The northernmost strand, the North Alki deformation zone, uplifted a beach terrace about 20 feet aligning with a 65-foot offset in the subsurface pre-Vashon deposits. The middle strand, the Mee Kwa Mooks deformation zone, displaced beach sediments about 8 feet and displayed shearing features. The southernmost strand, the Lowman Beach fault strand, displaced about 82 feet of pre-Vashon subsurface deposits (Booth et al., 2003). Their mapped locations are consistent with those identified by Blakely et al. (2002) (Figure 4).

4.0 FIELD & GEOSPATIAL ANALYTIC METHODS

Both field and geospatial analytic methods were used to identify anomalies on land in south Seattle. A field investigation was conducted to view in-situ Seattle bedrock to assist with understanding the contents of the geotechnical boring logs. A series of geospatial analytic methods processed thousands of geotechnical boring logs and displayed geologic cross sections correlating boring logs.

4.1 FIELD METHODS

Site visits were conducted on July 21, 2018 to examine in-situ Blakeley Formation and Tukwila Formation in preparation for identifying written descriptions of bedrock in boring logs. Blakeley Formation outcrops were examined at Alki Point in West Seattle and at Seward Park on the Bailey Peninsula. At Alki Point, the shallow marine sedimentary Blakeley Formation included cyclic sequences of sandstone, siltstone, and mudstone. Bedrock at Alki Point beach displays an anticline with near vertical

bedding. The bedding was measured to strike 130° parallel to Alki Beach and dip 40° east, progressively steepening and changing to an east-west orientation to the north. Example strike and dip measurements from south to north (strike 120°, dip 47° east; strike 123°, dip 50° east; strike 110°, dip 62° east; and strike 110°, dip 80° east before overturning and directing east-west with a strike of 100° and dip of 44° east) follow a folding pattern similar to Yount and Gower's 1991 map (Figure 5). Trace fossils were present in the mudstone where burrows from bivalves and gastropods were filled with more resistant material leaving positive relief in the mudstone surface. Volcanic pumice clasts approximately 0.5 inches in diameter and fossilized wood about 4 inches long by 2 inches wide were scattered in the sandstone. The presence of pumice and wood suggests some of the sand could have mixed with deposits from early Cascade Mountain Range eruptions. The deposits accumulated in marine water at the former Washington shoreline. The Blakeley Formation viewed at Seward Park had areas of competent vertical walls with spalling erosion creating a smooth face extending east to west. Conglomerate in the Blakeley Formation was examined on the west shore of Seward Park with rounded clasts up to 10 inches in diameter.

South of Boeing Field, Tukwila Formation is exposed in roadcuts along Airport Way South at the South Boeing Access Road. The Eocene Tukwila Formation is about 56 to 34 million years old and originated from the proto-Cascade Mountain Range (Troost and Booth, 2008). The volcanic rock seen along Airport Way was highly weathered light brown clay that easily crumbled to dust. The outcrop included hydrothermally altered zones of reddish brown to white precipitant and quartz veins.

4.2 GEOSPATIAL ANALYTIC METHODS

4.2.1 DATA ORIGIN

The Washington State Department of Natural Resources (DNR) compiled multiple reliable sources of published seismogenic faults across Washington State into a single GIS shapefile in 2016 (Figure 2). The strands within the Seattle Fault Zone were identified by several publications supplied by the U.S. Geological Survey (USGS); however, the main strands within the study area were mapped by Blakely et al. (2002) (Johnson et al., 2016). All the published faults within the geographic study area are inferred faults (Figure 4).

The University of Washington Pacific Northwest Center for Geologic Mapping Studies (GeoMapNW) began compiling geotechnical boring logs of subsurface geologic information into a GIS geodatabase in 1998 directed by Drs. Troost and Booth (Booth et al., 2005). The database has periodically been updated since the early 2000s but data from the City of Seattle were last added in 2005. A copy of the GeoMapNW database now resides at the Washington Geological Survey (WGS), where thousands of

additional borings and water wells have been added. A copy of the GeoMapNW database was used for this project. More recent (post 2005) geotechnical boring logs were obtained from WGS's subsurface database for use in this project. Boreholes were added from WGS's database if the borehole intersected bedrock and was located near Interstate 5 and Sound Transit's Link light rail route.

4.2.2 DATA PROCESSING

Much of this project involved processing and interpreting boring logs using Esri's ArcGIS 10.5.1. The GeoMapNW database held over 84,500 boreholes as of 2019. Over 18,000 boreholes were within the geographic study area for this project. To filter for the boring logs that contacted bedrock, a code was developed using the programming language Python in ArcGIS's ModelBuilder to query boring logs containing terms found in Blakeley Formation and Tukwila Formation geologic descriptions. This selection using Python was conducted on a copy of the original borehole exploration shapefile from the GeoMapNW geodatabase to ensure the original table connections and formatting were not disturbed. The copied borehole shapefile was first clipped to the study area to reduce the size of the dataset. The clipped borehole shapefile attribute table was then joined with the boring log's subsurface layer table. By linking the shapefile and table, a physical coordinate (x, y, z) was assigned to every subsurface layer in the study area. A "Status" field was added to the attribute table of the newly created shapefile for the subsurface layers to keep track of which layers contained bedrock. Next, Python was used to select subsurface layers by their attributes using key bedrock terms (such as sandstone, conglomerate, and bedrock, etc.) and wild cards ("%") to allow for variations in records (full list in Appendix A). Any subsurface layer that included a bedrock term was assigned a status of "Queried". Unselected layers were termed "Negative". Once the data in the shapefile were categorized into "Negative" or "Queried", the statuses were transferred to the original borehole shapefile (EXPLORATION.shp) in the GeoMapNW database to proceed to the next step using the borehole shapefile with intact connections to the nonspatial data tables such as the subsurface layer, geologic interpretation, subsurface comment, author, contractor, geologic unit, and source tables.

A "Status" field was added to the original borehole exploration shapefile (EXPLORATION.shp) in the GeoMapNW database. The statuses applied to the boreholes through the Python query were transferred from the copied borehole layer to the original borehole layer in the GeoMapNW database. The original borehole shapefile contained all boreholes within the GeoMapNW database, including the boreholes outside of the study area. The boreholes outside of the geographic study area received the status "Out of scope" and were displayed with no symbology. The boreholes not selected through the Python query process, meaning no bedrock was recorded in the log, were assigned a "Negative" status. The boreholes

attributed as “Queried” were individually opened to determine if the Python query did select bedrock positive boreholes. Receiving the status “Checked” meant the boring log did not contain bedrock and the Python selection was invalid. The Python selection was invalid in situations when a term such as “Rock” was not describing bedrock but instead described, for example, rock found within artificial fill. The boring logs intersecting bedrock were categorized as “Confirmed” (Figure 6). Additional fields were added to the original borehole shapefile to record the physical condition of the bedrock (Intact, Weathered, Completely Weathered), the bedrock description copied from the boring log, and the top of bedrock elevation. Ground surface elevations were extracted from 2016 3-foot LiDAR data for the boring logs within the study area (PSLC, 2016). The depth to top of bedrock was subtracted from the surface elevation to give the bedrock elevation in feet using ArcGIS’s Field Calculator. Another query was conducted based on the maximum depth reached by the borehole. All boreholes deeper than 200 feet in the study area were checked to confirm no bedrock positive boreholes were missed.

Additional boring logs were added to the borehole exploration shapefile and subsurface layer table from the WGS’s database and surface bedrock outcrops located in the field on July 21, 2018. Twenty-five boring logs were individually downloaded from the WGS database because they were located along the Link light rail and contained bedrock descriptions in the log. A surface elevation was extracted from the 2016 LiDAR for the fourteen field collected points. A “Source” field was added to the borehole exploration shapefile to note which boring logs originated from WGS (“DNR Data Portal”) and the field collection (“Field Collection DAM”).

4.2.3 DIFFERENTIATING BEDROCK FROM QUATERNARY DEPOSITS

Key bedrock geologic description terms, the material’s properties, and the contents of adjacent boreholes were taken into each assessment to differentiate between Tertiary bedrock and Quaternary deposits in the geotechnical boring logs. Strength properties and cementation were helpful in determining if the material was rock or glacially overridden Quaternary deposits. The most common bedrock seen in the boring logs were various states of intact, weathered, and completely weathered Blakeley Formation (Tb). Occasionally the boring log would state “Bedrock”, “Weathered Sandstone”, “Shale”, “Siltstone”, or “Mudstone”, etc. Other times the description would explain the color, weathered or fresh, intact or fractured, cemented, hard, stiff, dense, and abbreviated terms such as “weath S/S” or “SS” understood to be abbreviated for weathered siltstone or sandstone. When the descriptions were ambiguous, the neighboring boreholes were compared to see if there was a continuation of bedrock in the area. If the borehole was surrounded by non-bedrock materials, it was determined the ambiguous boring log was “negative” for bedrock. Additionally, the sequence of the strata in the stratigraphic column was taken into

consideration. If bedrock was identified above a Quaternary deposit, the boring log was deemed negative for bedrock because bedrock should not be within Quaternary deposits except in the case of a reverse fault tip. Quaternary deposits described in the boring logs included topsoil, artificial fill, fluvial deposits of sand, gravel, and cobbles, along with glacial deposits of clay, silt, sand, and till. The differentiation between bedrock and Quaternary deposits was conducted conservatively to reduce error of overestimating the presence of bedrock in Seattle.

4.2.4 CROSS SECTIONS

Once the boring logs were processed, cross sections were developed to help visualize the three-dimensional (3D) contact of Quaternary deposits and Tertiary bedrock within the study area. The Geologic Cross Section Tool in the ArcGIS Toolbox developed by University of Washington graduate students Schaefer, Schwiters, and Weiser (2018) was used to produce 108 cross sections (Figure 7; Appendix B). The Geologic Cross Section Toolbox includes three tools for creating, symbolizing, and exporting two-dimensional (2D) cross-sectional views of selected geotechnical boring logs from the GeoMapNW geodatabase along a selected linear path (Schaefer et al., 2018). The ground surface along the cross-section lines was generated from the 2016 3-foot LiDAR DEM. No vertical exaggeration was applied to the cross sections. A line was added to each profile shapefile in the 108 cross sections to connect the top of the bedrock from borehole to borehole.

4.2.5 BEDROCK TOPOGRAPHIC SURFACE

Contours from a triangular irregular network (TIN) topographic surface of the bedrock were generated in AutoCAD Civil 3D 2018 using all boreholes containing bedrock within the study area and 206 bedrock-negative boreholes. The bedrock-positive and -negative boreholes were exported from ArcGIS to two Excel spreadsheets, one for positive and one for negative, where the attributes were rearranged to a point number (Exploration ID), northing, easting, elevation, description format (PNEElD). For the bedrock-positive boring logs, the elevation values were the elevations at the top of bedrock. The elevation values for the bedrock-negative boring logs were the elevation at the bottom of the borehole. The bedrock-positive spreadsheet was divided into three spreadsheets, one for each category of bedrock condition: intact, weathered, and completely weathered. The spreadsheets were imported separately into AutoCAD Civil 3D and assigned to four separate point groups labeled as each respective bedrock condition and a fourth point group for bedrock-negative boreholes. A TIN surface was developed using the four point groups. The TIN generates hundreds of triangle-shaped planar surfaces from the points in 3D (Figure 8). Each triangle plane uses three points. The points are selected based on proximity and each triangle is connected along the sides to create a continuous topographic surface. The outer edge of the surface was

revised to remove inaccurate computer-generated estimations. From the TIN surface, contours were generated and set to an interval of fifty feet and exported from AutoCAD to ArcGIS.

4.2.6 IDENTIFYING ANOMALIES

Each of the 108 cross sections were evaluated manually to identify anomalies in the approximate bedrock surface. The anomalies were numbered and labeled as "Anomaly #". Anomalies were identified as abrupt changes in the bedrock surface elevation where the overlaying ground surface remained relatively flat (Figure 9). The vertical displacement in bedrock ranged from as little as 5 feet to over 1200 feet. Any anomaly seen in a cross section was illustrated as a short line segment in plan view using an Anomaly polyline shapefile. The anomalies were also recorded in the cross section profile shapefiles with a short vertical line (Figure 9). Anomalies were evaluated to determine if they could be traced laterally between cross sections north-south or east-west. The anomalies in the bedrock surface seen in the cross sections were compared to the surface topography with aerial photographs and a bare-earth DEM to confirm the subsurface features were not from modern alterations or glacial scouring as evident in the topography. Anomalies were then categorized as potential anthropogenic alterations, potential erosion, potential fold from compression, or potential fault offsets.

5.0 RESULTS

The geotechnical boring logs gave detailed descriptions of the Blakeley and Tukwila Formations. Blakeley Formation was described as sandstone, siltstone, mudstone, claystone, shale, and conglomerate. Some descriptions included trace fossils, highly jointed to massive structure, various density values depending on if the sample was intact or completely weathered, and the color of the sample such as brown, yellowish brown, tan, or gray. The boring logs containing Tukwila Formation described andesite, andesite breccia, volcanic breccia tuff, talus rock, and volcanic rock. The logs also included information about the samples being highly fractured, fractured, or massive, weak to hard, green to blue or gray color, iron staining, and pumice clasts. Some logs gave detailed joints measurements such as the description for Exploration 63959: "Highly to moderately weathered, massive, light gray, weak, clayey ANDESITIC TUFF with angular pumice clasts; highly fractured with joints at 0, 15, 40, 50, 60 and 90 degrees (Tvc) R2".

The process of selecting bedrock-positive boring logs reduced the number of boreholes from 18,000 to 1700 boreholes within the study area. The boring logs for these 1700 boreholes were evaluated individually by checking each subsurface layer to validate if the borehole did contact bedrock, reducing the number of boreholes to 809 containing bedrock within the study area (Figure 6). There were 170

boreholes with a maximum depth of 200 feet or greater. Only 30 of those 170 boreholes reached 300 feet or deeper. Out of the bedrock-confirmed boreholes, 238 boreholes intersected intact bedrock, 477 boreholes reached weathered bedrock, and 94 boreholes contained completely weathered bedrock (Table 1).

Over 75 anomalies were initially identified in the 108 cross sections. The process of aligning anomalies laterally reduced the number of anomalies from 75 to 66 as multiple anomalies connected (Figure 10; Appendix C). With the lateral aligning of anomalies, the 66 anomalies intersected the 108 cross sections at approximately 166 total locations. For example, Anomaly 1 was originally identified in five cross sections but in order to align the anomaly laterally, the anomaly intersected a total of seven cross sections. Anomaly 1 did not initially appear in those two remaining cross sections because of a limited amount of data between boreholes along those cross sections. Thirty-three anomalies were laterally extensive across southeast Seattle while 34 anomalies were only identified in one cross section each. Characteristics of each anomaly at each of the 166 cross section intersections were recorded in an Excel spreadsheet (Appendix C). Recorded characteristics included the Anomaly identification number, the interpreted type of anomaly (anomaly category: fault, compression fold, anthropogenic alteration, or erosion), offset direction, bedrock elevation, vertical and horizontal bedrock offset, and which cross section the anomaly appeared on.

Anomaly 1 is the longest anomaly laterally aligning with strands identified by Blakely et al. (2002) and Booth et al. (2003) (Figure 10). Anomaly 1 aligned with the Mee Kwa Mooks deformation zone of Booth et al. (2003) and B1 of Blakely et al. (2002); the north side of the anomaly dropped in elevation as the south uplifted. Anomalies 1 and 5 intersected cross section G1-1’ between boreholes 59399 and 10729 (Figure 11). The difference between the top of bedrock is more than 928 feet between borehole 59399 and 10729. Borehole 10729 is on the east bank of the Duwamish waterway directly south of 59399 about 1 mile from Harbor Island to Kellogg Island. East of cross section G1-1’ on Interstate 5, the vertical displacement in bedrock is 1212 feet between exploration 59399 and 33016. Exploration 33016 is the northernmost bedrock positive borehole on Interstate 5 about 1.3 miles from borehole 59399. Borehole 33016 separates Anomalies 1 and 5 on Interstate 5 (Figure 11). The pattern of anomalies suggests a general stair-step profile with the bedrock surface decreasing in elevation toward the North Alki deformation zone north of Anomaly 1.

Many borings align with Interstate 5 through the Seattle Fault Zone. One cross section, cross section B1-1’, along Interstate 5 south of Eddy Street near the north end of Boeing Field, revealed an irregular

bedrock surface with eight anomalies spanning 800 feet (Figure 12). The vertical displacements in the bedrock surface ranged from 7 to 53 feet. The anomalies are located close together and include both uplifted and dropped bedrock steps. Similar features were seen in other cross sections such as cross section D18-18' along Martin Luther King Jr. Way South from South Oregon Street to South Holden Street (Figure 13). This cross section displayed approximately 17 anomalies.

The overlying Quaternary strata were examined along each anomaly to see if there were signs of offset in the younger deposits. Every cross section displays multiple unconformities in the Quaternary strata. The inconsistency of deposits limited the ability to identify deformation in the Quaternary deposits over a potential fault offset anomaly because the unconformities look like faults but could also be caused by erosion and deposition.

6.0 DISCUSSION

The anomalies could be faults, compressional features, erosional features, and/or the result of human alterations (Figure 14; Appendix C). Thirty-three of the 66 identified anomalies were inferred to be potential faults (Table 2; Appendix C). Anomalies were interpreted as faults when neighboring cross sections showed the same sense of motion, such as when neighboring north blocks moved in the same direction from cross section to cross section. Additionally, if the ground surface was flat with no signs of major construction or potential slope failure to explain for the offset in bedrock surface, the anomaly was identified as a potential fault. The anomaly was categorized as a compression feature if it was a minor change in bedrock elevation before or after an inferred fault, implying the bedrock surface may have folded due to the pressure around the fault plane (Figure 15). Erosional features included a change in bedrock elevation from potential glacial scour, fluvial erosion, wave erosion, or mass wasting from hillslope failure. Potential erosional features were supported by surface characteristics highlighted in the bare-earth DEM (Figure 16). Human alterations, especially near major infrastructure such as Interstate 5, included areas where bedrock had been removed for the grading of hillslopes or installation of bridge overpass footing (Figure 17). The anthropogenic inferred anomalies were typically in localized areas and not seen continuing in neighboring cross sections.

Construction investigations for Interstate 5 supplied a dense and reliable source of boring logs. Cross section B1-1' depicted eight anomalies, Anomaly 29 and Anomalies 31-37, along 800 feet of Interstate 5 (Figure 12). All anomalies except Anomaly 31 are interpreted to be potential fault offsets. Anomaly 31 is inferred to have been the result of anthropogenic alterations to the hillslope from the grading for highway construction because the cross-section path from exploration 41973 to 41972 traveled uphill at an oblique

angle across the road cut and the bedrock elevation increased 43.6 feet. Bedrock could have been removed at the base of the slope creating this 40-foot difference in elevation. Additionally, exploration 41973 at the base of the slope is capped with gravel, unlike exploration 41972, suggesting some form of human modification to the base of the road cut. There are no neighboring boring logs or cross sections to this stretch of Interstate 5 limiting the ability to confirm or deny these interpretations. North of cross section B1-1', cross section C1-1' shows a similar frequency of anomalies on Interstate 5 (Figure 17). Along 550 feet of Interstate 5, six anomalies, Anomaly 13 and 15-19, were identified intersecting cross section C1-1'. Anomaly 13 and 19 are interpreted as potential faults because they align with suspected faults to the east and west. Anomalies 15-18 are thought to be caused by human alterations to the landscape because aerial imagery shows an Interstate 5 overpass, Corson Ave South off ramp, and South Lucile Street bridge passing directly above this section of cross section C1-1' explaining the deformed bedrock surface if material was excavated and replaced for the construction of the bridge and highway. Anomalies along Interstate 5 are spaced feet apart and highlight many inconsistencies in the subsurface strata. Some can be explained as human alterations to the landscape as seen in cross section C1-1', but others have the potential of being fault offsets.

Anomalies 1, 14, 19, 22, 52, 54, and 57 are interpreted to be continuations of fault strands mapped by Blakely et al. (2002), Booth et al. (2003), Liberty and Pratt (2008), Barnett et al. (2010), and Cowell (2018) (Table 2; Figure 10 and 18). Anomaly 1 is interpreted to be a continuation of B1 of Blakely et al. (2002) and the Mee Kwa Mooks deformation zone of Booth et al. (2003). Anomaly 1 could connect east to Anomaly 14 and the eastern continuation of B of Blakely et al. (2002) in Seward Park and Lake Washington. The connection between Anomalies 1 and 14 are based on the geotechnical boring logs, anomaly motion, and the mapped northern limits of Blakeley Formation outcrops (Figure 10). Anomaly 14 displays the same north-down displacement mapped by Cowell (2018) and Blakely et al. (2002) suggesting the previously mapped thrust fault by Blakely et al. (2002) may cross Seward Park farther north than currently located, or, there are more fault offsets in the area than previously identified. Anomaly 19 could connect to the Lowman Beach fault strand of Booth et al. (2003) and B2 of Blakely et al. (2002) based on the lateral placement and north-down displacement of the anomaly and fault strand. Anomalies 19 or 22 could continue east aligning with the visible fault trace mapped by Barnett et al. (2010) on Mercer Island. Farther south, Anomaly 52 could connect to the south Mercer Island inferred faults mapped by Blakely et al. (2002) and Liberty and Pratt (2008). Anomaly 52 terminates farther inland than the previously noted faults due to a limited resource of boring logs (Figure 18). Anomaly 52 is interpreted to connect west to Anomaly 54 on Interstate 5 and possibly farther southwest to Anomaly 57 following parallel to C of Blakely et al. (2002) (Figure 10).

The bedrock surface generated from the 809 bedrock-positive and 206 bedrock-negative boreholes in AutoCAD Civil 3D helped visualize the bedrock paleotopography by displaying a TIN surface (Figure 19). The 206 bedrock negative boreholes were included to give a more accurate shape to the approximate bedrock surface. For example, the approximate bedrock surface along cross section E16-16' would pull flat between boreholes 1428 and 1746 (Figure 16). By adding the two negative-bedrock boreholes, 4076 and 1745, a depression was modeled in the bedrock surface contours. The two negative boreholes' elevations at the bottom of the boring were included as upper bounds to the bedrock surface. Bedrock-negative boreholes were not added to the TIN surface if the borehole did not reach deeper than the nearby bedrock elevation, such as the negative boreholes along cross section G1-1' between borehole exploration 59399 and 10729 (Figure 11). The contours from the TIN were set at a fifty-foot interval and compared to the identified anomalies. The software AutoCAD allowed for an interactive 3D view of the bedrock surface. The contours and TIN surface supported the anomalies by modeling the bedrock surface deformation as seen with Anomaly 13 in Figure 20. Cross section D21-21' identified an abrupt drop in bedrock elevation from borehole 2842 north of Anomaly 13 to 3106 south of Anomaly 13. Exploration 2842 contacted bedrock 0.4 feet below the surface while exploration 3106 drilled a maximum depth of 41.5 feet without reaching bedrock. The two boreholes are laterally separated by 42 feet. By including the bedrock-negative boring log 3106 in the AutoCAD generated surface, the contours modeled the deformation pattern seen in cross section D21-21'. The contours modeled more anomalies than what was identified in the cross sections such as the drop in elevation from 50 feet to -650 feet at the south end of Boeing Field where a bedrock-negative boring log (Exploration 10733) drilled a maximum depth of 686 feet without contacting bedrock.

A conceptual drawing of a cross sectional view through Seattle shows the irregularity in the bedrock surface through the Seattle Fault Zone (Figure 21). The diagram compiles features displayed in multiple cross sections but mainly cross section D18-18' which had the most anomalies and followed Martin Luther King Jr. Way South in Rainier Valley, Seattle (Figure 13). The deeper portions of the conceptual drawing are based on seismic reflection scans presented by Pratt et al. (2015). The bedrock surface had distinct uplifted and subsided steps on either side of the potential faults. The north-south compression forms an undulating bedrock surface concealing fold-propagated faults. The potential faults appear closer together moving north towards the boundary between the Seattle uplift and Seattle basin where the greatest vertical displacement occurs.

The anomalies identified through borehole correlation and the mapping between cross sections displayed the complexity of the 3D framework of the Seattle Fault Zone. The strain produced by the Cascadia

Subduction Zone and north-south crustal shortening has created the deformed bedrock seen in the cross sections. The frequency of parallel anomalies in localized areas suggests the strain along one anomaly can splay into numerous anomalies.

7.0 LIMITATIONS & ASSUMPTIONS

The anomalies and bedrock topographic map were derived from geotechnical boring logs recorded in the GeoMapNW geodatabase and are from public and private entities. New drilling was not conducted for this project, restricting the subsurface mapping to existing data resulting in zones of no data. Over 16,200 boreholes within the study area were not drilled deep enough to contact bedrock. In some areas there was a dense population of boreholes in a linear pattern with very few neighboring boreholes to the east or west. A single cross section was generated with no parallel cross sections to check against for quality control. This situation was present, for example, along Interstate 5 where a single cross section displayed eight anomalies (Figure 12). These anomalies inferred to be potential faults were neither supported nor denied due to the absence of boreholes on either side of the cross section.

Bedrock outcrops in Seattle were difficult to locate and access due to limited outcrop exposure and extensive surface alterations both by humans and nature. The few outcrops visited were exposed at low tide at Alki Point, along a highway off ramp on Boeing Access Road, and in the vegetated Seward Park. Other outcrops would require access to private land. Bedrock outcrops have been buried by Quaternary deposits. Urbanization has removed and covered some bedrock outcrops as seen along Interstate 5 and the Duwamish waterway. All these surface alterations have reduced access to bedrock outcrops requiring mapping of strands of the Seattle Fault Zone to rely on minimally invasive assessments such as drilling, high resolution seismic reflection data, and aeromagnetic data.

The bedrock condition and quality of sample descriptions restricted the data processing. Some bedrock positive boreholes only reached weathered bedrock. It was assumed when a borehole reached weathered bedrock, intact bedrock must be below resulting in the “Confirmed” borehole status. Due to the abundance of boring logs describing weathered bedrock, some descriptions resembled Quaternary glacial deposits such as “compact silt” which could be glacially overridden silty glacial deposits or siltstone bedrock. In these situations, the surrounding boreholes were consulted in an attempt to determine if bedrock was indeed encountered.

Using the Cross Section Tool was a learning process. It was discovered the output was more accurate if the selected borehole directly crosses the cross-section polyline. The earlier cross sections were not

revised due to time restrictions unless the cross section was viable to the identification of an anomaly. In those cases, the cross section was remade for a more accurate display and interpretation.

8.0 CONCLUSION

The processing of 18,000 boring logs identified 66 major anomalies for future investigation into the location of fault strands of the Seattle Fault Zone. Of those anomalies, 33 were interpreted as possible faults. Geotechnical boring logs gave detailed descriptions of Tertiary deposits beneath the City of Seattle. The AutoCAD generated TIN surface modeled the paleotopographic features of the bedrock surface revealing irregular terrain in south Seattle. Changes in the bedrock surface elevation between boring locations from about 5 feet to over 1200 feet were identified as anomalies. Anomaly 1 highlighted a drop in bedrock elevation ranging from 928 to 1212 feet within the Duwamish waterway and near Interstate 5 illustrating a possible stair-step structure to the northern edge of the Seattle Fault Zone. South of Anomaly 1, where the density of available boreholes increased, anomalies became closer together geographically suggesting strain was distributed among numerous anomalies showing the complexity of the 3D structure within the Seattle Fault Zone or that more closely spaced borings show more accurately the irregularity in the bedrock surface. Anomalies 1, 14, 19, 22, 52, 54 and 57 appear to connect to previously mapped faults while other anomalies may indicate the location of new strands. The anomalies identified in southeast Seattle in this research contributes new interpretations into the path of potential fault strands from Puget Sound to Lake Washington. The identification of faults by the correlation of boreholes was proven successful and could be applied to other complex fault zones around the world.

9.0 FUTURE WORK

The data and maps presented in this project were the preliminary steps toward locating strands of the Seattle Fault Zone. As previously stated, some anomalies could be faults while others likely represent compressional features, geomorphic erosion, or human alterations.

- Further investigation into the anomalies could be done at a finer scale than this project's broad approach. More detail can be collected through field and seismic investigations to better understand the anomaly origin.
- The borehole data was processed for Alki Point in West Seattle and the southern extents of the study area in north Allentown where the Link light rail crosses the Duwamish waterway. Cross sections and anomalies were not generated for these two areas because of the abundance of work conducted in southeast Seattle. These areas should be evaluated in more detail.
- More data should be added to the bedrock surface contours. The contours generated in AutoCAD Civil 3D illustrated the basic bedrock surface using bedrock-positive boreholes and a few hand

selected bedrock-negative boreholes. Additional data such as more boring logs, ground surface breaklines, and features identified in seismic reflection data should be added to these contours to increase their accuracy.

- The anomalies and topographic map of the bedrock surface identified through borehole correlation should be used in further analysis to assist in the accurate identification of strands of the Seattle Fault Zone.
- The lateral extents of the anomalies identified as continuations of mapped faults should be evaluated with detailed subsurface mapping of Quaternary deposits.
- Newly identified potential fault location should be further evaluated by geophysical methods and detailed evaluations of overlying Quaternary deposits.

10.0 REFERENCES

AMEC Earth and Environmental Inc., and PanGEO Inc., 2004, Geotechnical Engineering Report Central Link Light Rail D 755 Procurement No. RTA/LR 106-98 King County, Washington, 2-91M-14550-0.

Atwater, B.F. and Moore, A.L., 1992, A tsunamic about 1000 years ago in Puget Sound, Washington, Science, v. 258, iss. 5088, p. 1614.

Barnett, E.A., Haugerud, R.A., Sherrod, B.L., Weaver, C.S., Pratt, T.L., and Blakely, R.J., 2010, Preliminary atlas of active shallow tectonic deformation in the Puget Lowland, Washington, U.S. Geological Survey, Open-File Report 2010-1149, 32 p.

Blakely, R.J., Wells, R.E., Weaver, C.S., and Johnson, S.Y., 2002, Location, structure, and seismicity of the Seattle Fault zone, Washington: Evidence from aeromagnetic anomalies, geologic mapping, and seismic-reflection data, Geological Society of America Bulletin, v. 114, no. 2, p. 169-177.

Booth, D.B., Troost, K.G., and Shimel, S.A., 2003, Landfall of the Seattle fault zone, West Seattle, WA, Geological Society of America Abstracts with Program, v. 35, no. 6, p. 479.

Booth, D.B., Troost, K.G., and Shimel, S.A., O'Neal, M.A., and Wisher, A.P., 2005, New Geologic Mapping and Geologic Database for the Urbanized Puget Lowland, Western Washington State, USA, p. 259-266, in Soller, D.R. ed., 2005, Digital Mapping techniques '05 – Workshop Proceedings, U.S. Geological Survey, Open-File Report 2005-1428.

Brocher, T.M., Wells, R.E., Lamb, A.P., and Weaver, C.S., 2017, Evidence for distributed clockwise rotation of the crust in the northwest United States from fault geometries and focal mechanisms, Tectonics, v. 36, p. 787-818.

Bucknam, R.C., Hemphill-Haley, E., and Leopold, E.B., 1992, Abrupt Uplift Within the Past 1700 Years at Southern Puget Sound, Washington: Science, v. 258, p. 1611-1614.

Cowell, K.J., 2018, Geophysical Investigation of a Geologic Unconformity at Seward Park – Seattle, WA [Masters thesis]: University of Washington.

Johnson, S., Potter, C., and Armentrout, J., 1994, Origin and evolution of the Seattle fault and Seattle basin, Washington, Geology, v. 22, no. 1, p. 71-74.

Johnson, S.Y., Dadisman, S.V., Childs, J.R., and Stanley, W.D., 1999, Active tectonics of the Seattle fault and central Puget Sound, Washington – Implications for earthquake hazards, The Geological Society of America Bulletin, v. 111, p. 1042-1053.

Johnson, S.Y., Blakely, R.J., Brocher, T.M., Haller, K.M., Barnett, E.A., Bucknam, R.C., Haeussler, P.J., Pratt, T.L., Nelson, A.R., Sherrod, B.L., Wells, R.E., Lidke, D.J., Harding, D.J., and Kelsey, H.M., compilers, 2016, Fault number 570, Seattle Fault Zone, in Quaternary fault and fold

database of the United States: U.S. Geological Survey website, http://earthquake.usgs.gov/hazards/qfaults (Accessed 06/02/2019).

Liberty, L.M., and Pratt, T.L., 2008, Structure of the Eastern Seattle Fault Zone, Washington State: New Insights from Seismic Reflection Data, Bulletin of the Seismological Society of America, v. 98, no. 4, p. 1681-1695.

Nelson, A.R., Johnson, S.Y., Kelsey, H.M., Wells, R.E., Sherrod, B.L., Pezzopane, S.K., Bradley, L.A., Koehler, R.D.III., and Bucknam, R.C., 2003, Late Holocene earthquakes on the Toe Jam Hill fault, Seattle fault zone, Bainbridge Island, Washington, The Geological Society of America Bulletin, v. 115, no. 11, p. 1388-1403.

Porter, S.C. and Swanson, T.W., 1998, Radiocarbon age constraints on rates of advance and retreat of the Puget Lobe of the Cordilleran Ice Sheet during the last glaciation: Quaternary Research, v. 50, p. 205-213.

Pratt, T.L., Troost, K.G., Odum, J.K., and Stephenson, W.J., 2015, Kinematics of shallow backthrusts in the Seattle fault zone, Washington State, Geosphere, v. 11, no. 6, p. 1948-1974.

Puget Sound Lidar Consortium (PSLC), 2016, 2016 King County Delivery 1 Bare Earth Filegeodatabase, http://pugetsoundlidar.ess.washington.edu/lidardata/restricted/projects/2016king_county_1.html

Schaefer, J., Schwitters, D., and Weiser, M., 2018, Geologic Cross Section Toolbox Instructions: University of Washington.

Sherrod, B.L., 2002, Late Quaternary Surface Rupture Along the Seattle Fault Zone Near Bellevue, Washington, American Geophysical Union, Fall Meeting, Abstract #S21C-12.

Troost, K.G., and Booth, D.B., 2008, Geology of Seattle and the Seattle Area, in Baum, R., Godt, J, and Highland, L. eds., Landslides and Engineering Geology of the Seattle, Washington, Area, Geol. Soc. Amer., Special Papers XX, p. 1-37, 2 plates.

Troost, K.G., and Booth, D.B., Wisher, A.P., and Shimel, S.A., 2005, The Geologic Map of Seattle – a Progress Report: U.S. Geological Survey Open-File Report, 2005-1252, scale 1:24,000.

Yount, J.C., Dembroff, G.R., and Barats, G.M., 1985, Map showing depth to bedrock in the Seattle 30’ by 60’ Quadrangle, Washington: U.S. Geological Survey, Miscellaneous Field Studies Map, scale 1:100,000.

Yount, J.C., and Gower, H.D., 1991, Bedrock Geologic Map of the Seattle 30’ by 60’ Quadrangle, Washington: U.S. Geological Survey, scale 1:100,000.

Zehfuss, P.H., Atwater, B.F., Vallance, J.W., Brenniman, H., and Brown, T.A., 2003, Holocene lahars and their by-products along the historical path of the White River between Mount Rainier and Seattle, Geological Society of America, Field Guide 4, p. 209-223.

11.0 TABLES

Table 1: Geotechnical Boring Log Statistics. The statistics of the processed boring logs assisted in the understanding of the state of bedrock in Seattle.

GEOTECHNICAL BORING LOG STATISTICS		NUMBER
TOTAL BORING LOGS IN STUDY AREA		18,000
BEDROCK TERM SELECTION: NEGATIVE		16,300
BEDROCK TERM SELECTION: POSITIVE		1,700
QUERY CHECKED (NEGATIVE)		891
QUERY CONFIRMED		890
DEPTH (FEET)	0-200	639
	>200	170
	>300	30
BEDROCK QUALITY	INTACT	238
	WEATHERED	477
	COMPLETELY WEATHERED	94

Table 2: Correlation of Potential Fault Anomalies and Known or New Strands in the Seattle Fault Zone. Thirty-three of the 66 anomalies were interpreted as potential fault offsets. Some anomalies were interpreted as continuation of existing fault strands. See Appendix C for more information about all 66 Anomalies.

ANOMALY	CROSS SECTIONS INTERSECTED BY ANOMALY	AMOUNT OF POTENTIAL VERTICAL OFFSET (FEET)	CONTINUATION OF FAULT	NEW POTENTIAL FAULT
1, 14	G 1-1', C 24-24', C 25-25', D 18-18', D 19-19', E 2-2', E 4-4', E 12-12', E 13-13'	928 TO 1212	B OF BLAKELY ET AL (2002), MEE KWA MOOKS OF BOOTH ET AL. (2003), COWELL (2018)	NO
2, 14	D 18-18', D 19-19', E 15-15'	10 TO 39	B OF BLAKELY ET AL (2002), COWELL (2018)	YES/NO
3	D 18-18', D 19-19'	23 TO 29		YES
4	D 19-19'	20		YES
5, 14	G 1-1', C 24-24', C 25-25', D 18-18', D 19-19', E 2-2', E 4-4', E 7-7', E 8-8', E 9-9', E 15-15'	23 TO 928	B OF BLAKELY ET AL (2002), COWELL (2018)	YES/NO
8	D 19-19'	45		YES
9	D 20-20', D 21-21'	16 TO 21		YES
11	D 20-20', D 21-21'	39 TO 43		YES
13	C 1-1', C 13-13', D 18-18', D 20-20', D 21-21', E 2-2', E 3-3', E 6-6', E 9-9'	7 TO 41		YES
14	E 12-12', E 13-13'	-	B OF BLAKELY ET AL (2002), COWELL (2018)	NO
19	C 1-1', C 3-3', C 5-5', C 10-10', C 12-12', C 13-13', C 23-23', D 18-18'	1 TO 38	B2 OF BLAKELY ET AL (2002), LOWMAN BEACH FAULT STRAND OF BOOTH ET AL. (2003), BARNETT ET AL. (2010)	NO
21	C 1-1', C 3-3', C 4-4', C 8-8'	10 TO 33		YES
22	D 18-18', E 3-3', E 6-6', E 9-9'	9 TO 54	BARNETT ET AL. (2010)	NO
26	C 2-2'	12		YES
29	B 1-1', D 18-18'	9 TO 53		YES
30	E 10-10', E 11-11'	16 TO 22		YES
32	B 1-1'	19		YES
33	B 1-1'	7		YES
34	B 1-1'	8		YES
35	B 1-1'	8		YES
36	B 1-1'	14		YES
37	B 1-1'	6		YES
44	D 18-18'	14		YES
48	A 7-7', A 15-15'	4 TO 14		YES
49	D 9-9', D 18-18', D 23-23'	3 TO 8		YES
50	A 2-2', A 3-3', A 7-7', A 16-16', A 24-24', D 1-1', D 2-2', D 3-3', D 4-4', D 5-5', D 6-6', D 7-7', D 8-8', D 17-17', D 18-18'	8 TO 44		YES
52, 54, 57	A 22-22', D 6-6', D 18-18', D 22-22', G 1-1'	6 TO 135	C OF BLAKELY ET AL. (2002), LIBERTY AND PRATT (2008)	YES/NO
53	A 3-3', A 6-6', A 24-24'	18 TO 103		YES
55	D 18-18'	12		YES
56	A 3-3', A 6-6', A 7-7', D 18-18', E 3-3', E 17-17'	6 TO 103		YES
58	F 1-1', F 2-2', F 3-3', F 4-4', F 5-5', G 1-1'	12 TO 176		YES

12.0 FIGURES

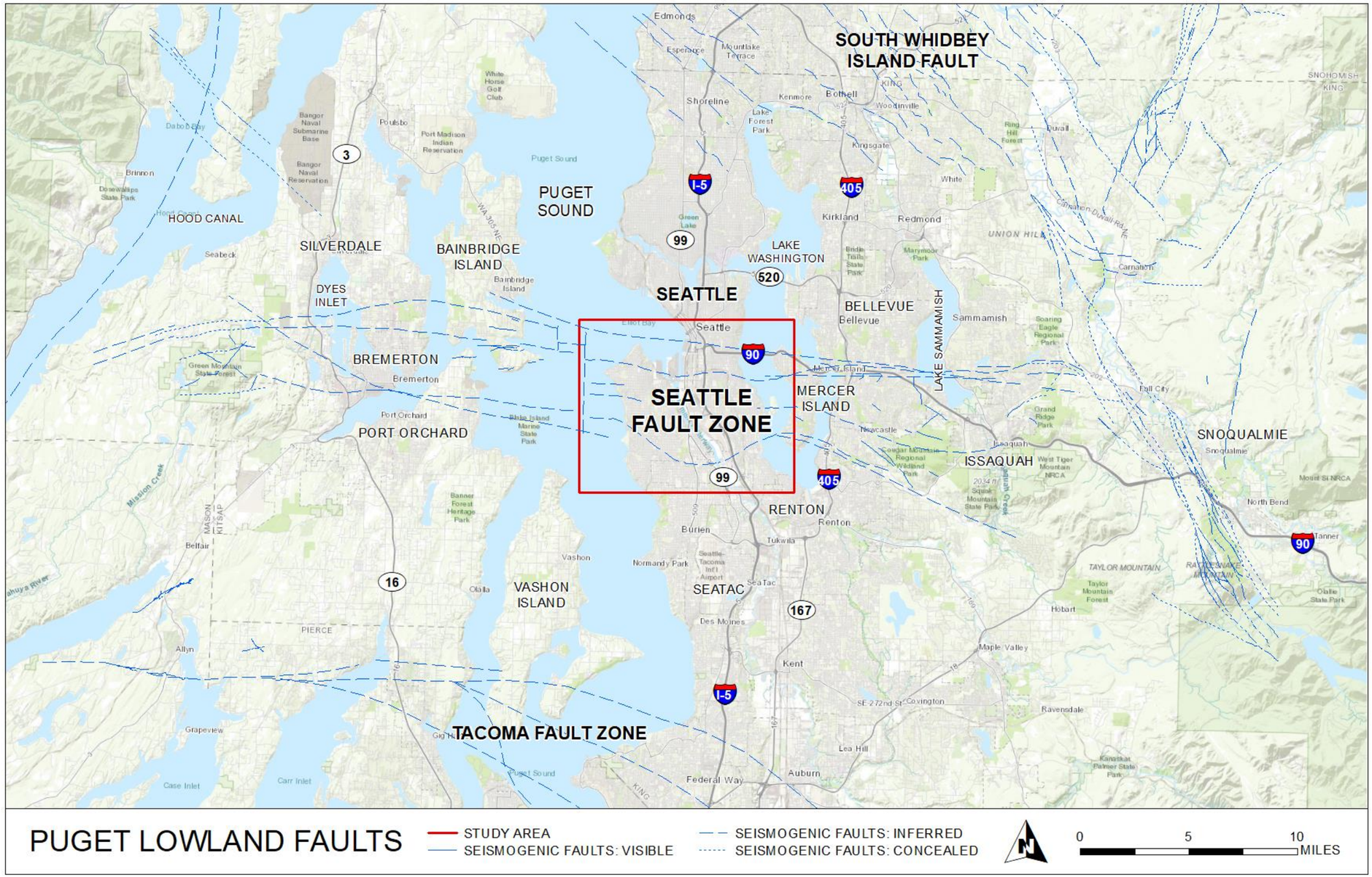

Figure 1: Puget Lowland Faults. The Seattle Fault Zone spans approximately 50 miles from west of Bremerton to east of Issaquah with the South Whidbey Island Fault Zone to the northeast and Tacoma Fault Zone to the south. The seismogenic fault locations are provided by Washington State Department of Natural Resources as a compilation of active faults mapped by multiple sources (Johnson et al., 2016).

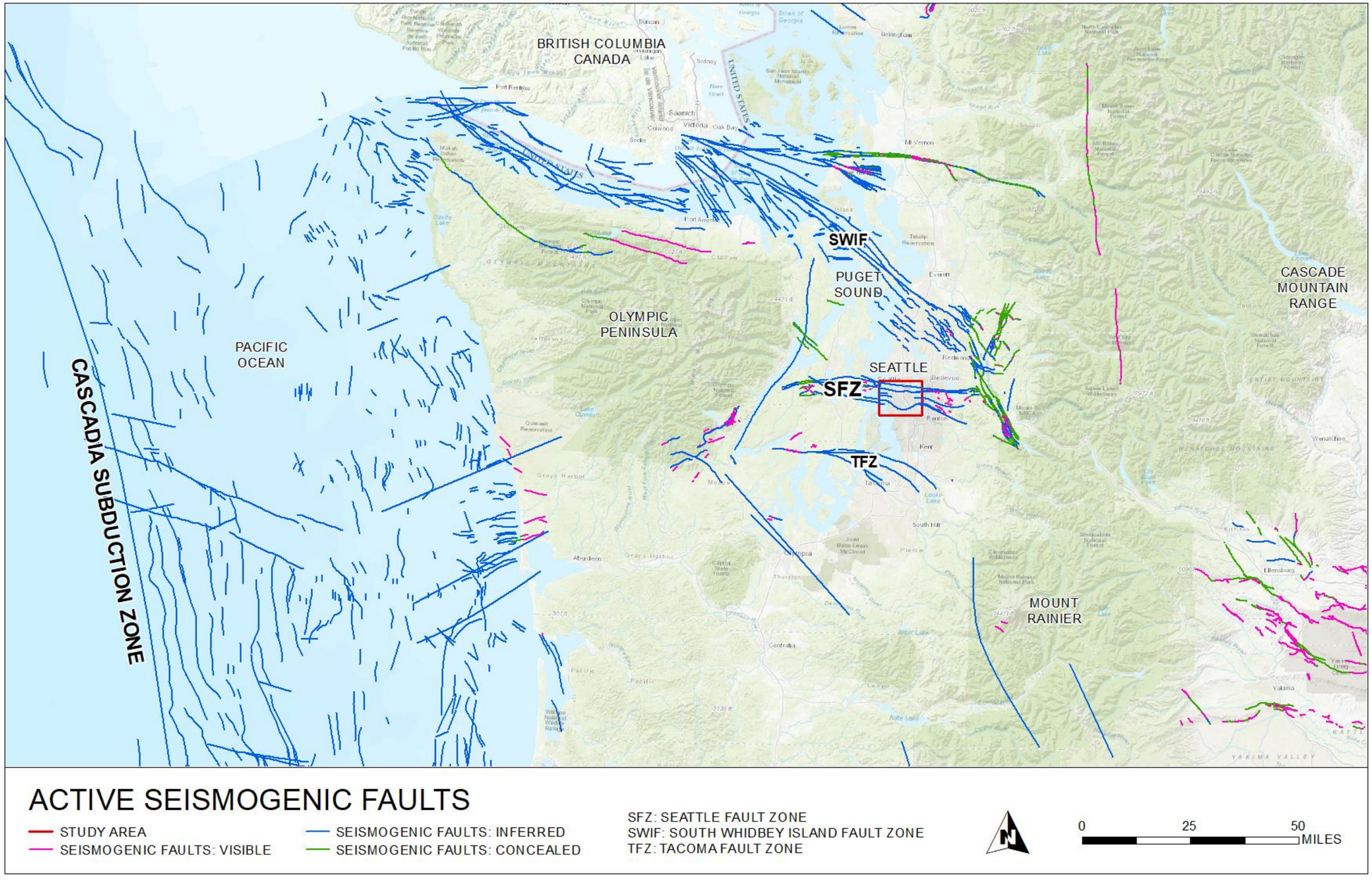

Figure 2: Active Seismogenic Faults. The Cascadia Subduction Zone off the western coast of the U.S. along with north-south compression has developed multiple faults and fault zones in western Washington. Most faults are inferred, especially off the coast and within the Puget Lowland. The seismogenic faults are provided by Washington State Department of Natural Resources as a compilation of active faults mapped by multiple sources (Johnson et al., 2016).

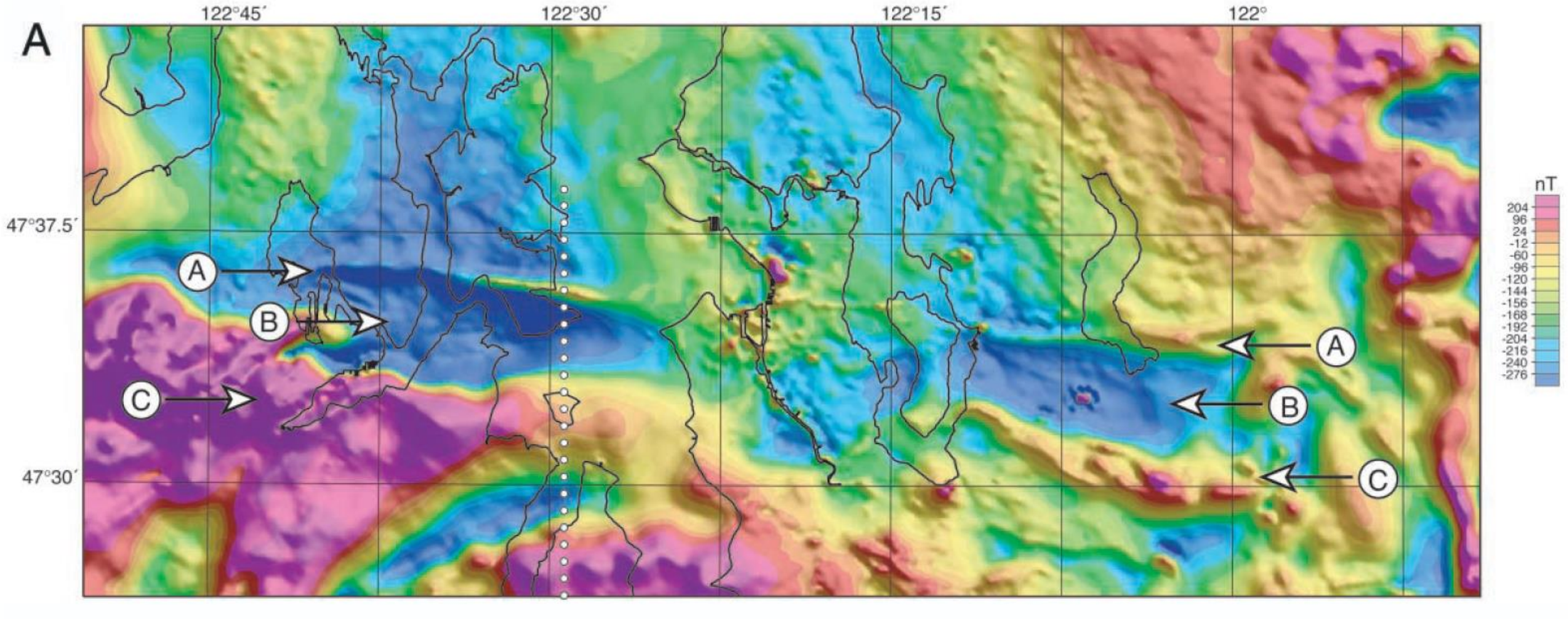

Figure 3: Aeromagnetic Anomalies. Blakely et al. (2002) identified three magnetic anomalies using aeromagnetic surveys. These anomalies are related to the structure of the steeply dipping Blakely Harbor Formation (Anomaly A), steeply dipping Blakeley Formation (Anomaly B), and Tukwila Formation (Anomaly C). The anomalies identified as A, B, and C represent the locations of inferred fault strands. The warm colors indicate highest magnetic bedrock and anthropogenic features. Magnetic profiles were generated by Blakely et al. (2002) along the white dotted line (adapted from Blakely et al., 2002).

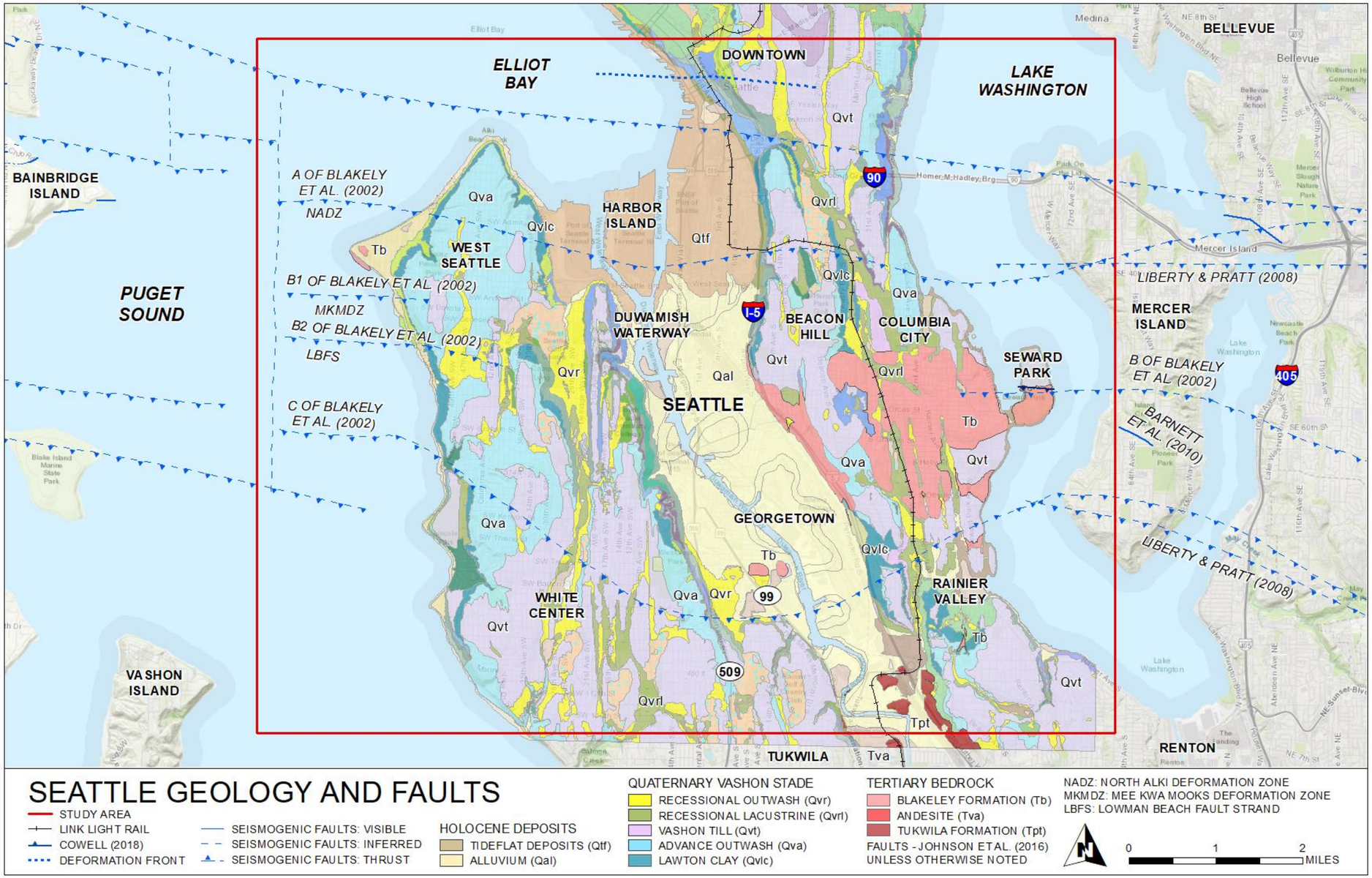

Figure 4: Seattle Geology and Faults. The study area focused on southeast Seattle where Blakeley Formation (light red) is exposed at the ground surface. The Quaternary and Tertiary units were mapped by Troost et al. (2005). The seismogenic faults are provided by Washington State Department of Natural Resources as a compilation of active faults mapped by multiple sources (Johnson et al., 2016). The Deformation Front was digitized from Pratt et al. (2015). A potential fault strand was digitized in Seward Park based on Cowell (2018). The Link light rail route was provided by City of Seattle's GIS database. Not all geologic units were included in this map.

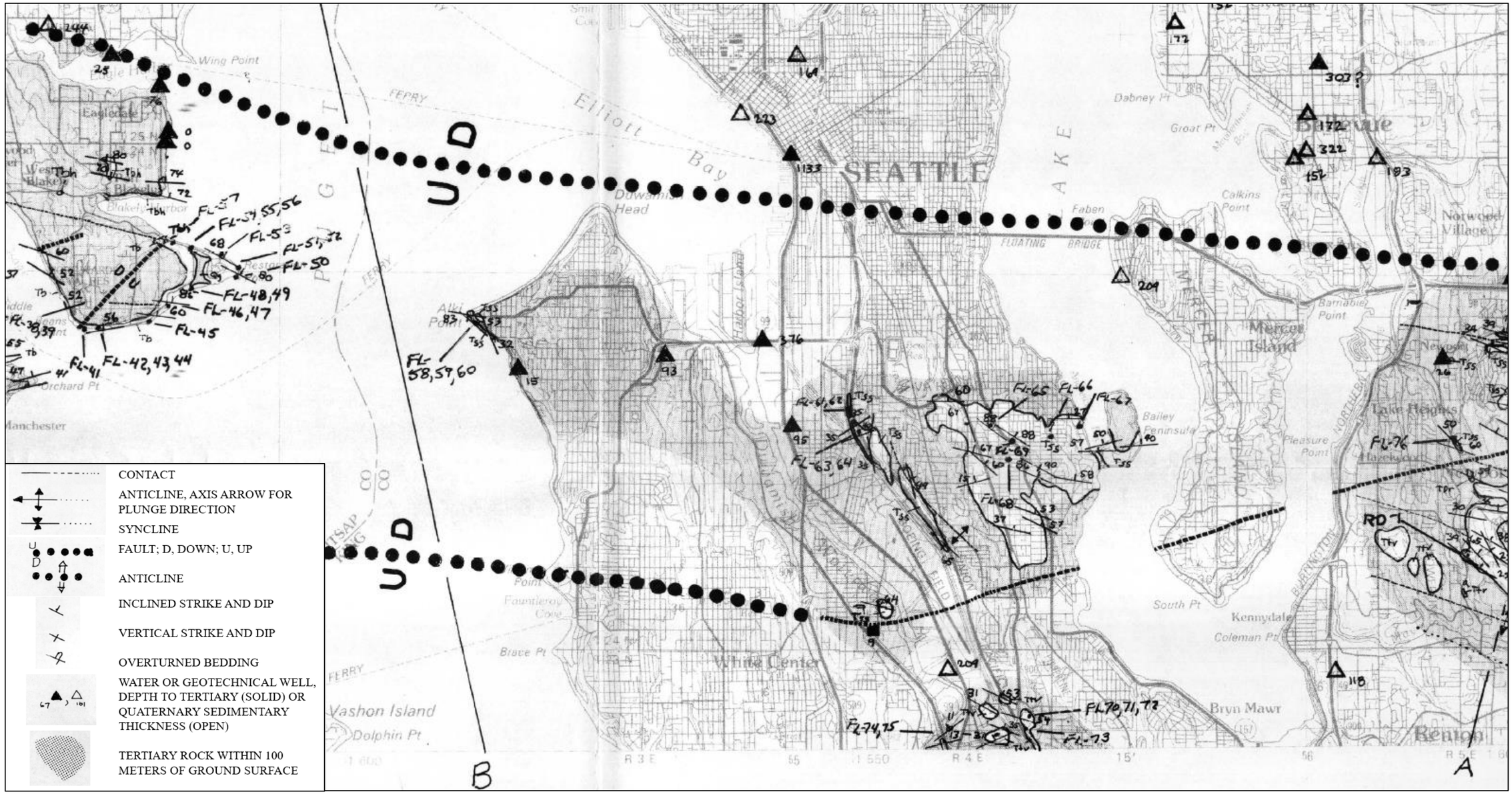

Figure 5: Seattle Bedrock Structure. Yount and Gower (1991) mapped the exposed bedrock outcrops (solid black lines) in south Seattle from 1978-1982. They identified steeply dipping strata, anticlines, and vertical bedding (adapted from Yount and Gower, 1991).

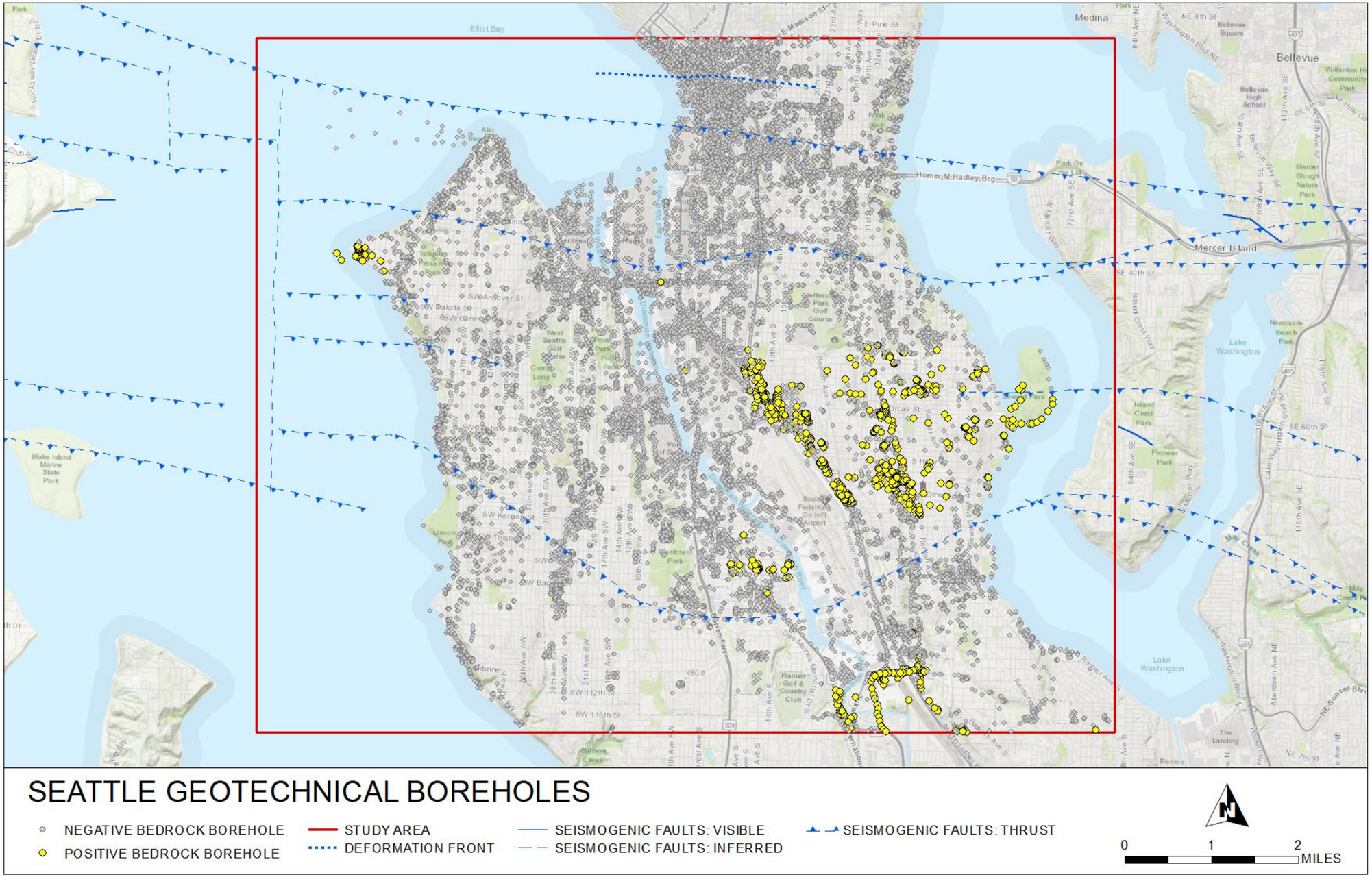

Figure 6: Seattle Geotechnical Boreholes. The yellow points represent the boreholes that encountered bedrock; while the grey points indicate the borehole did not reach bedrock. Data is from the GeoMapNW Database.

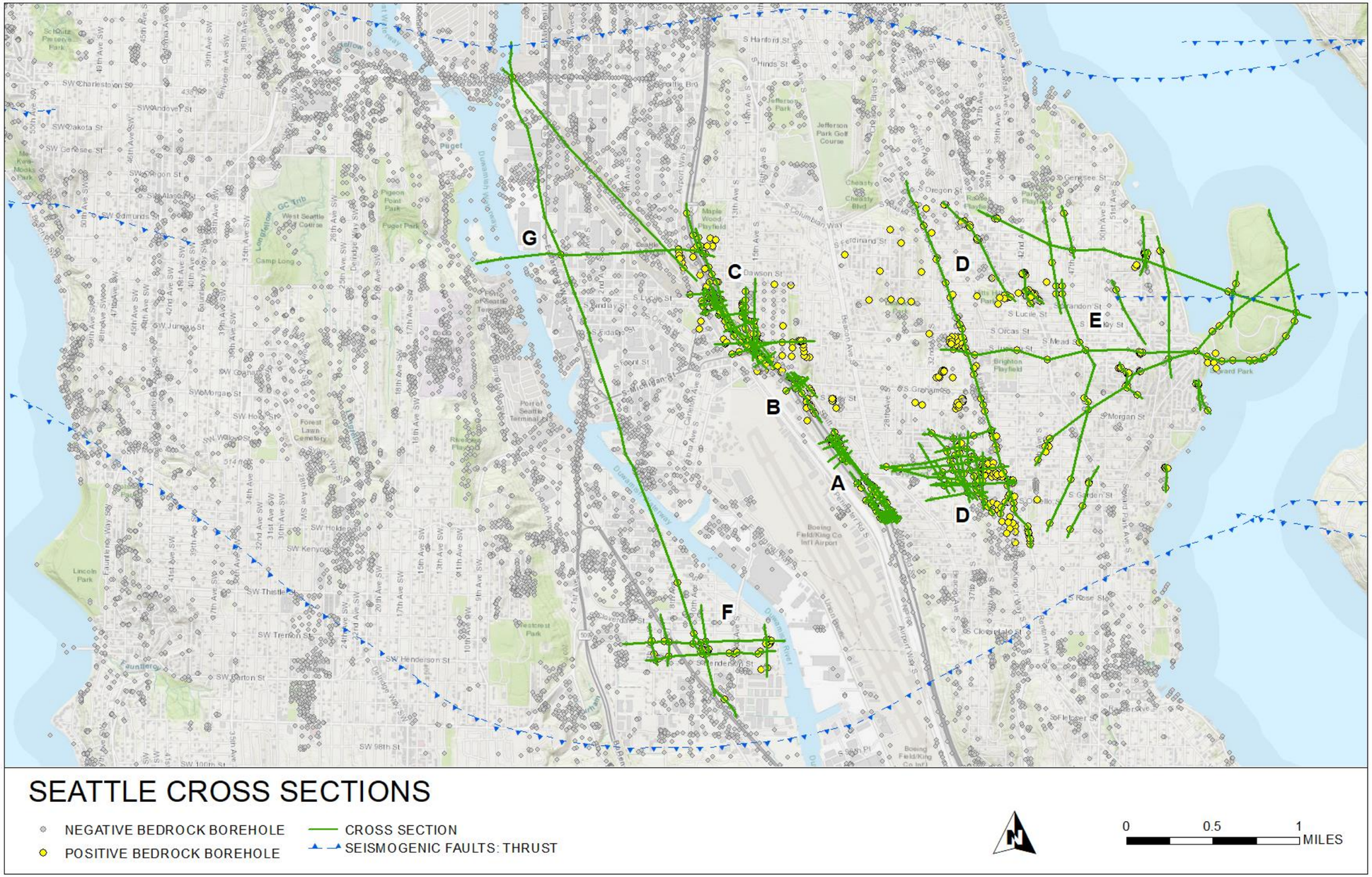

Figure 7: Seattle Cross Sections. The green lines show the location of the 108 cross sections generated for southeast Seattle. The cross sections were conducted in groups around bedrock-positive boreholes (A-G). For a more detailed view, see Appendix B.

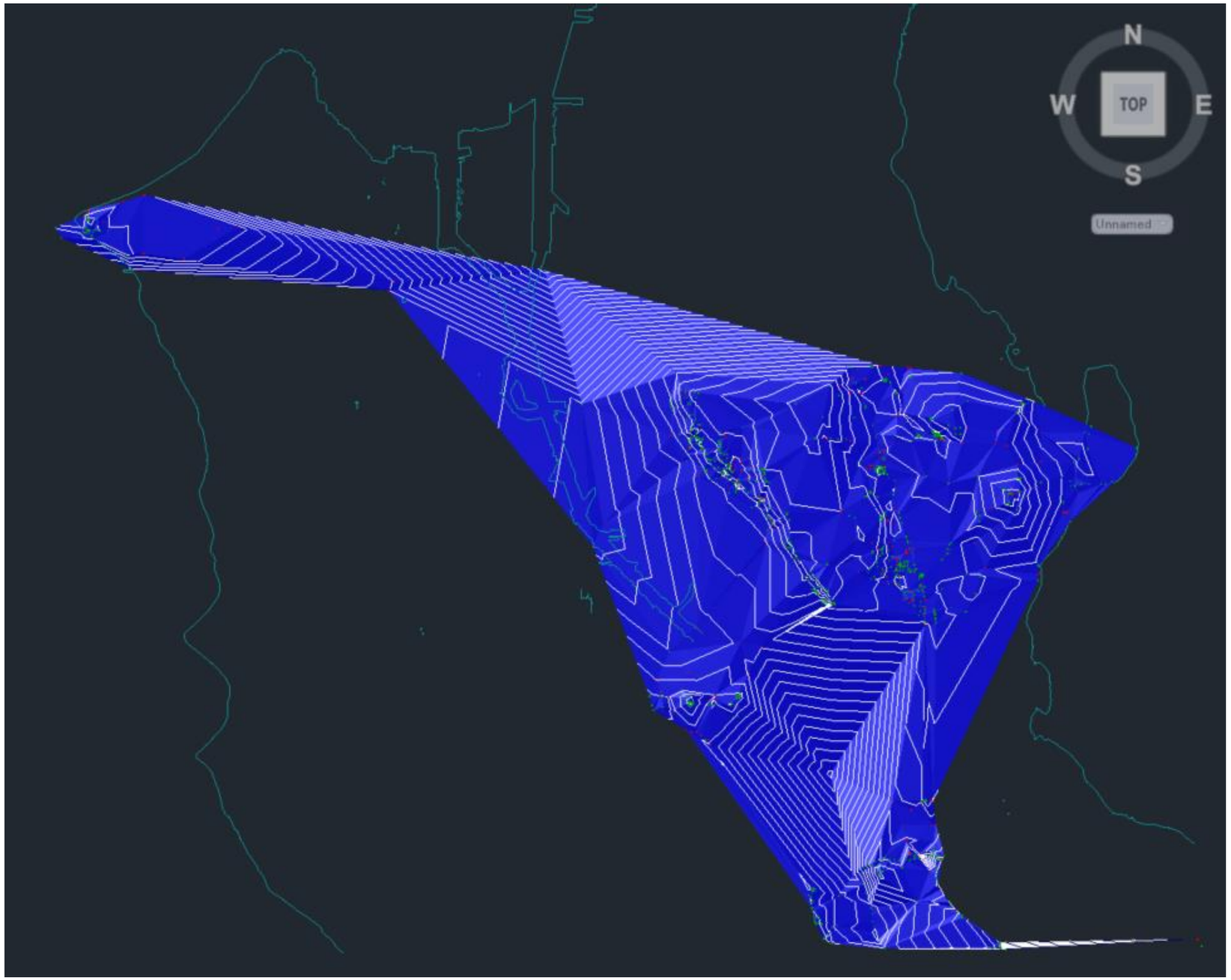

Figure 8: AutoCAD Civil 3D TIN Surface. The bedrock topography in south Seattle was generated in AutoCAD Civil 3D as a TIN surface (blue) using bedrock-positive and -negative boring logs. See Figure 19 for contour elevaions.

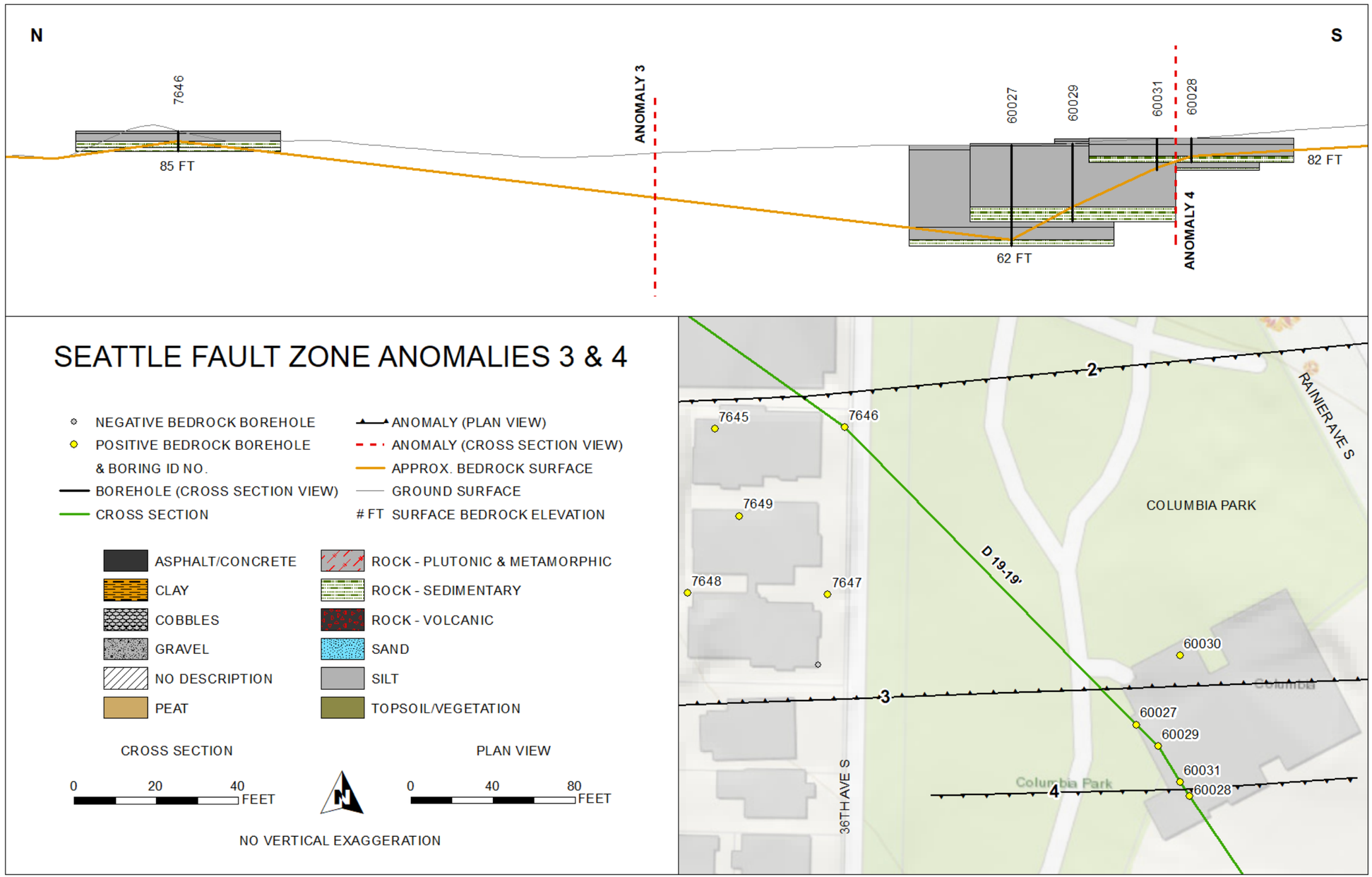

Figure 9: Seattle Fault Zone Anomalies 3 & 4. Anomaly 2-4 intersected cross section D19-19' within Columbia Park. The change in depth to bedrock surface between borehole exploration 7646 and 60027 (Anomaly 3) displays the typical deformation to the approximate bedrock surface identified as an anomaly. The approximate bedrock surface slopes about 6 degrees between Anomalies 2 and 3 and then increases to about 25 degrees between Anomalies 3 and 4 (Appendix C).

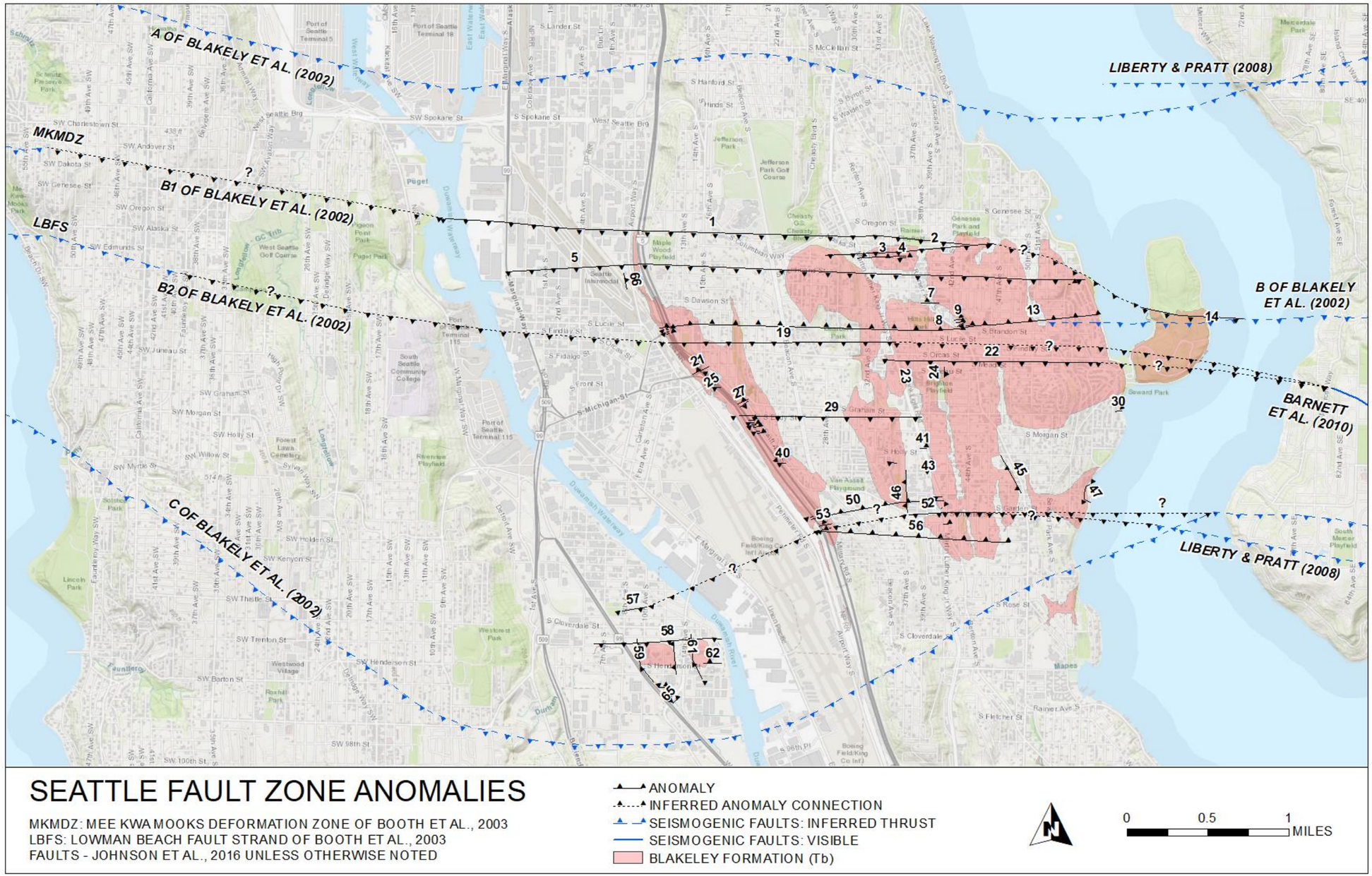

Figure 10: Seattle Fault Zone Anomalies. The 66 anomalies identified by borehole correlation were centered around bedrock outcrops with Anomalies 1, 14, 19, 22, 52, 54, and 57 potentially connecting to existing known strands of the Seattle Fault Zone.

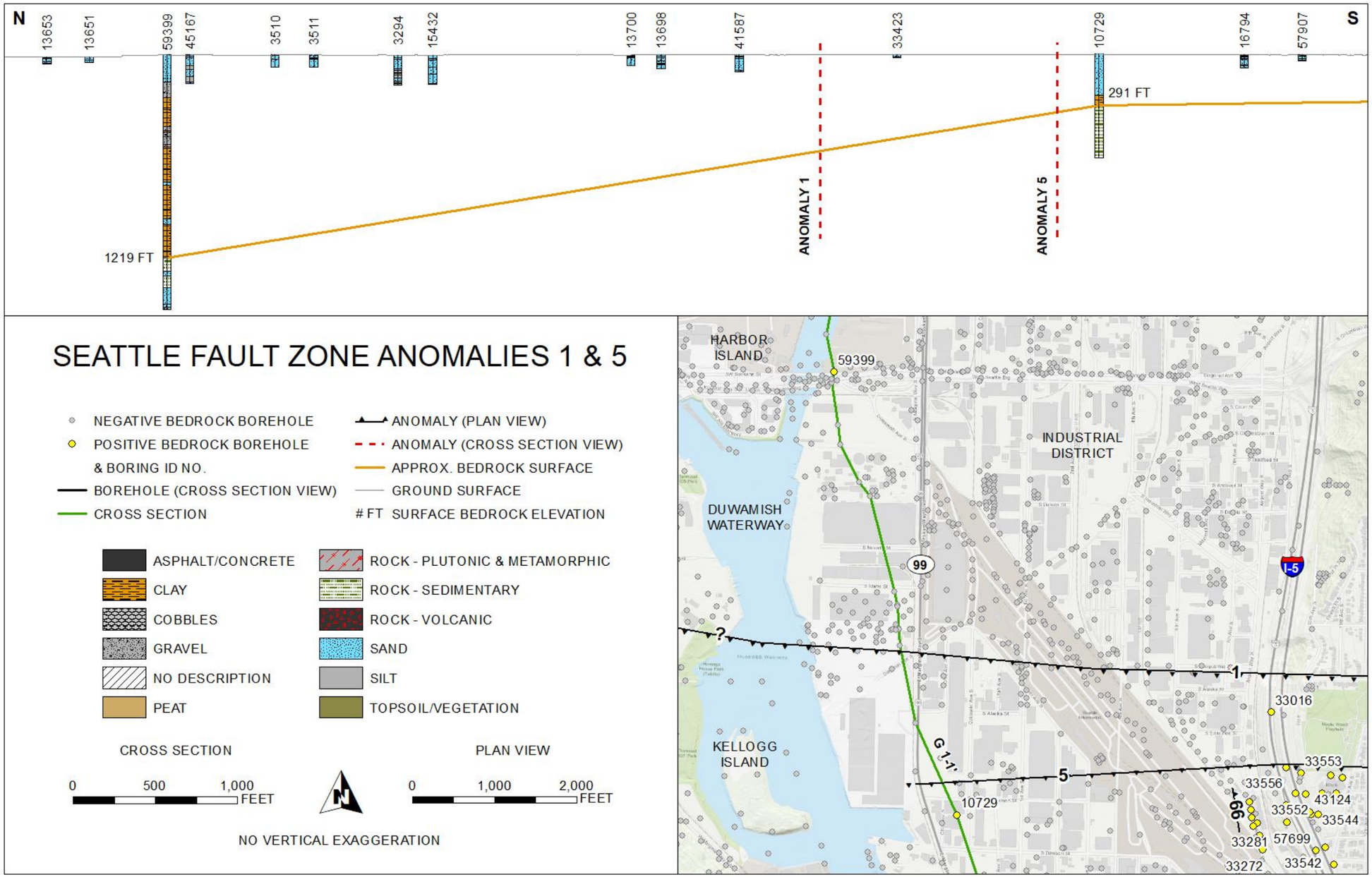

Figure 11: Seattle Fault Zone Anomalies 1 & 5. The greatest vertical offset in bedrock elevation was seen along cross section G1-1' with Anomaly 1 in the Duwamish waterway and Interstate 5. Borehole 59399 reached bedrock 1235 feet below the surface at an elevation of 1219 feet. The closest bedrock-positive borehole (10729) contained bedrock 928 feet above borehole 59399. The bedrock offset from exploration 59399 to 33016, located near Interstate 5, was 1212 vertical feet.

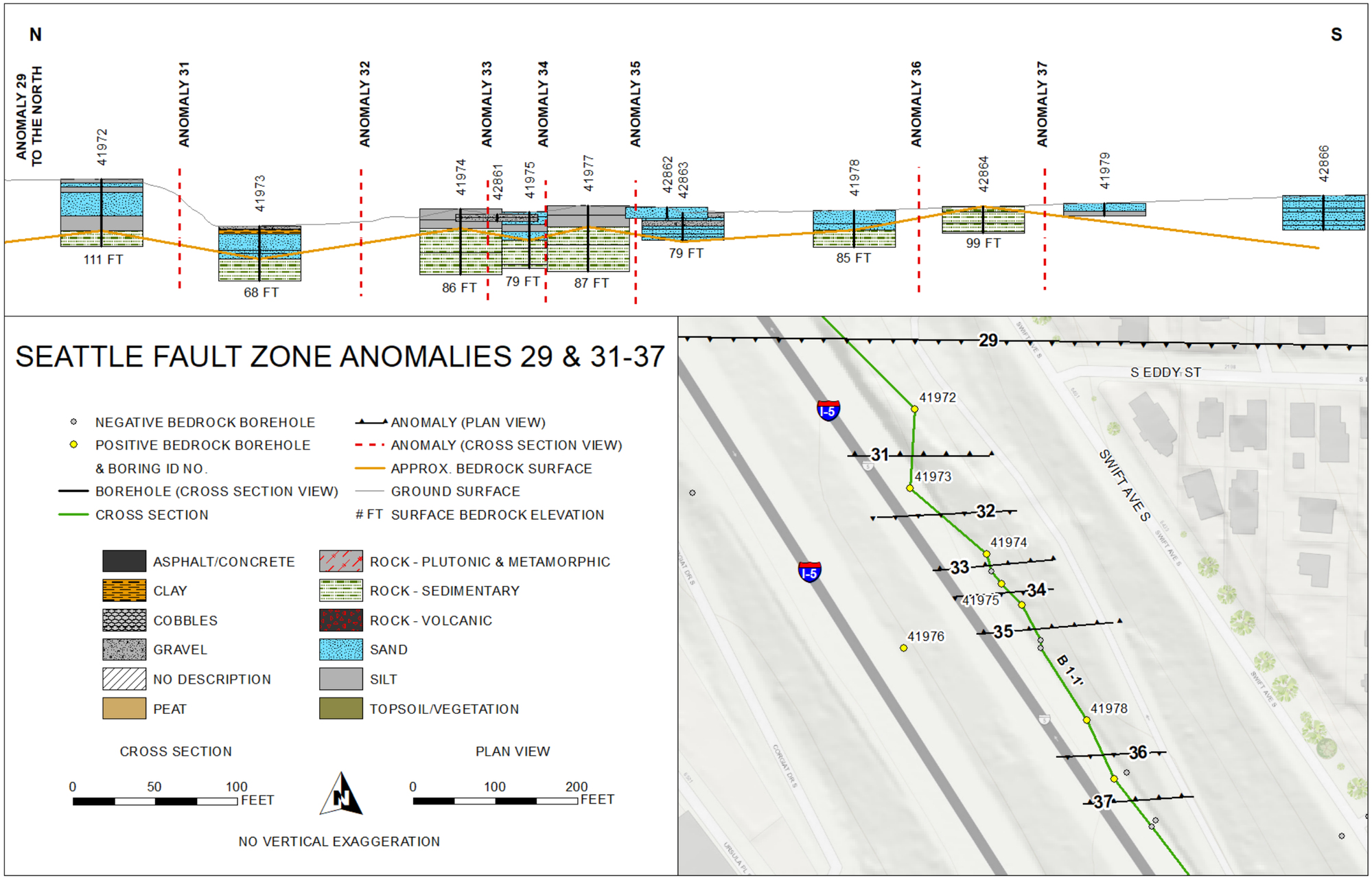

Figure 12: Seattle Fault Zone Anomalies 29 & 31-37. Eight anomalies were identified along 800 feet of Interstate 5, cross section B1-1', with vertical displacements in the bedrock surface ranging from 7 - 53 feet.

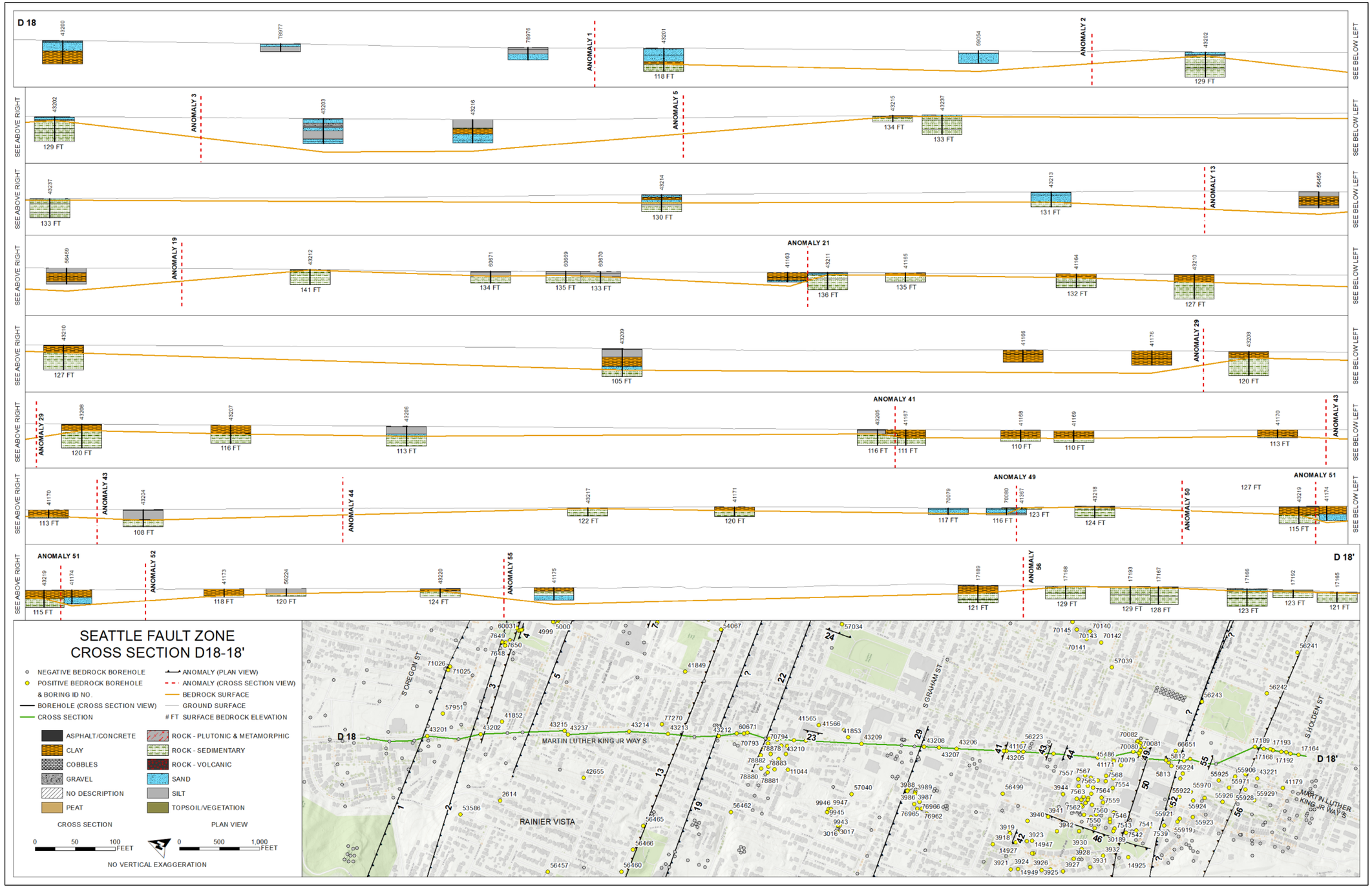

Figure 13: Seattle Fault Zone Cross Section D18-18'. Cross Section D18-18' was one of the longest cross sections. This one cross section highlighted 17 anomalies along Martin Luther King Jr. Way South in Rainier Vista.

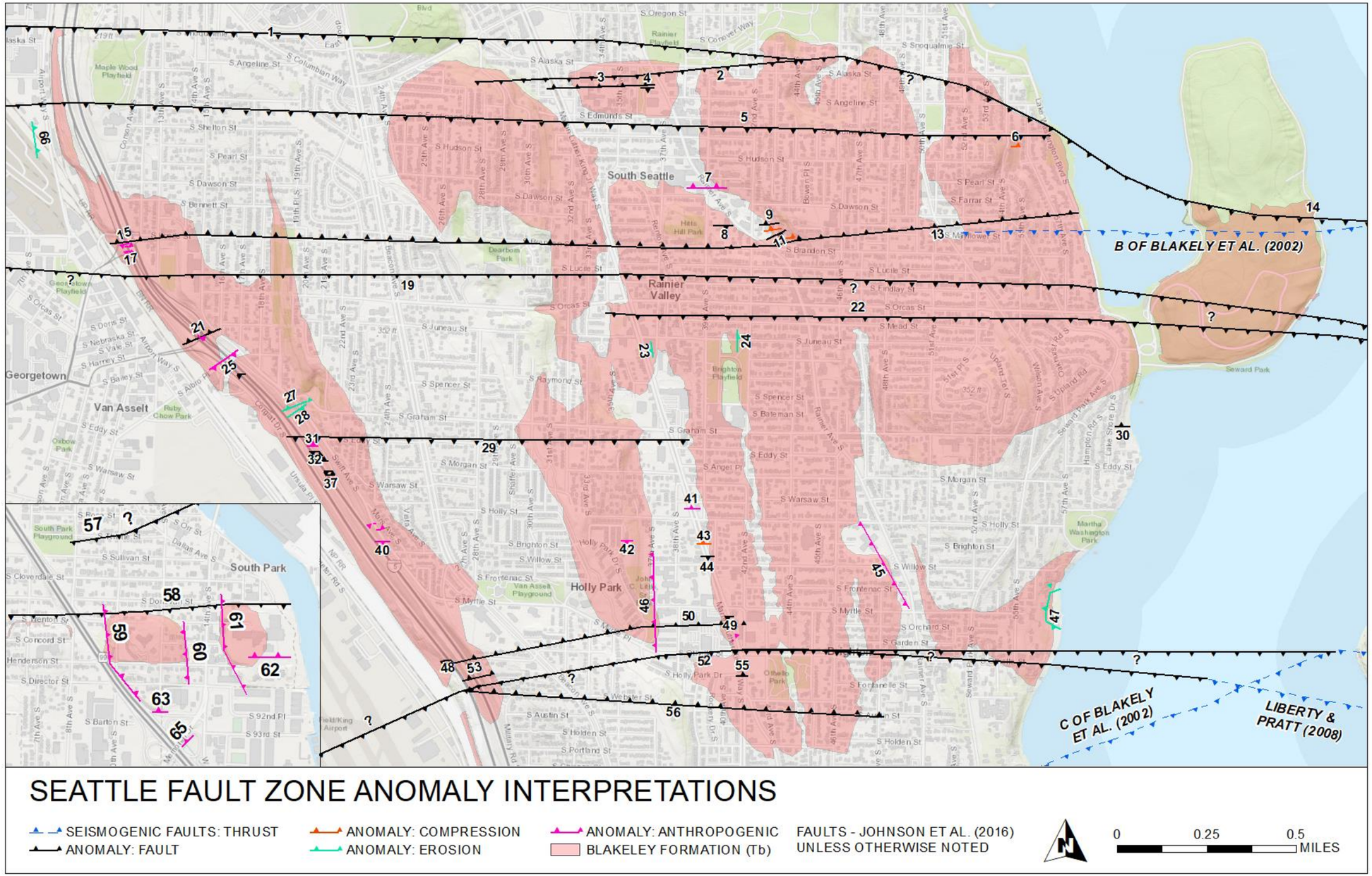

Figure 14: Seattle Fault Zone Anomaly Interpretation. The anomalies were interpreted as alterations caused by human influences (Anthropogenic), tectonic strain features (Compression), material removed by erosion (Erosion) or inferred faults (Fault).

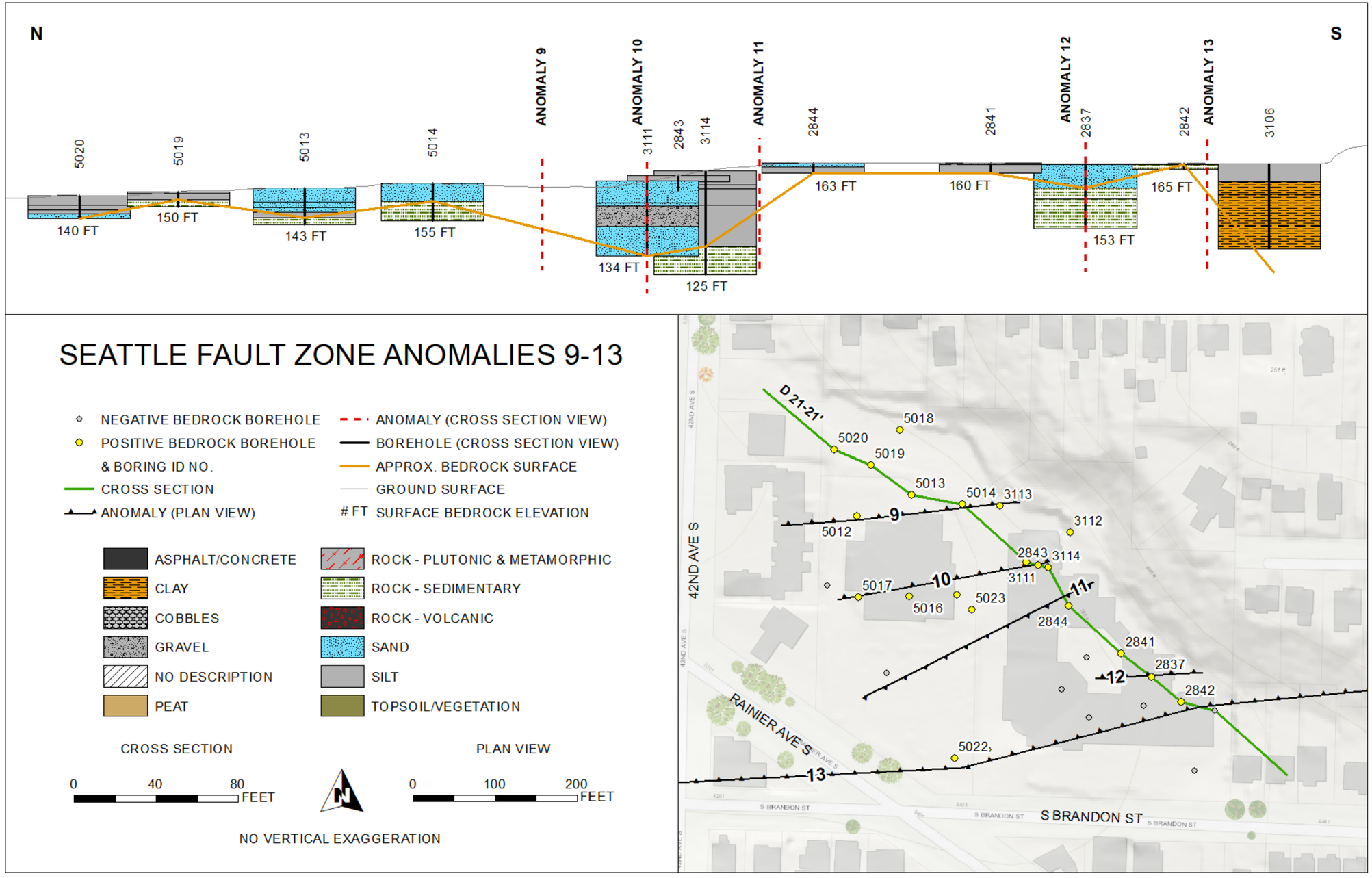

Figure 15: Seattle Fault Zone Anomalies 9-13. Anomalies 9 and 12 were inferred as compressional features bordering a larger fault-inferred anomaly, Anomaly 13, along cross section D21-21'.

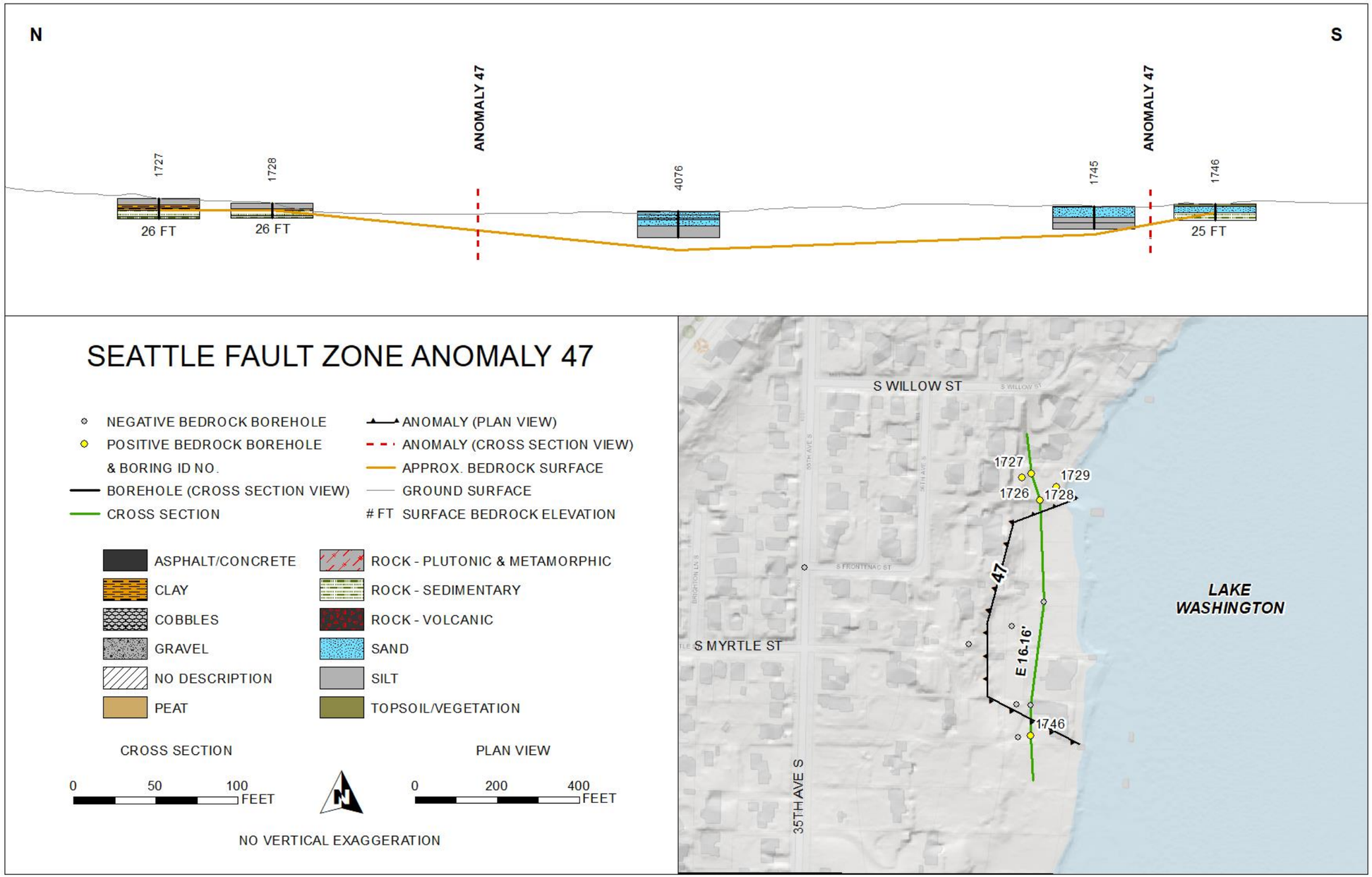

Figure 16: Seattle Fault Zone Anomaly 47. Anomaly 47 on cross section E16-16' appeared to follow a curved depression in the bedrock surface on the shore of Lake Washington. This anomaly was inferred as an erosional feature such as a potential slope failure where waves removed the toe of the slope.

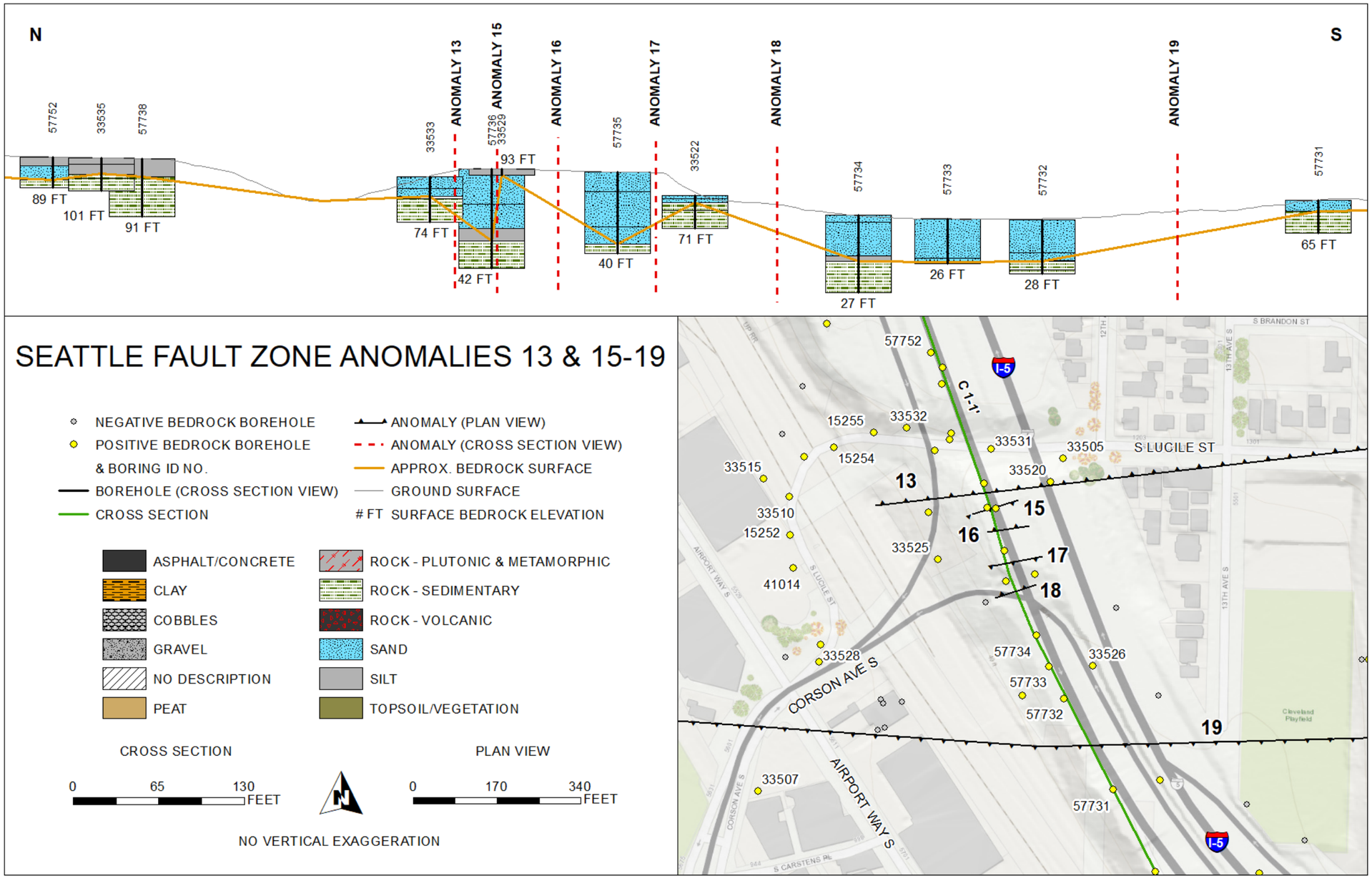

Figure 17: Seattle Fault Zone Cross Section C1-1’. Anomalies 13 and 15-19 are located along 550 feet of cross section C1-1’ on Interstate 5. Anomalies 13 and 19 are potentially fault offsets and extend laterally east. Anomalies 15-18 are suspected human alterations to the bedrock possibly from the construction of the on/off ramp to Interstate 5 or from a former ravine.

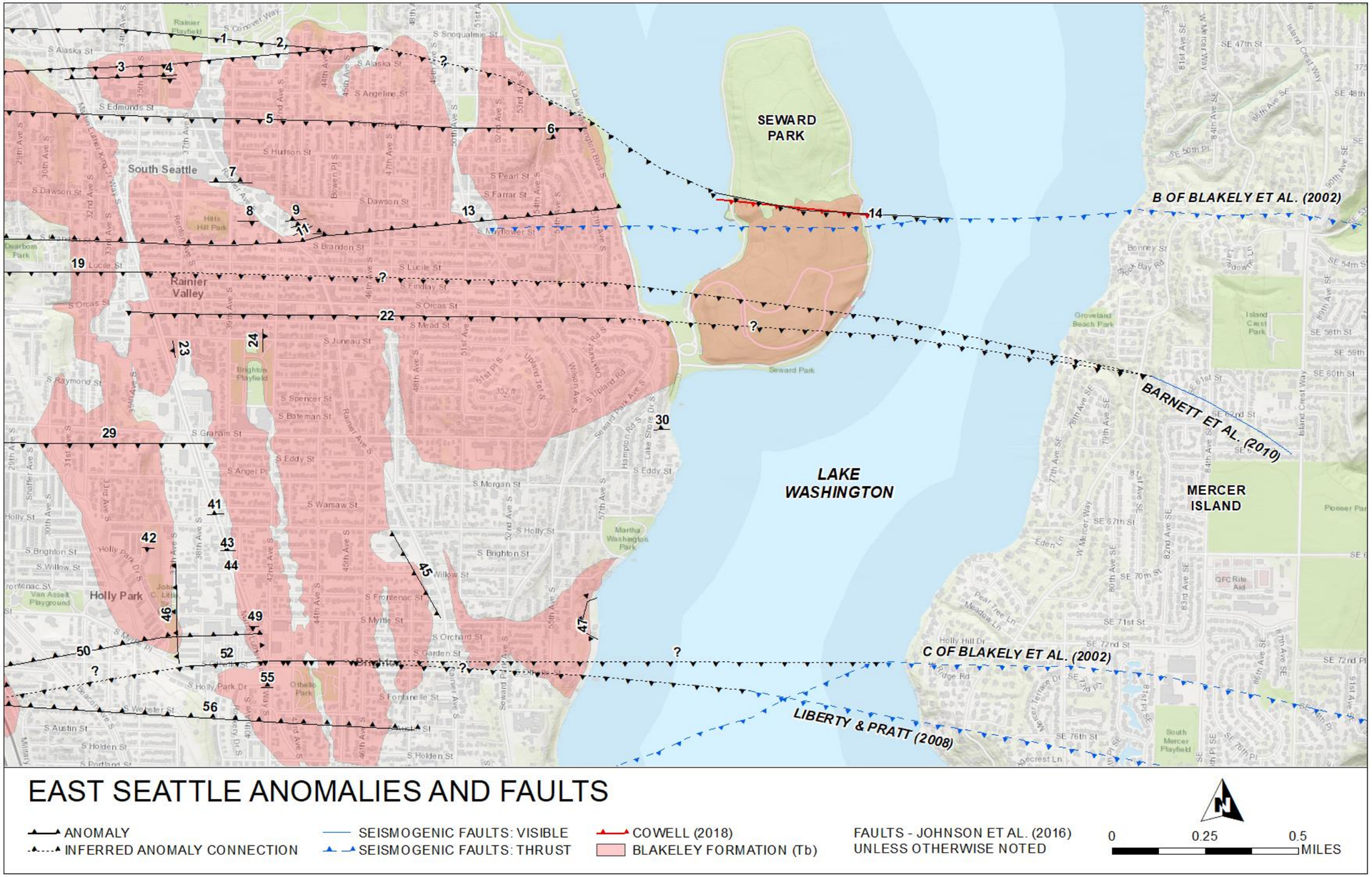

Figure 18: East Seattle Anomalies & Faults. Anomalies 14, 22, and 52 potentially connect to mapped fault strands on Mercer Island and within Lake Washington. These anomalies display the same sense of motion as the strands mapped by Blakely et al. (2002) and Liberty and Pratt (2008). Anomaly 14 overlapped Cowell's (2018) mapped anomaly in Seward Park.

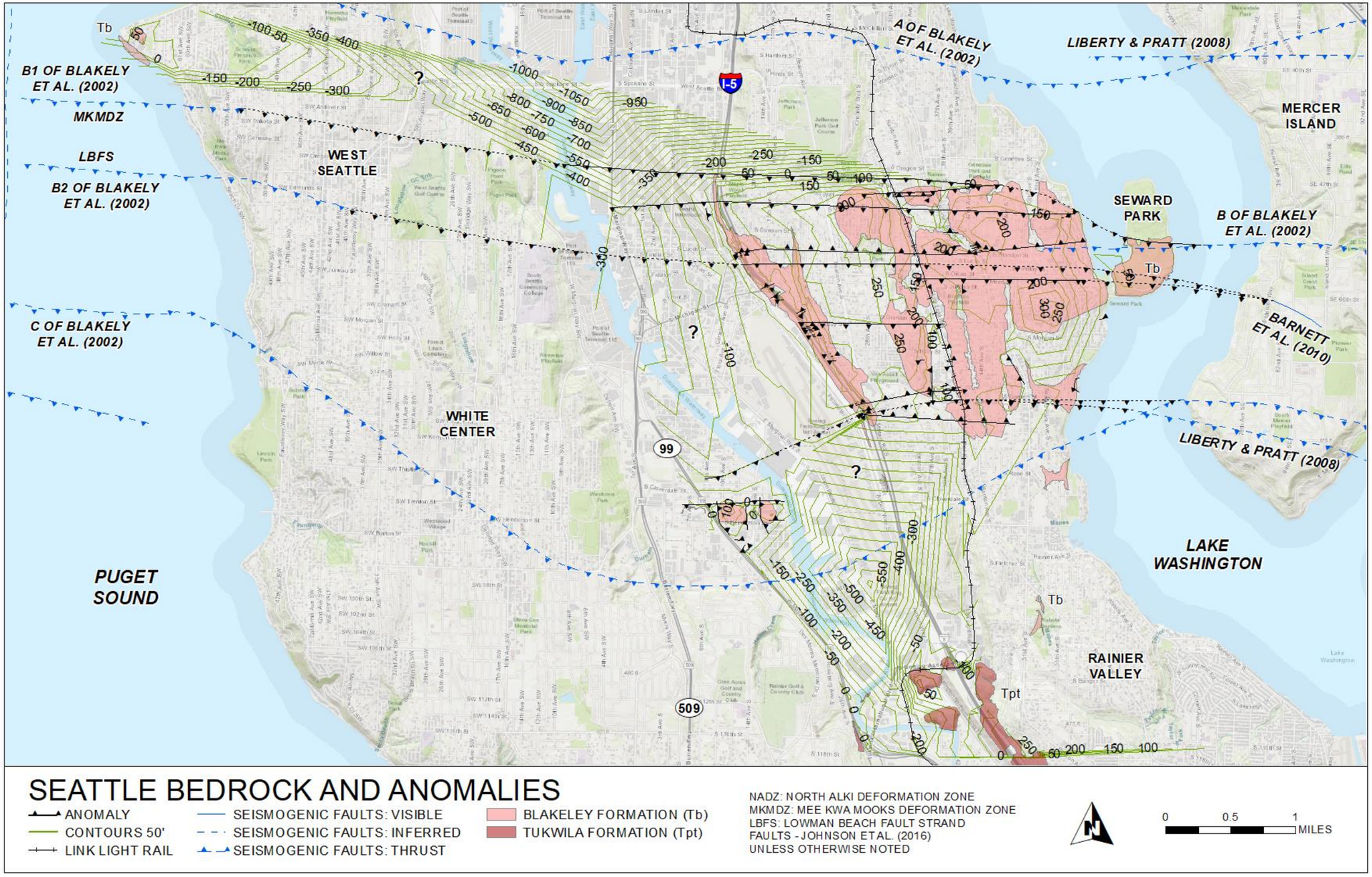

Figure 19: Seattle Bedrock and Anomalies. The bedrock surface contours were generated in AutoCAD Civil 3D using a triangulation method between boreholes containing bedrock and not containing bedrock in southeast Seattle. The contours are shown at a 50-foot interval.

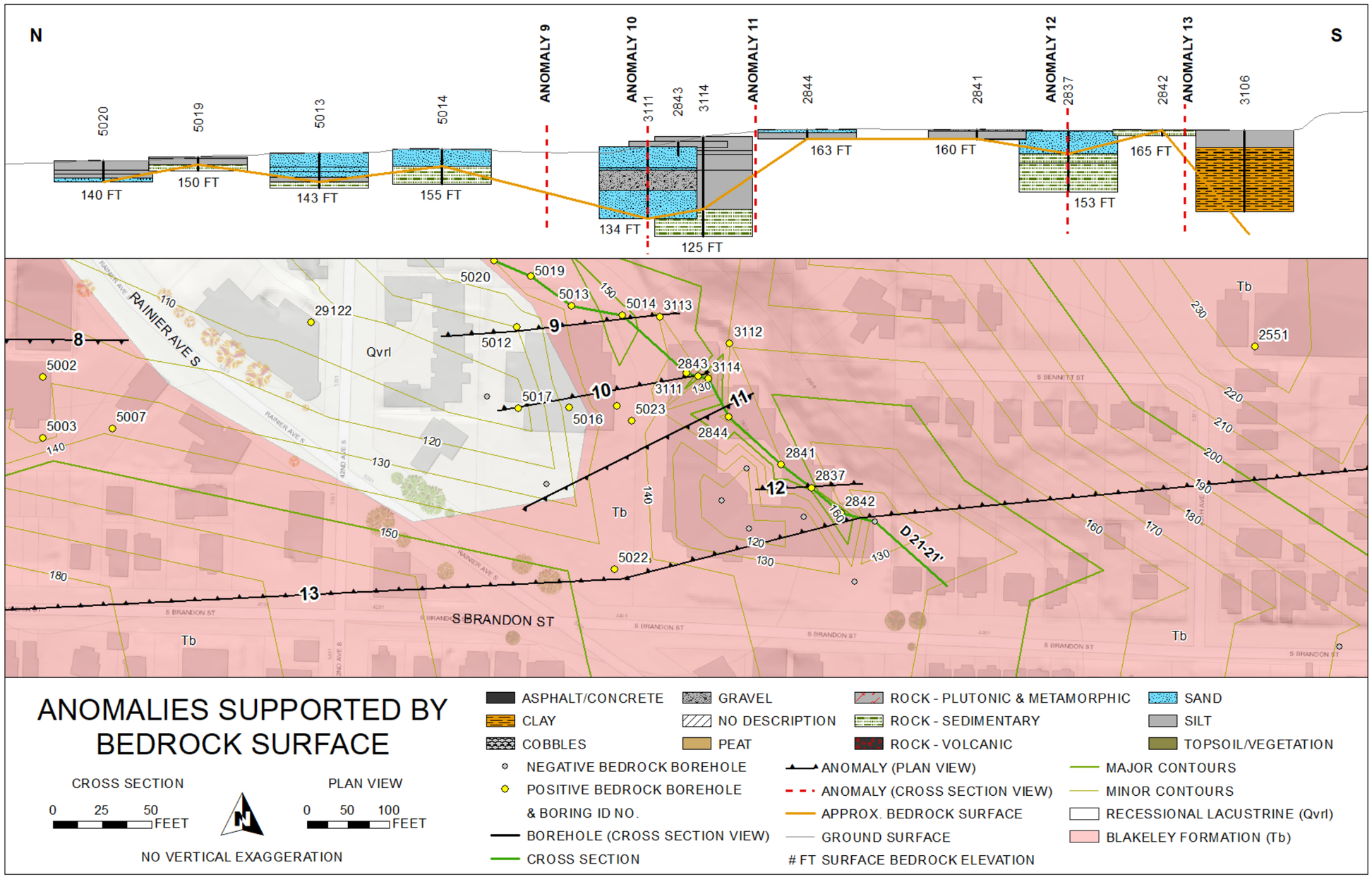

Figure 20: Anomalies Supported by Bedrock Surface Contours. The contours generated for the bedrock surface supported the location of anomalies by indicating changes in the surface elevation. For example, the contours north of Anomaly 13 show a change in slope as the contours become closer together.

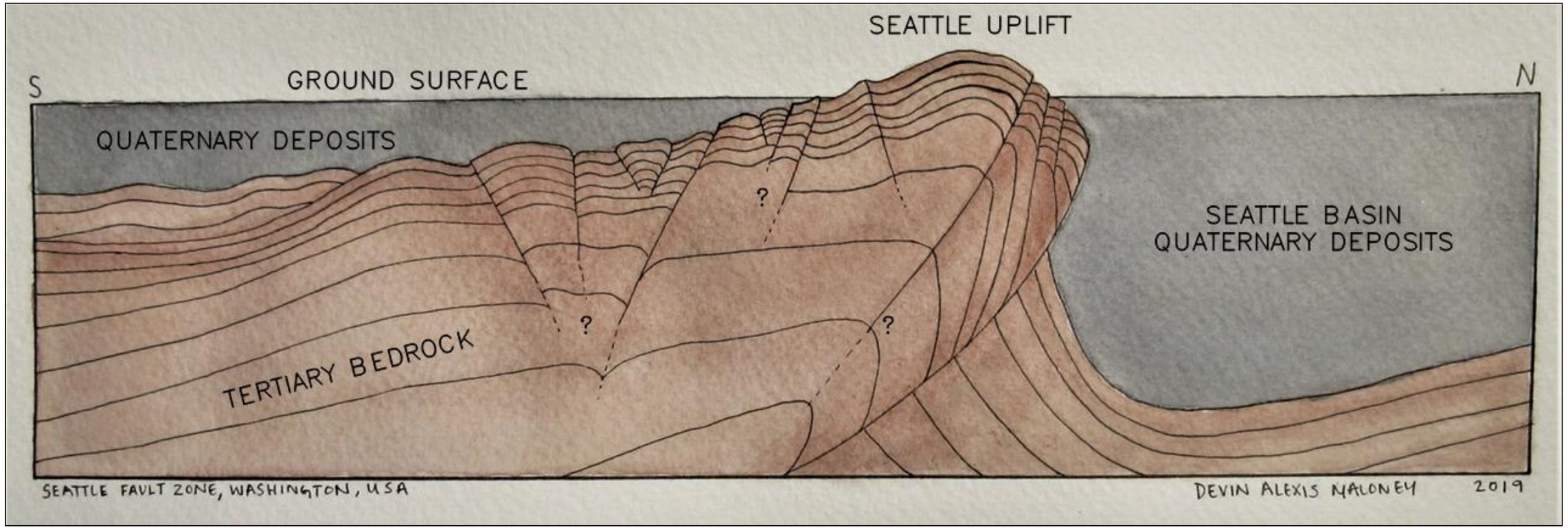

Figure 21: Seattle Fault Zone Conceptual Drawing. The general structure of the Seattle Fault Zone displays a stair-step decent into the Seattle basin with the frequency of faults increasing from south to north. Strain is distributed along numerous parallel faults increasing the complexity of the Seattle Fault Zone structure. Not to scale.

APPENDIX A: BEDROCK TERMS

Select by Attributes:
SUBSURF_LAYER_LAYER_DESC LIKE '%bedrock%'

Bedrock terms used for data processing:

Blakeley	Sedimentary	Limestone
blakeley	sedimentary	limestone
BLAKELEY	SEDIMENTARY	LIMESTONE
Blakely	Volcanic	Conglomerate
blakely	volcanic	conglomerate
BLAKELY	VOLCANIC	CONGLOMERATE
Formation	Sandstone	Fossil
formation	sandstone	fossil
FORMATION	SANDSTONE	FOSSIL
Bedrock	Siltstone	Fossiliferous
bedrock	siltstone	Igneous
BEDROCK	SILTSTONE	Andesite
Harbor	Mudstone	ANDESITE
harbor	mudstone	Basalt
HARBOR	MUDSTONE	Quartzite
Tertiary	Claystone	Volcaniclastic
tertiary	claystone	Tuff
TERTIARY	CLAYSTONE	tuff
Renton	Rock	TUFF
Shale	rock	
shale	ROCK	
SHALE		

APPENDIX B: CROSS SECTIONS

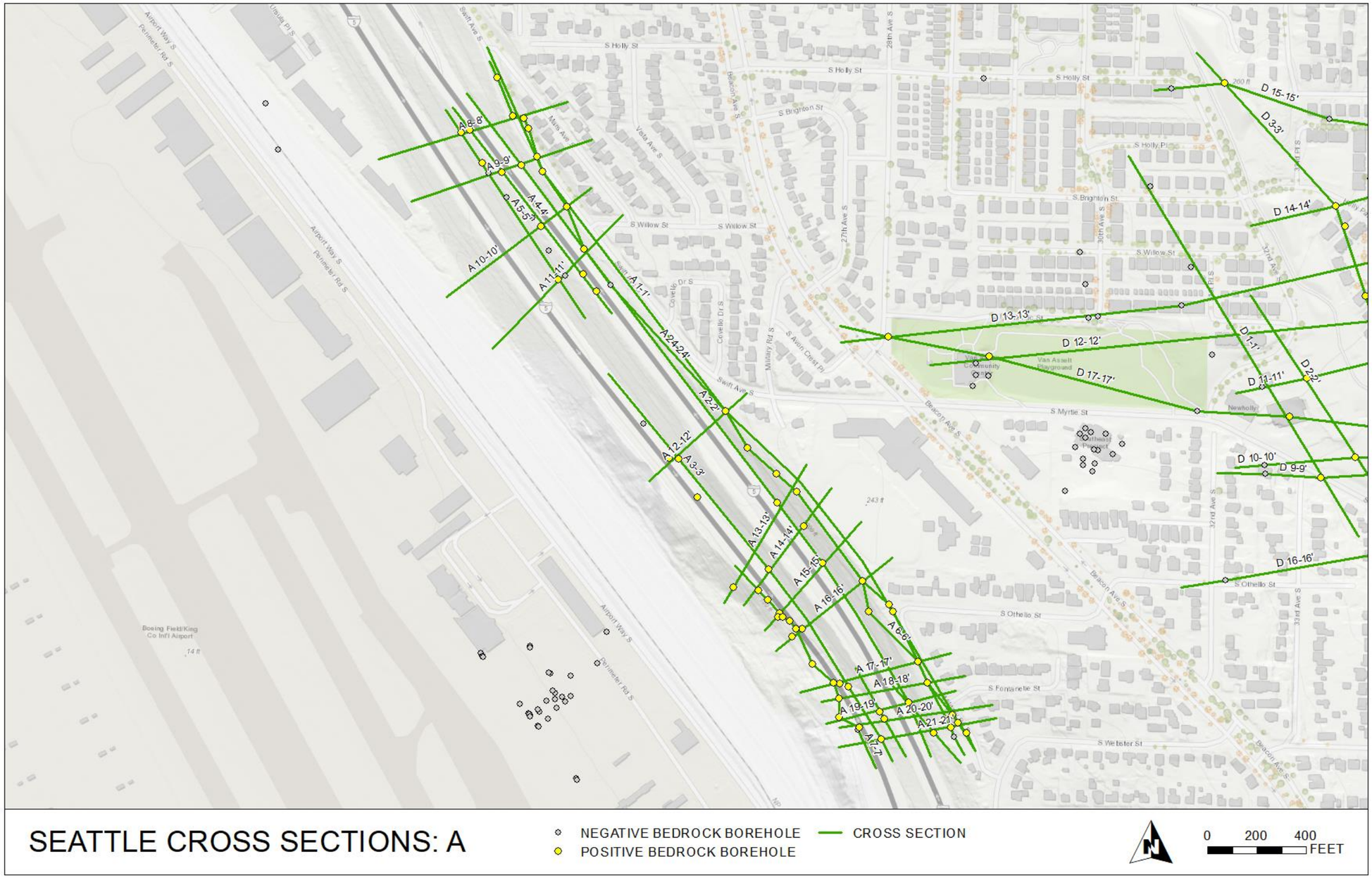

Seattle Cross Sections: A. Group A contains 24 cross sections on or near Interstate 5. See Figure 7.

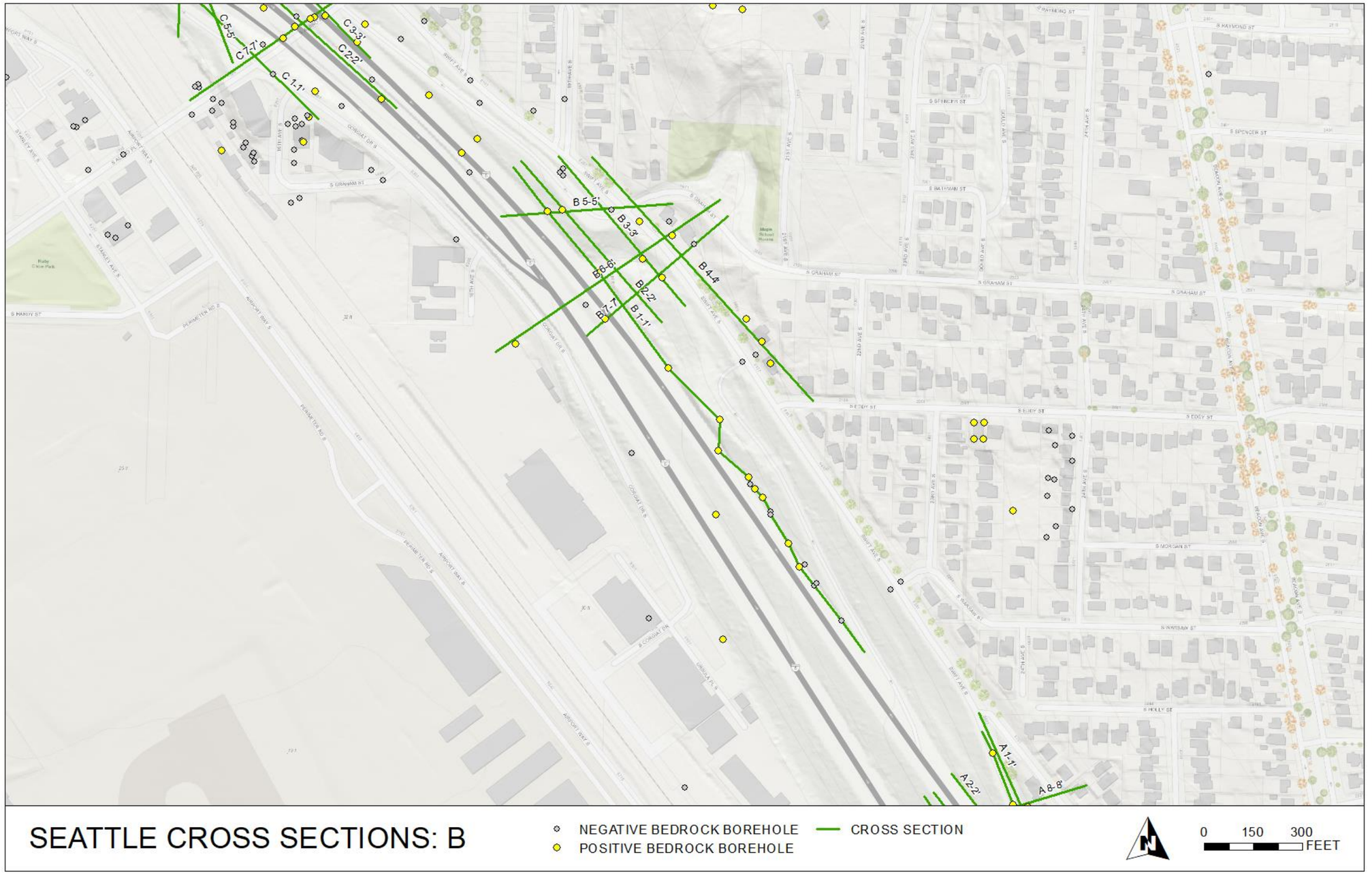

Seattle Cross Sections: B. Group B contains 7 cross sections on or near Interstate 5. See Figure 7.

Seattle Cross Sections: C. Group C contains 26 cross sections on or near Interstate 5. See Figure 7.

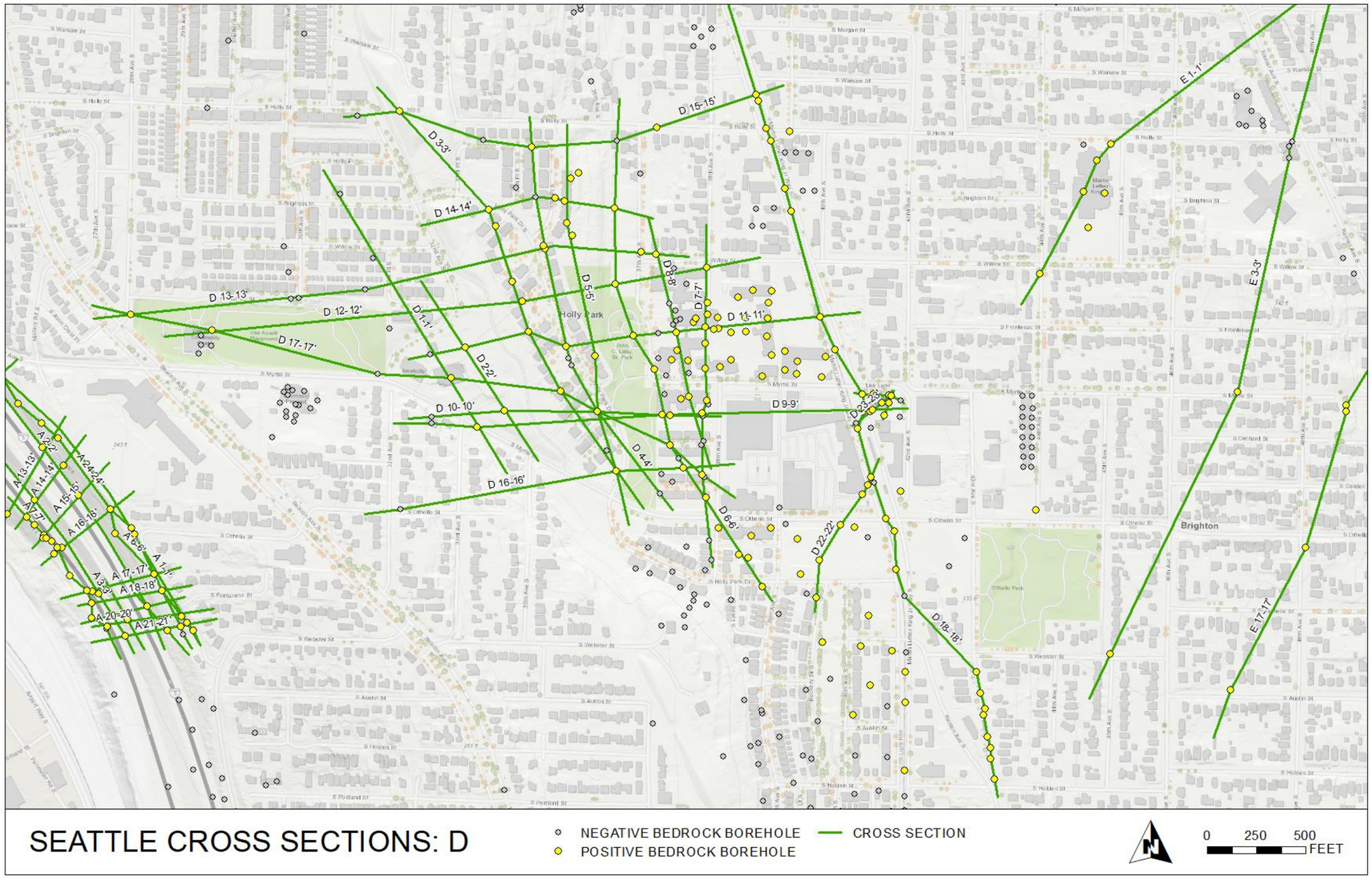

Seattle Cross Sections: D. Group D contains 25 cross sections in southeast Seattle. See Figure 7.

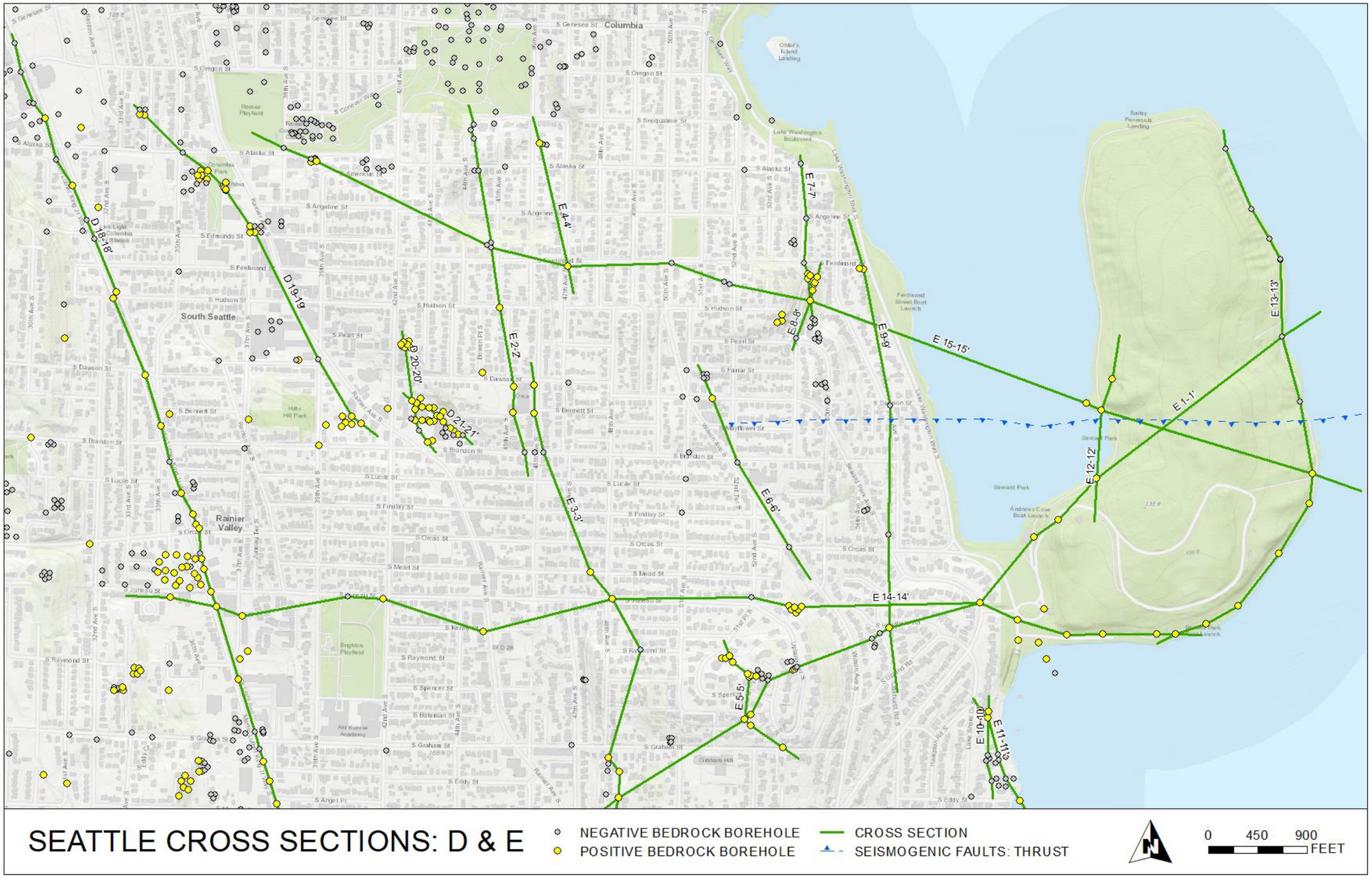

Seattle Cross Sections: D & E North. Group E contains 17 cross sections in southeast Seattle near Lake Washington. See Figure 7.

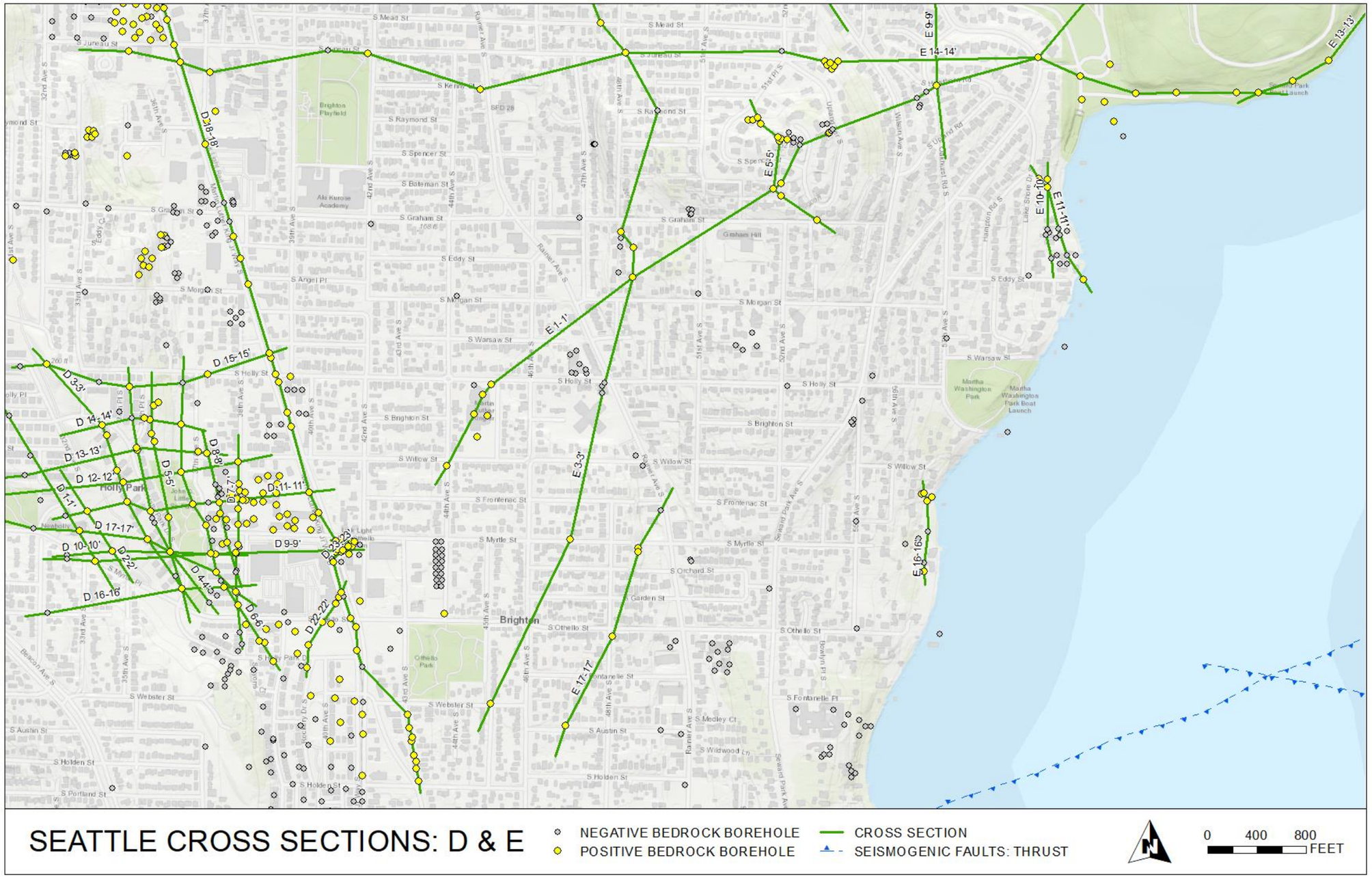

Seattle Cross Sections: D & E South. Group E contains 17 cross sections in southeast Seattle near Lake Washington. See Figure 7.

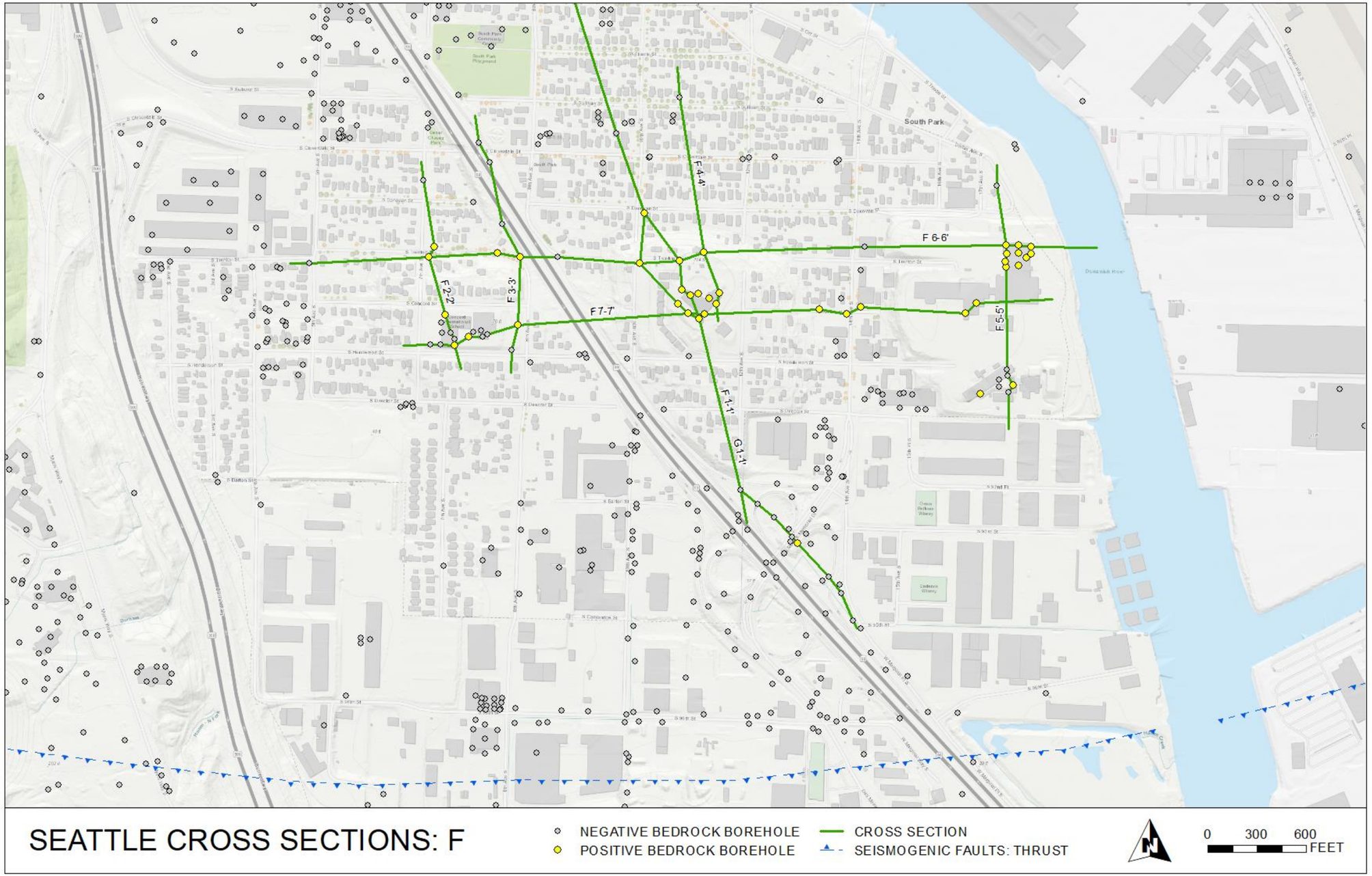

Seattle Cross Sections: F. Group F contains 7 cross sections in south Seattle on the west side of the Duwamish waterway. See Figure 7.

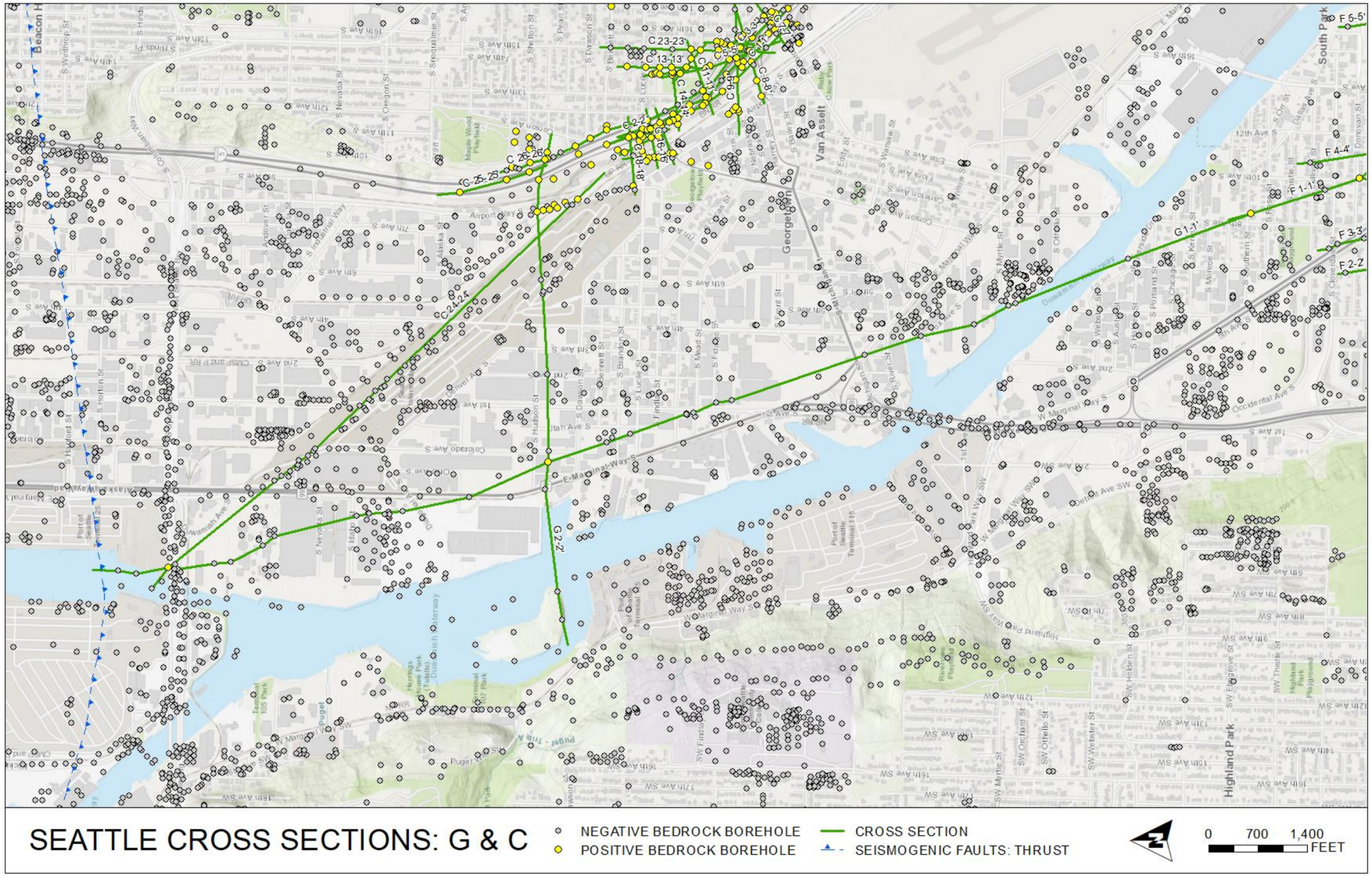

Seattle Cross Sections: G & C. Group G contains 2 cross sections within the Duwamish valley. See Figure 7.

APPENDIX C: ANOMALIES

SEATTLE FAULT ZONE ANOMALIES MALONEY, D.A., 2019			SUBSURFACE GEOLOGIC UNITS ASPHALT/CONCRETE, CLAY, COBBLES, GRAVEL, NO DESCRIPTION, PEAT, ROCK - PLUTONIC & METAMORPHIC, ROCK - SEDIMENTARY, ROCK - VOLCANIC, SAND, SILT, TOPSOIL/VEGETATION						
ANOMALY	ANOMALY CATEGORY	OFFSET DIRECTION	EXPLORATION ID		BEDROCK ELEVATION (FEET)		BEDROCK OFFSET (FEET) VERTICAL	HORIZONTAL	SLOPE (DEGREES)	CROSS SECTION
1	FAULT	DOWN TO NORTH	59399	10729	-1219.0	-291.1	927.94	5595.98	9.42	G 1-1'
1	FAULT	DOWN TO NORTH	59399	33272	-1219.0	-6.9	1212.11	7818.52	8.81	C 24-24'
1	FAULT	DOWN TO NORTH	33016	-	49.31	-	-	-	-	C 25-25'. NO BEDROCK NORTH OF CROSS SECTION.

1	FAULT	DOWN TO NORTH	43201	-	118.10	-	-	-	-	D 18-18'. NO BEDROCK NORTH OF CROSS SECTION.
			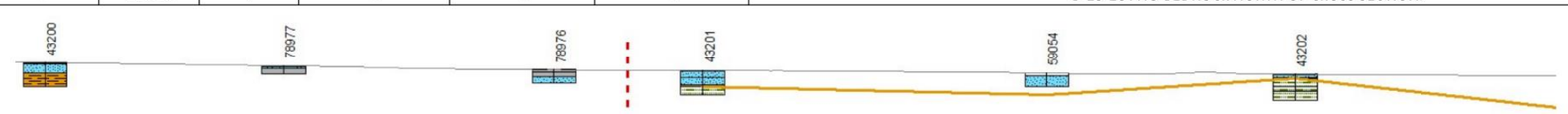							
1	FAULT	DOWN TO NORTH	71025	-	120.78	-	-	-	-	D 19-19'. NO BEDROCK NORTH OF CROSS SECTION.
										
1	FAULT	DOWN TO NORTH	-	-	-	-	-	-	-	E 2-2'. NO BEDROCK NORTH OF 56445. ANOMALY 2 MAY PASS BETWEEN 14464 AND 29143 CONNECTING TO THE EASTERN ANOMALY.
										
1	FAULT	DOWN TO NORTH	-	59516	-	61.12	-	-	-	E 4-4'. NO BEDROCK NORTH OF CROSS SECTION.
										
2	FAULT	DOWN TO NORTH	59054	43202	118.8	128.6	9.8	283.0	1.98	D 18-18'
										
2	FAULT	DOWN TO NORTH	71025	7646	120.78	85.16	35.63	763.68	2.67	D 19-19'. POTENTIAL COMPRESSION PUSHING BEDROCK UP JUST SOUTH OF 71025 BEFORE ANOMALY 1 CROSSES.
										

2	FAULT	DOWN TO NORTH	56217	2573	17.28	56.64	39.36	303.78	7.38	E 15-15'
			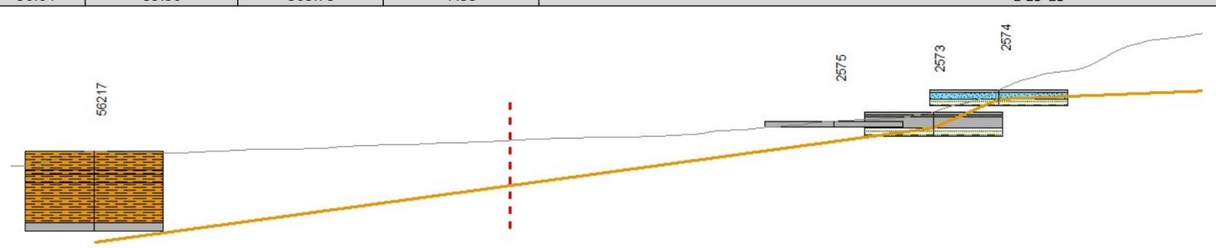							
3	FAULT OR SLOPE	UP TO NORTH	43202	43203	128.6	99.3	29.26	336.0	4.98	D 18-18'
			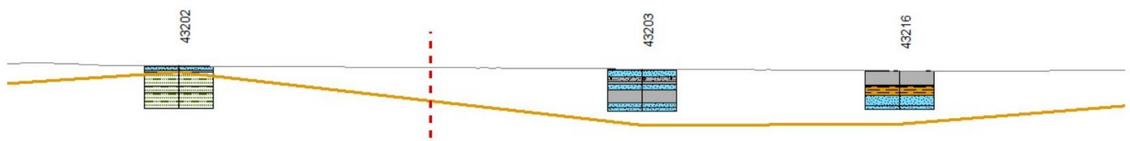							
		UP TO NORTH	7646	60027	85.2	62.2	22.99	203.0	6.46	D 19-19'
			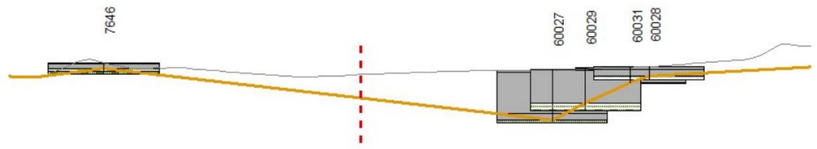							
4	FAULT OR SLOPE	DOWN TO NORTH	60027	60028	62.20	82.43	20.23	43.50	24.94	D 19-19'
			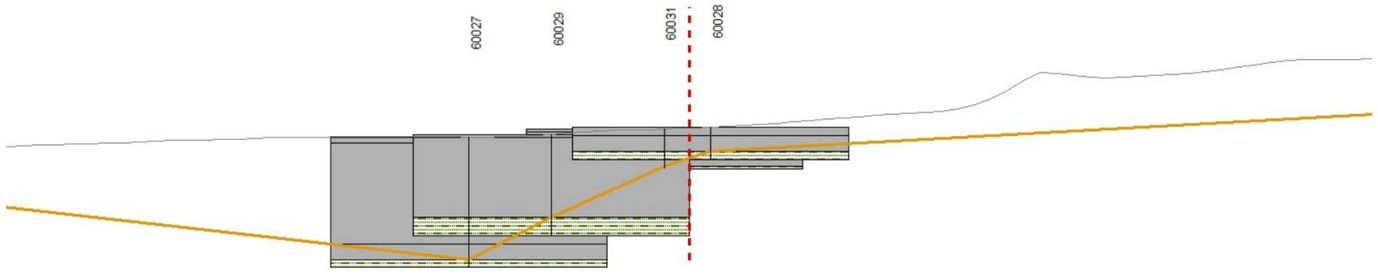							
5	FAULT	DOWN TO NORTH	59399	10729	-1219.02	-291.08	927.94	5595.98	9.42	G 1-1'. LACK OF DATA TO CONFIRM OR DENY ANOMALY 5 CROSSES G 1-1'.
			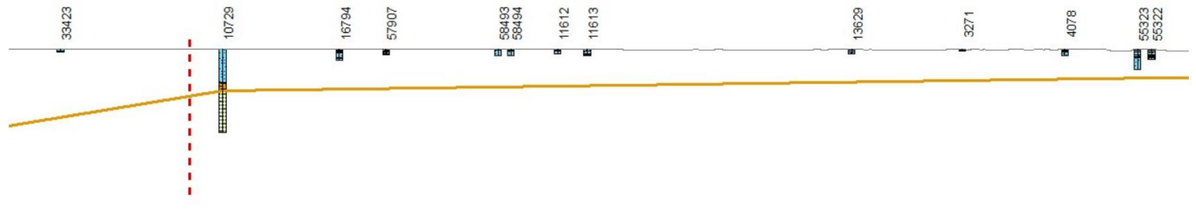							

5	FAULT	DOWN TO NORTH	-	33272	-	-6.91	-	-	-	C 24-24'. LACK OF DATA TO CONFIRM OR DENY ANOMALY 5 CROSSES C 24-24'.
			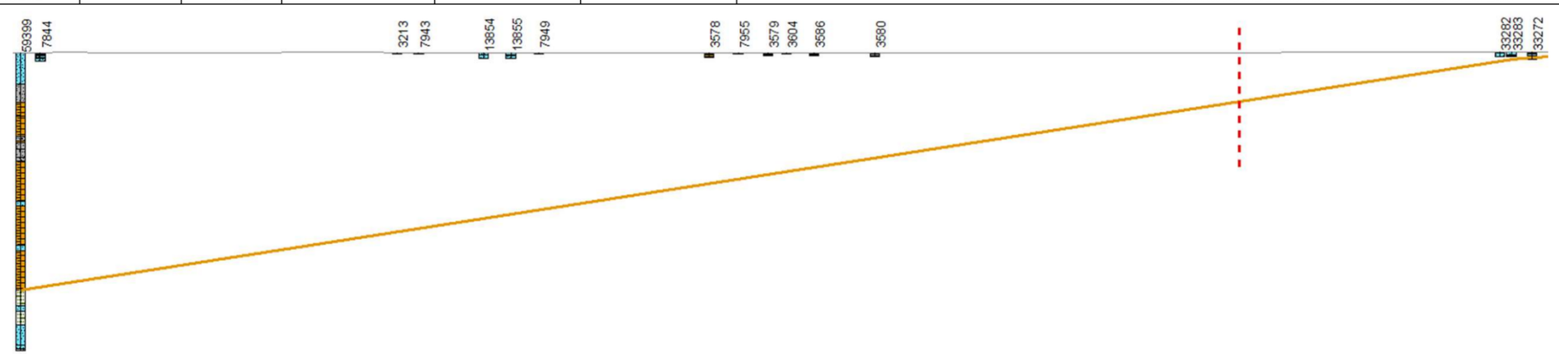						
5	FAULT	DOWN TO NORTH	33016	33559	49.31	131.37	82.06	695.98	6.72	C 25-25'
										
5	FAULT	DOWN TO NORTH	43216	43215	100.54	133.64	33.10	525.35	3.60	D 18-18'
			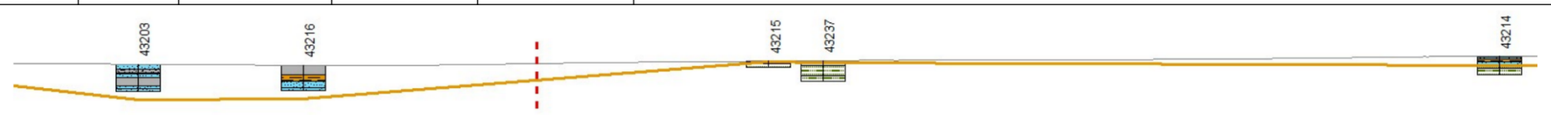							
5	FAULT	-	4998	56219	106.39	83.29	23.10	1290.97	1.03	D 19-19'. LACK OF DATA TO CONFIRM OR DENY ANOMALY 5 CROSSES D 19-19'.
			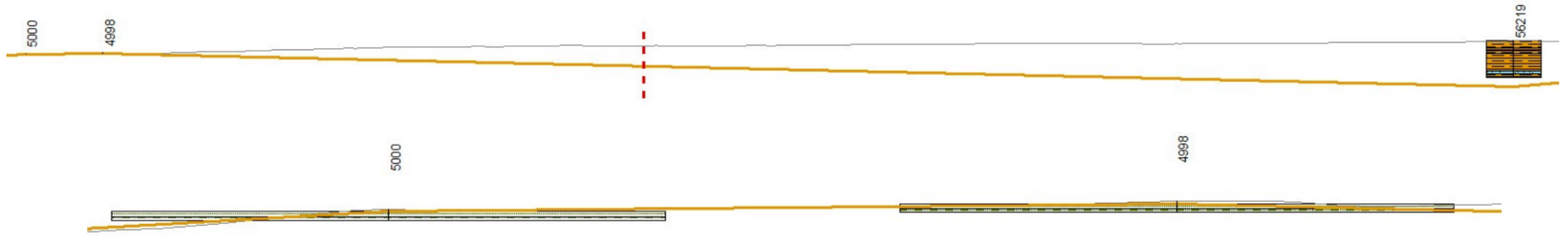							

5	FAULT	DOWN TO NORTH	3375	56445	192.64	223.17	30.53	553.70	3.16	E 2-2'
										
5	FAULT	DOWN TO NORTH	59516	56443	61.12	171.55	110.43	1148.26	5.49	E 4-4'. LACK OF DATA TO CONFIRM OR DENY ANOMALY 5 CROSSES E 4-4'. POSSIBLE EROSION OR FAULT DISPLACEMENT DROPPED BEDROCK ELEVATION TO THE NORTH.
										
5	FAULT	DOWN TO NORTH	2574	56443	67.49	171.55	104.05	2482.03	2.40	E 15-15'. ANOMALY 5 CROSSES E 15-15' TWICE (WEST AND EAST OF 56443).
			56443	55442	171.55	88.21	83.34	2235.50	2.14	
										
5	FAULT	DOWN TO NORTH	56207	1859	92.02	122.10	30.08	102.74	16.32	E 7-7'
			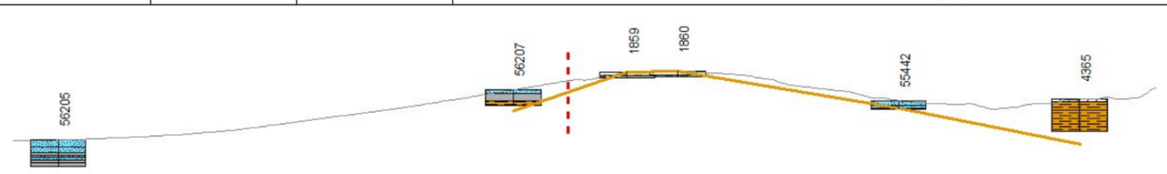							
5	FAULT	DOWN TO NORTH	-	1864	-	72.24	-	-	-	E 8-8'
			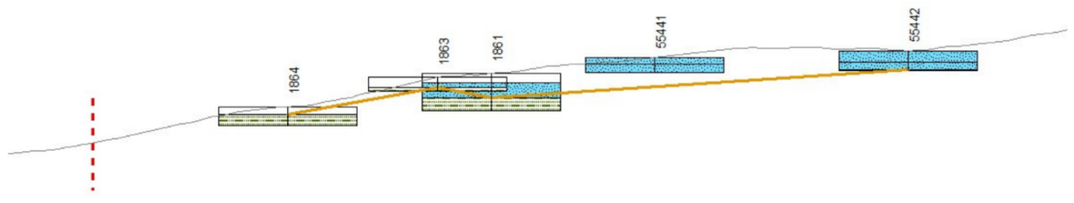							

5	FAULT	DOWN TO NORTH	-	29340	-	45.73	-	-	-	E 9-9'
			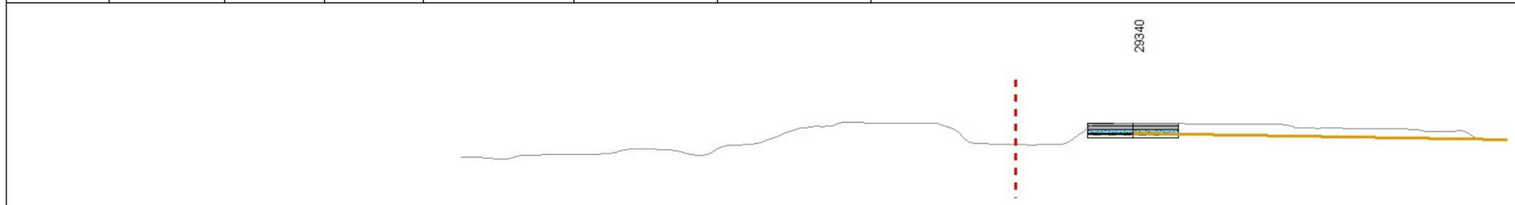						
6	COMPRESSION FOLD	UP TO NORTH	1863	1861	82.62	77.67	4.94	19.42	14.28	E 8-8'. POTENTIAL COMPRESSION FEATURE SOUTH OF ANOMALY 5.
			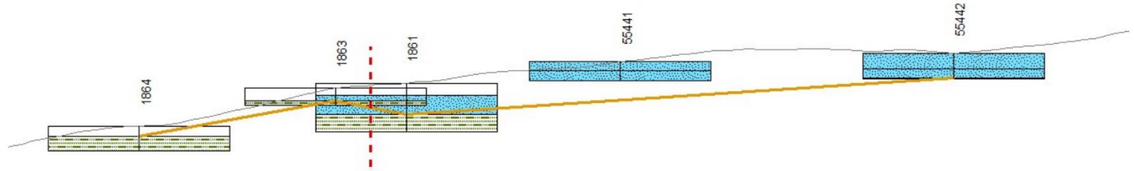						
7	ANTHROPOGENIC ALTERATION	UP TO NORTH	4998	56219	106.39	83.29	23.10	1290.97	1.03	D 19-19'. POSSIBLE ANTHROPOGENIC ROAD GRADE SOUTH OF ANOMALY 5.
									
8	FAULT	DOWN TO NORTH	56219	5002	83.29	128.74	45.46	601.89	4.32	D 19-19'
									
9	FAULT	UP TO NORTH	5012	5017	119.93	104.12	15.81	99.52	9.03	D 20-20'
									
9	FAULT	UP TO NORTH	5014	3111	155.31	134.36	20.95	104.61	11.32	D 21-21'
			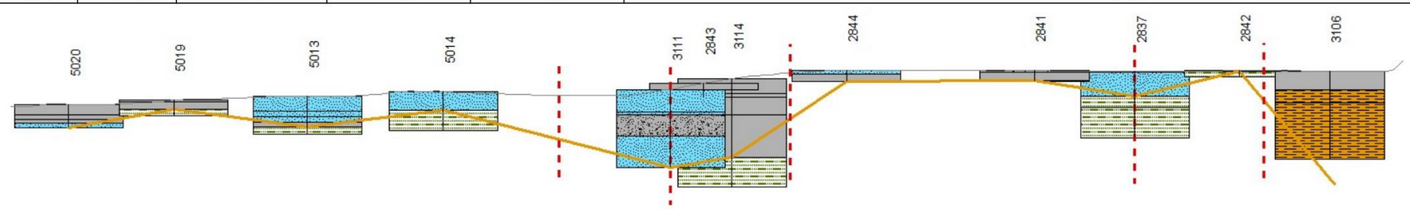						

10	COMPRESSION FOLD	UP TO NORTH	5012	5017	119.93	104.12	15.81	99.52	9.03	D 20-20'. POTENTIAL SYNCLINE FROM COMPRESSION BELOW 5017.
			5017	5022	104.12	146.97	42.85	227.92	10.65	
			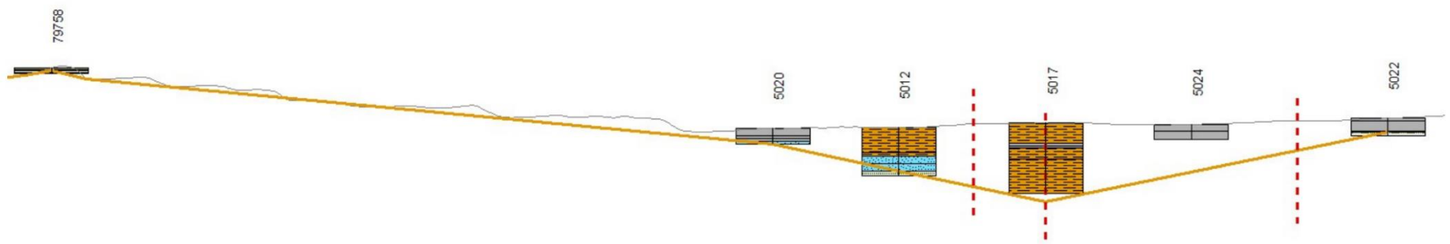							
10	COMPRESSION FOLD	UP TO NORTH	5014	3111	155.31	134.36	20.95	104.61	11.32	D 21-21'. POTENTIAL SYNCLINE NEAR 3111 FROM COMPRESSION.
			3114	2844	124.62	163.34	38.72	13.05	71.37	
			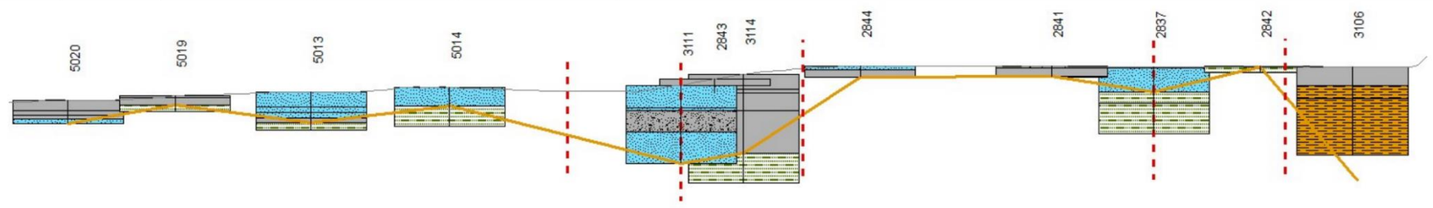							
11	FAULT	DOWN TO NORTH	5017	5022	104.12	146.97	42.85	227.92	10.65	D 20-20'
			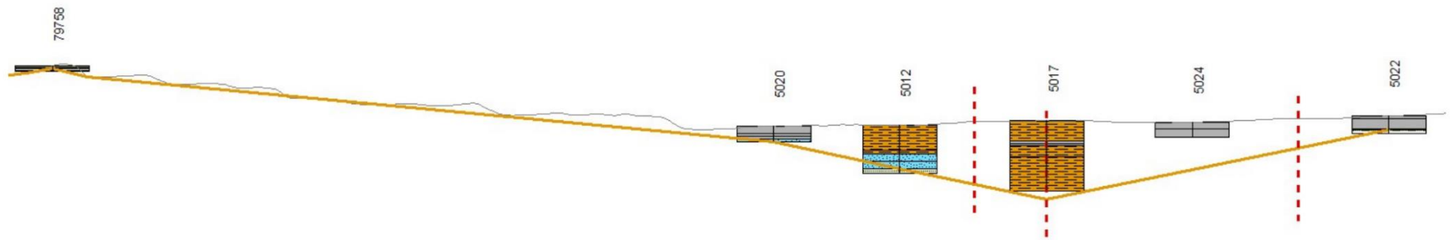							
11	FAULT	DOWN TO NORTH	3114	2844	124.62	163.34	38.72	13.05	71.37	D 21-21'
			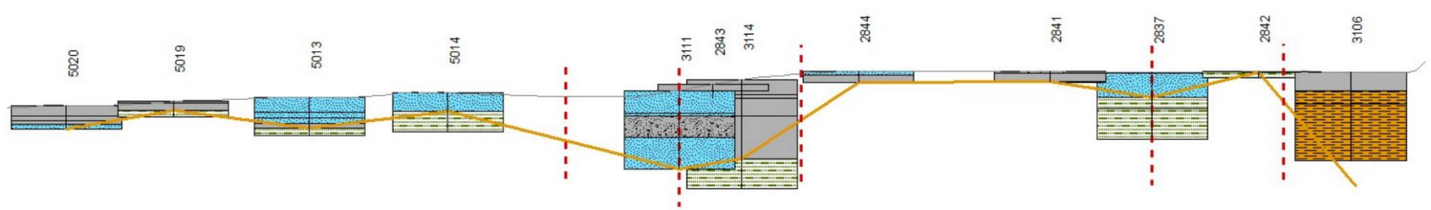							

12	COMPRESSION FOLD	UP TO NORTH	2841	2837	160.3045	152.7807	7.5238	46.2038	9.25	D 21-21'. POTENTIAL SYNCLINE FROM COMPRESSION.
			2837	2842	152.7807	164.50	11.72	47.96	13.73	
			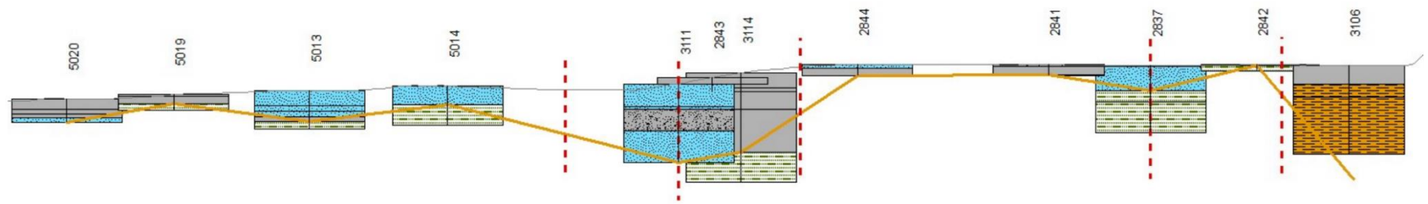							
13	FAULT	UP TO NORTH	33533	57736	76.43	41.94	34.49	48.28	35.54	C 1-1'. POSSIBLE ANTHROPOGENIC ROAD GRADE OR FAULT. NO NEIGHBORING CROSS SECTION TO VERIFY LATERAL ANOMALIES.
			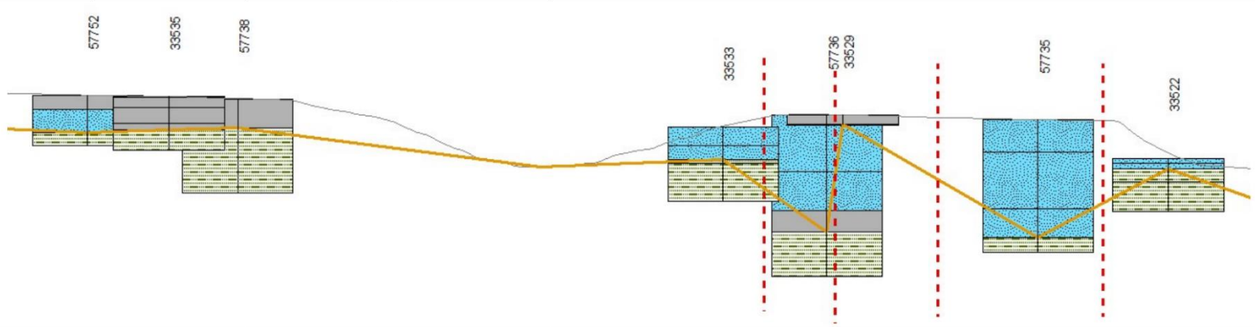							
13	FAULT	UP TO NORTH	46777	46568	162.08	132.26	29.82	257.10	6.62	C 13-13'
			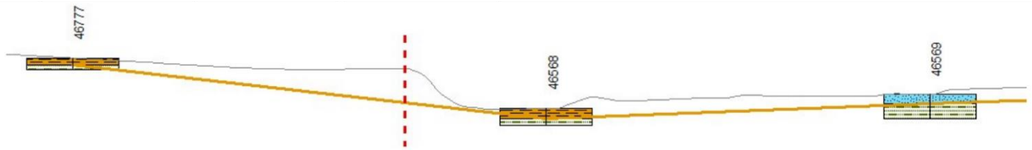							
13	FAULT	UP TO NORTH	43213	56459	131.03	123.96	7.07	334.09	1.21	D 18-18'
										
13	FAULT	UP TO NORTH	5022	-	146.97	-	-	-	-	D 20-20'. NO BEDROCK SOUTH OF 5022.
			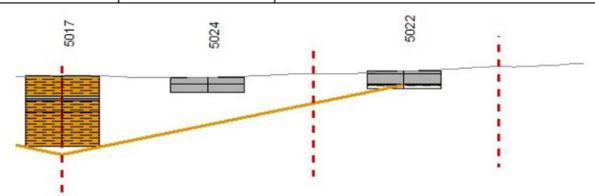							

13	FAULT	UP TO NORTH	2842	3106	164.50	123.34	41.16	41.74	44.60	D 21-21'
			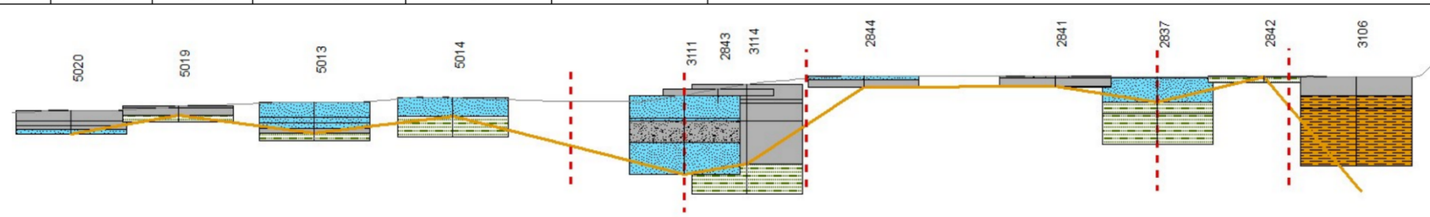							
13	FAULT	UP TO NORTH	2551	56260	236.45	195.09	41.36	380.01	6.21	E 2-2'
										
13	FAULT	UP TO NORTH	2554	56259	218.43	193.87	24.56	371.13	3.79	E 3-3'
										
13	FAULT	UP TO NORTH	14660	-	180.39	-	-	-	-	E 6-6'
										
13	FAULT	UP TO NORTH	29340	56211	45.73	26.43	19.30	1260.45	0.88	E 9-9'
										
14	FAULT	DOWN TO NORTH	-	100012	-	35.64	-	-	-	E 12-12'. NO BEDROCK NORTH OF 100012.
										
14	FAULT	DOWN TO NORTH	-	17403	-	26.47	-	-	-	E 13-13'
										

15	ANTHROPOGENIC ALTERATION	DOWN TO NORTH	57736	33529	41.94	92.56	50.62	18.49	69.93	C 1-1'. POSSIBLE ANTHROPOGENIC ROAD GRADE OR FAULT. NO NEIGHBORING CROSS SECTION TO VERIFY LATERAL ANOMALIES.
			33529	57735	92.56	39.78	52.78	88.44	30.83	C 1-1'. POSSIBLE ANTHROPOGENIC ROAD GRADE OR FAULT. NO NEIGHBORING CROSS SECTION TO VERIFY LATERAL ANOMALIES.
16	ANTHROPOGENIC ALTERATION	UP TO NORTH								

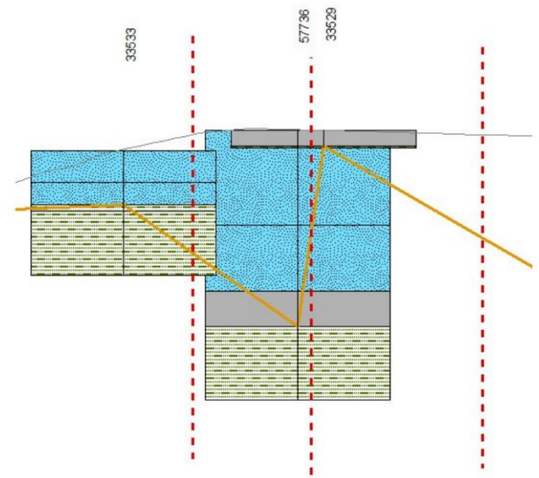

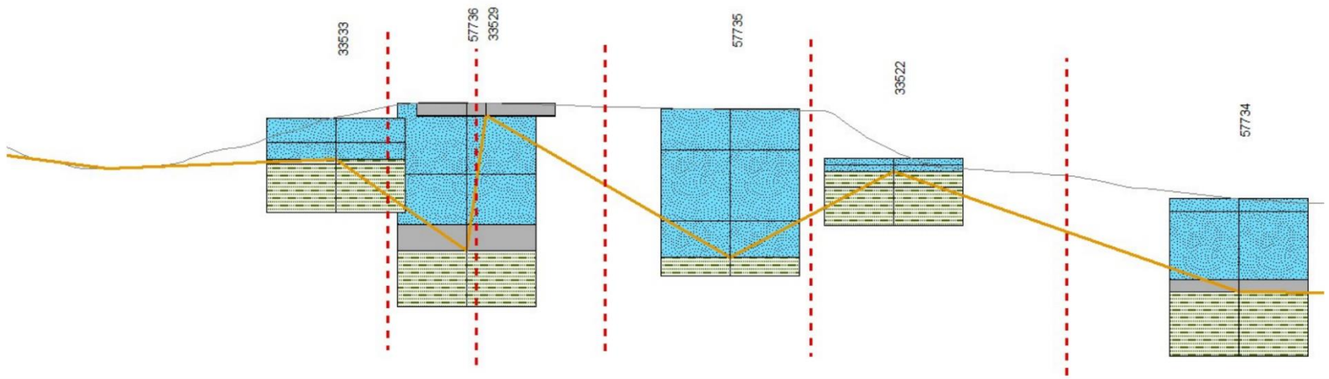

17	ANTHROPOGENIC ALTERATION	DOWN TO NORTH	57735	33522	39.78	70.98	31.21	61.67	26.84	C 1-1'. POSSIBLE ANTHROPOGENIC ROAD GRADE OR FAULT. NO NEIGHBORING CROSS SECTION TO VERIFY LATERAL ANOMALIES.
			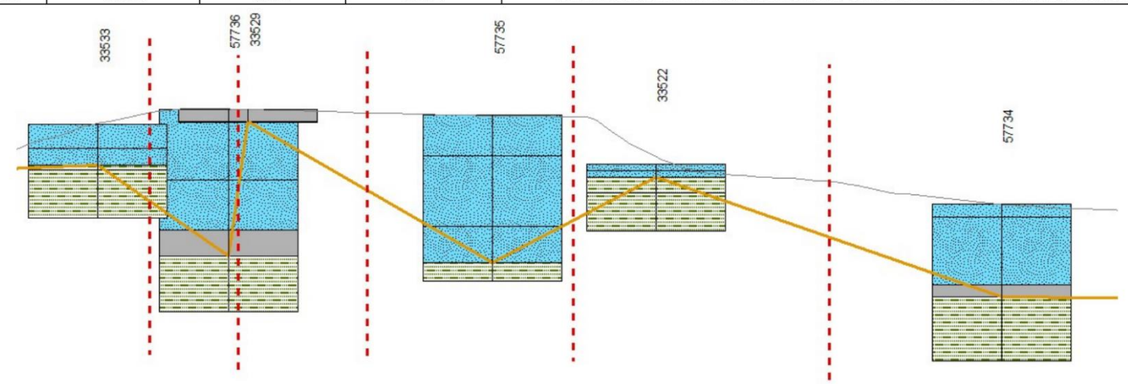						
17	ANTHROPOGENIC ALTERATION	DOWN TO NORTH	33531	100040	66.97	87.38	20.41	269.25	4.34	C 2-2'. LIMITED DATA BETWEEN 33531 AND 10040.
			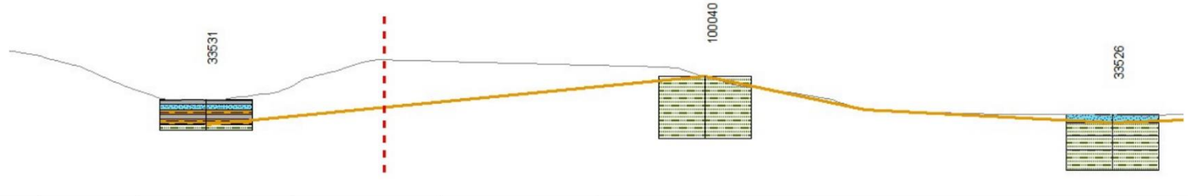						
18	ANTHROPOGENIC ALTERATION	UP TO NORTH	33522	57734	70.98	26.68	44.30	125.09	19.50	C 1-1'. POSSIBLE ANTHROPOGENIC ROAD GRADE OR FAULT. NO NEIGHBORING CROSS SECTION TO VERIFY LATERAL ANOMALIES.
			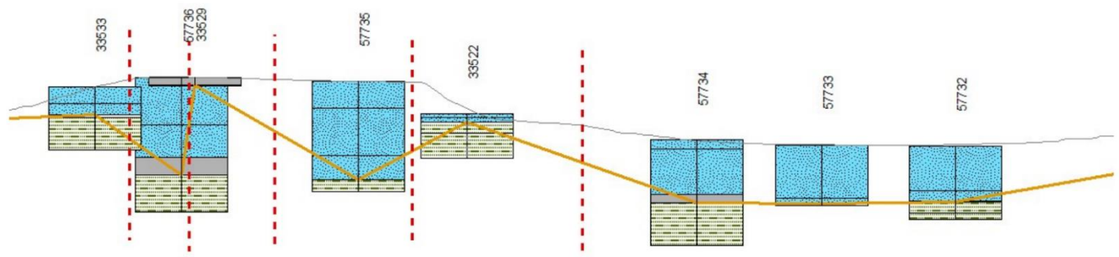						
19	FAULT	DOWN TO NORTH	57732	57731	27.60	65.10	37.50	26.68	54.57	C 1-1'.
			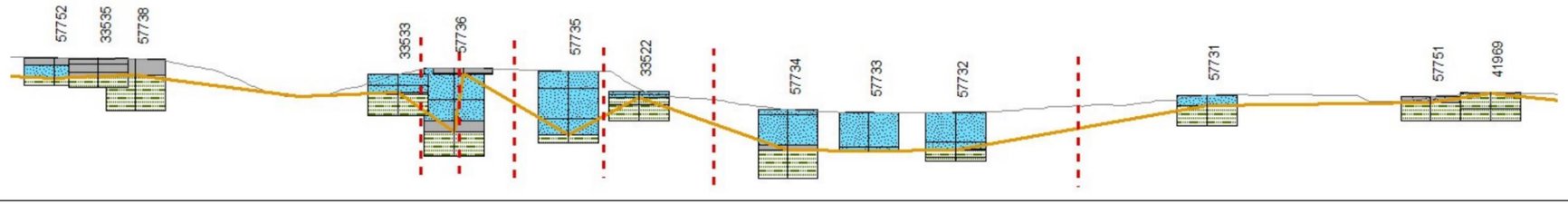						

19	FAULT	DOWN TO NORTH	33526	33519	62.05	74.97	12.92	269.12	2.75	C 2-2'.
			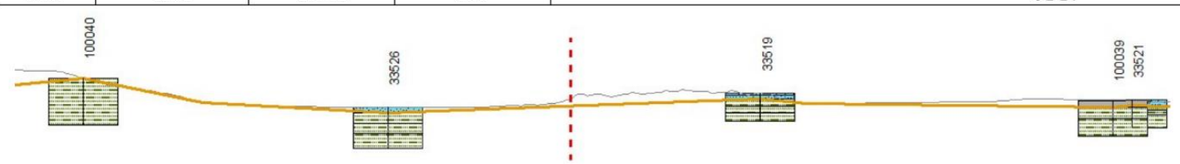							
19	FAULT	DOWN TO NORTH	-	41967	-	60.49	-	-	-	C 3-3'. LACK OF DATA TO CONFIRM OR DENY ANOMALY 15 CROSSES C 3-3'.
			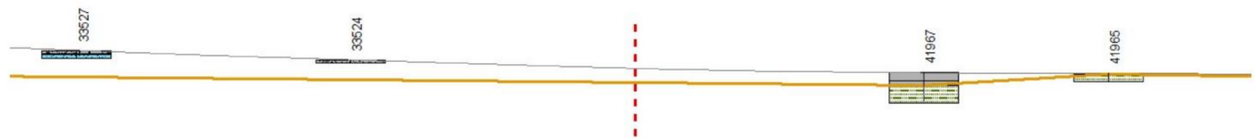							
19	FAULT	DOWN TO NORTH	32684	41960	113.62	112.66	0.96	377.70	0.15	C 5-5'. LACK OF DATA TO CONFIRM OR DENY ANOMALY 15 CROSSES C 5-5'.
			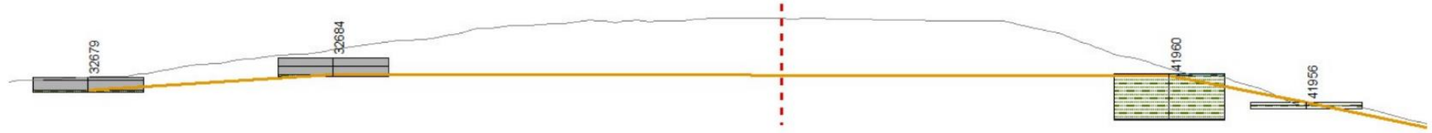							
19	FAULT	DOWN TO NORTH	32684	46571	113.62	133.82	20.19	137.00	8.38	C 10-10'
			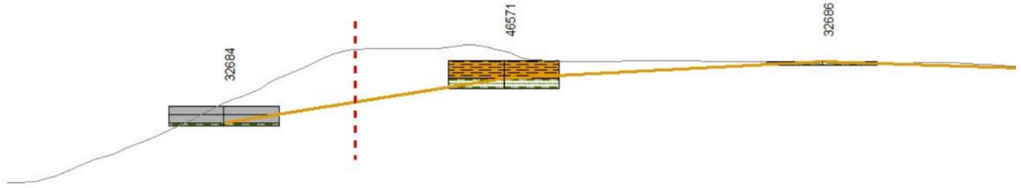							
19	FAULT	DOWN TO NORTH	32680	46571	124.71	133.82	9.11	203.32	2.56	C 12-12'
			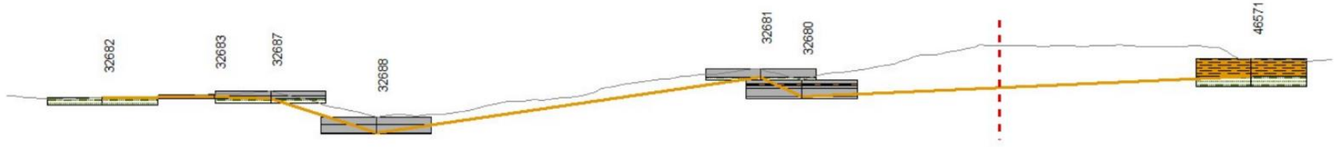							
19	FAULT	UP TO NORTH	46570	46571	147.10	133.82	13.28	210.92	3.60	C 13-13'
			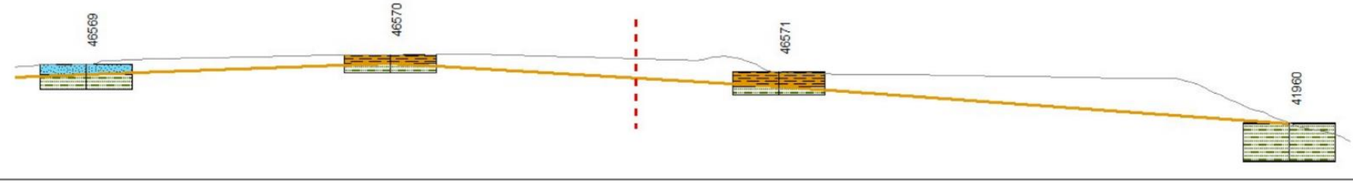							

19	FAULT	DOWN TO NORTH	42587	42589	128.11	137.57	9.46	270.83	2.00	C 23-23'
			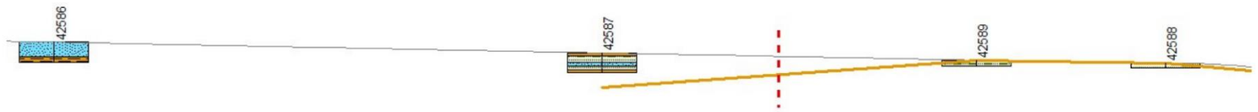							
19	FAULT	DOWN TO NORTH	56459	43212	123.96	141.22	17.26	304.00	3.25	D 18-18'
			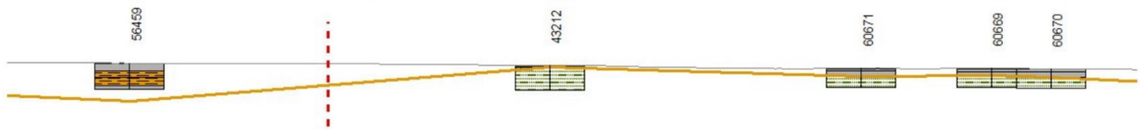							
20	ANTHROPOGENIC ALTERATION	DOWN TO NORTH	42591	42590	59.71	47.60	12.11	30.70	21.52	C 8-8'. POSSIBLE ANTHROPOGENIC ROAD GRADE ON I-5.
			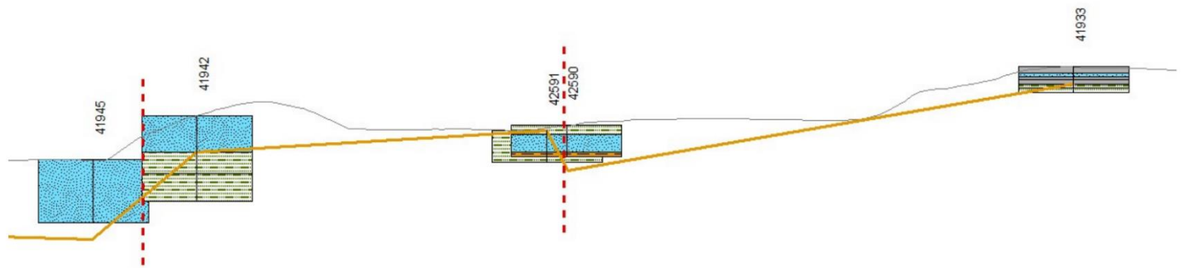							
21	FAULT	UP TO NORTH	41945	41942	17.04	49.92	32.87	51.39	32.60	C 8-8'
			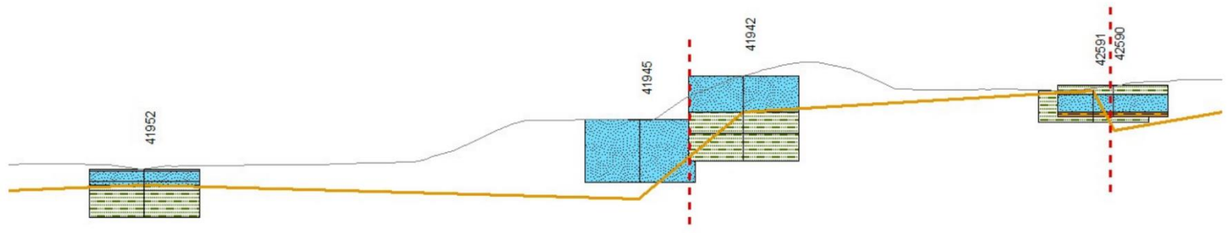							
21	FAULT	UP TO NORTH	41942	-	49.92	-	-	-	-	C 1-1'. LACK OF DATA TO CONFIRM OR DENY ANOMALY 21 CROSSES C 1-1'.
			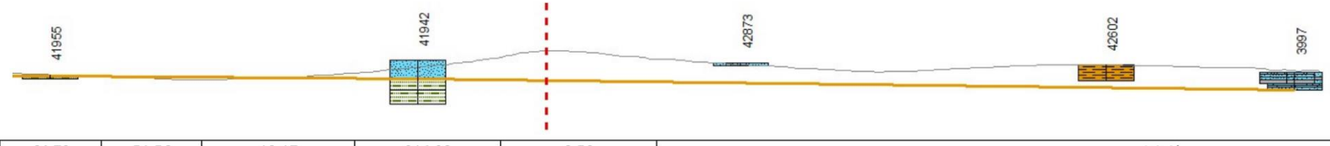							
21	FAULT	UP TO NORTH	41938	41932	64.72	51.56	13.17	214.98	3.50	C 3-3'
										

21	FAULT	UP TO NORTH	46574	41933	91.67	81.54	10.13	43.01	13.26	C 4-4'
										
22	FAULT	DOWN TO NORTH	41163	43211	126.57	135.61	9.03	50.28	10.19	D 18-18'. POTENTIAL COMPRESSION FEATURE SOUTH OF ANOMALY SEEN BETWEEN 43209 AND 43210.
			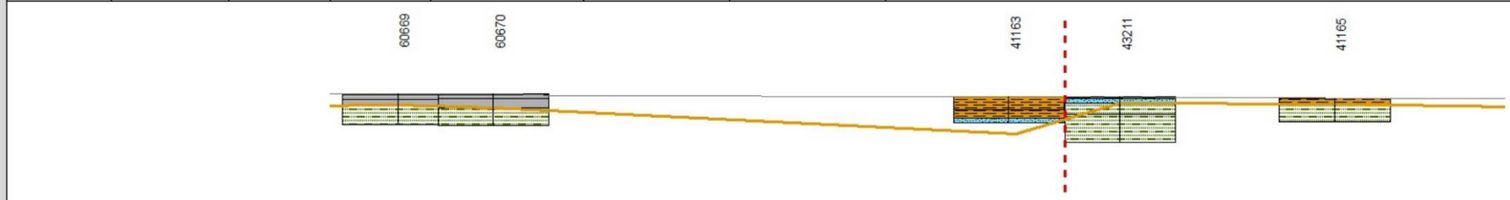							
22	FAULT	DOWN TO NORTH	56259	56613	193.87	165.86	28.01	1173.84	1.37	E 3-3'
										
22	FAULT	DOWN TO NORTH	-	-	-	-	-	-	-	E 6-6'. BEDROCK EXPOSED ON HILL SOUTH OF ANOMALY.
			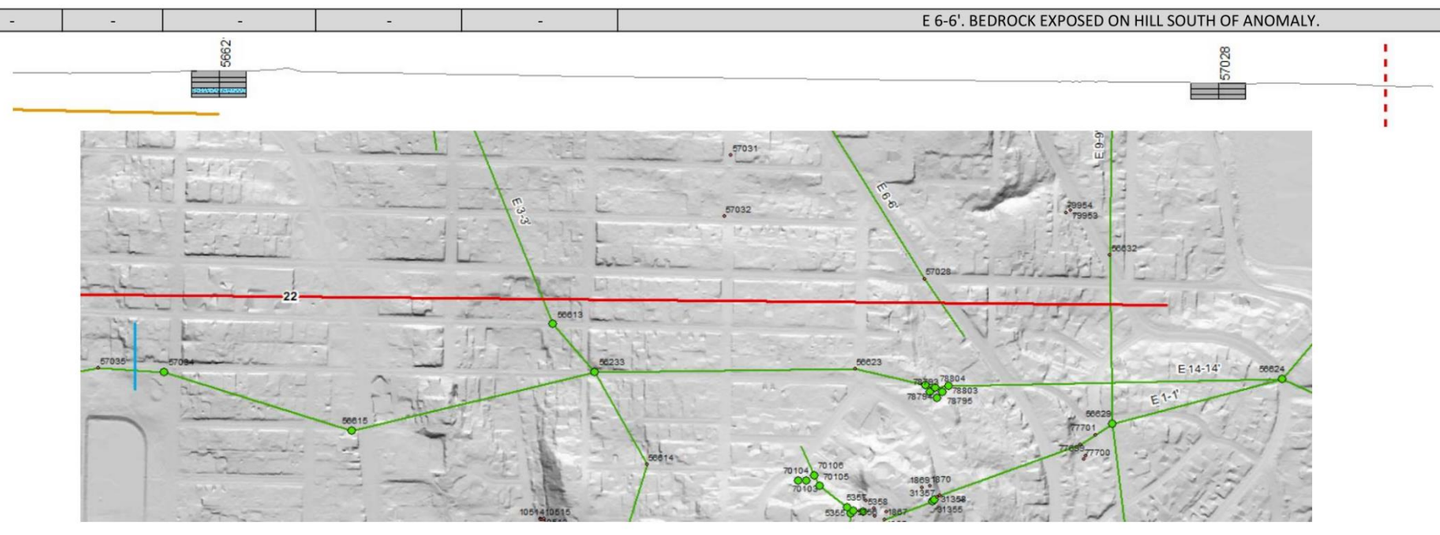								

22	FAULT	DOWN TO NORTH	56632	56629	74.31	128.01	53.70	848.00	3.62	E 9-9'
			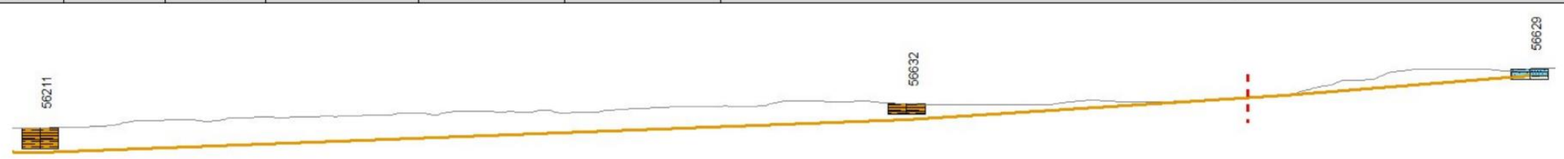							
23	EROSION	UP TO WEST	43210	41565	126.59	112.43	14.17	255.60	3.17	E 14-14'. POTENTIAL GLACIAL EROSION.
			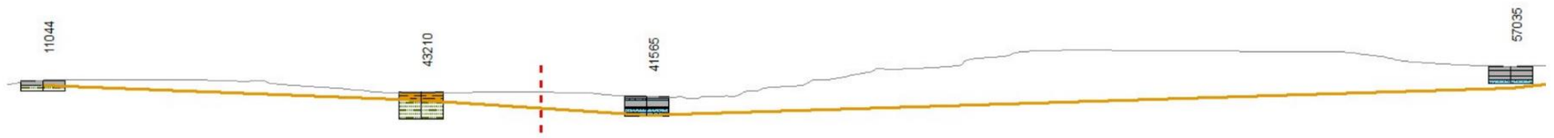							
24	EROSION	DOWN TO WEST	57035	57034	146.37	185.33	38.96	321.51	6.91	E 14-14'. POTENTIAL GLACIAL EROSION.
										
25	ANTHROPOGENIC ALTERATION	DOWN TO NORTH	41942	3997	49.92	39.23	10.68	49.92	12.08	C 1-1'. LACK OF DATA TO CONFIRM OR DENY ANOMALY 25 CROSSES C 1-1'. POTENTIAL ANTHROPOGENIC ALTERATION FOR CONSTRUCTION OF S ALBRO PL BRIDGE CROSSING I-5.
			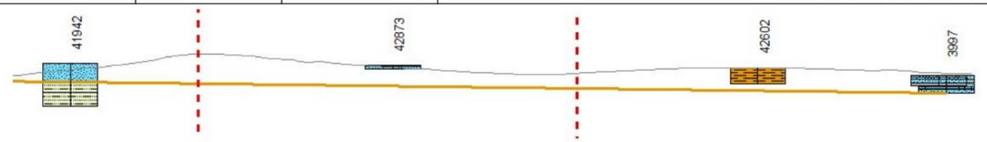							
25	ANTHROPOGENIC ALTERATION	DOWN TO NORTH	41925	41479	43.19	49.83	6.65	29.87	12.54	C 2-2'. POTENTIAL ANTHROPOGENIC ALTERATION FOR CONSTRUCTION OF S ALBRO PL BRIDGE CROSSING I-5.
			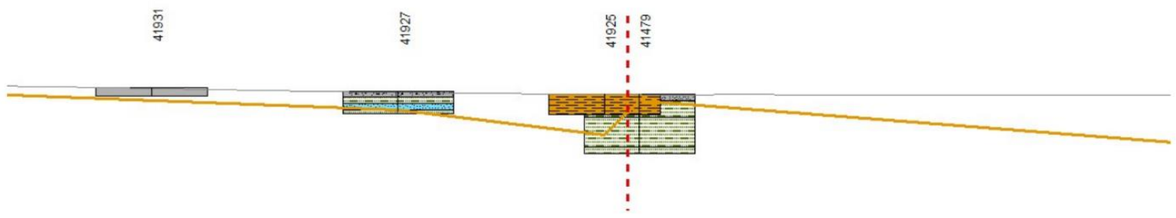							
25	ANTHROPOGENIC ALTERATION	DOWN TO NORTH	41932	41478	51.56	50.85	0.71	356.45	0.11	C 3-3'. LACK OF DATA TO CONFIRM OR DENY ANOMALY 25 CROSSES C 3-3'. POTENTIAL ANTHROPOGENIC ALTERATION FOR CONSTRUCTION OF S ALBRO PL BRIDGE CROSSING I-5.
										

25	ANTHROPOGENIC ALTERATION	DOWN TO NORTH	42880	41919	51.51	62.28	10.77	67.89	9.01	C 4-4'. POTENTIAL ANTHROPOGENIC ALTERATION FOR CONSTRUCTION OF S ALBRO PL BRIDGE CROSSING I-5.
			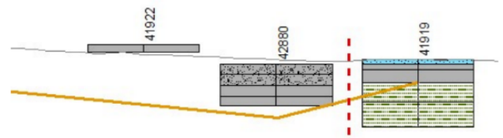							
26	FAULT	DOWN TO NORTH	42614	41928	37.29	49.50	12.22	67.94	10.19	C 2-2'
										
27	EROSION	UP TO NORTH	41949	41959	61.00	53.15	7.85	243.14	1.85	B 1-1'. LACK OF DATA TO CONFIRM OR DENY ANOMALY 27 CROSSES B 1-1'. POTENTIAL LANDSLIDE/RAVINE DEPOSIT REGRADE.
			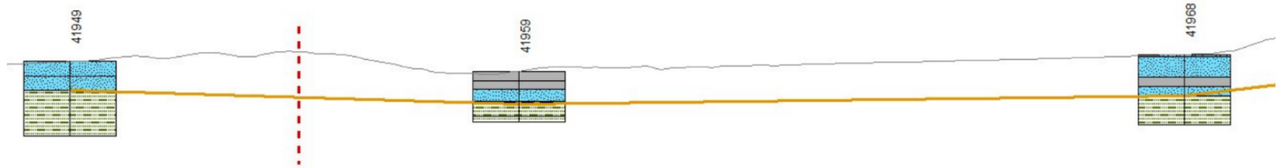							
27	EROSION	UP TO NORTH	41950	41958	97.29	77.47	19.82	221.87	5.11	B 2-2'. POTENTIAL LANDSLIDE OR OLD RAVINE.
			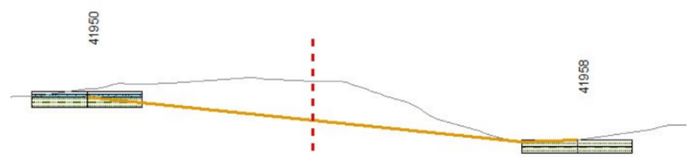							
27	EROSION	UP TO NORTH	-	-	-	-	-	-	-	B 3-3'. POTENTIAL LANDSLIDE OR OLD RAVINE.
			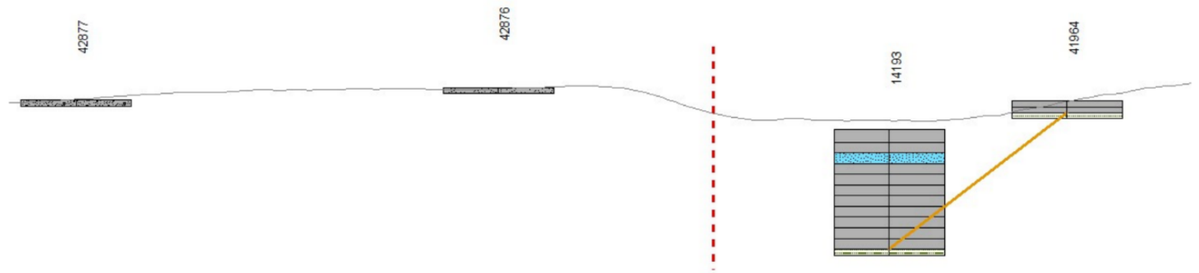							

27	EROSION	UP TO NORTH	41957	72803	118.22	66.30	51.92	109.82	25.30	B 4-4'. POTENTIAL LANDSLIDE OR OLD RAVINE.
			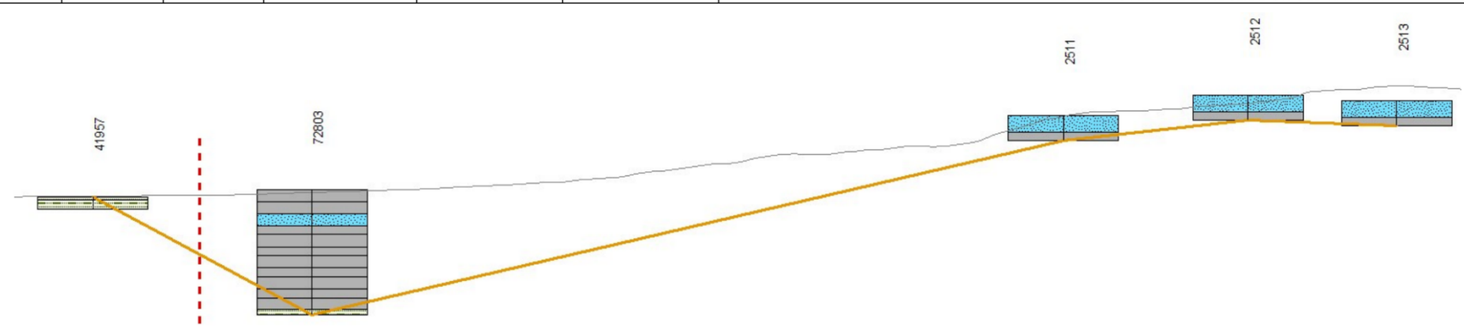							
28	EROSION	DOWN TO NORTH	41959	41968	53.15	57.85	4.70	360.44	0.75	B 1-1'. POTENTIAL LANDSLIDE/RAVINE DEPOSIT REGRADE.
			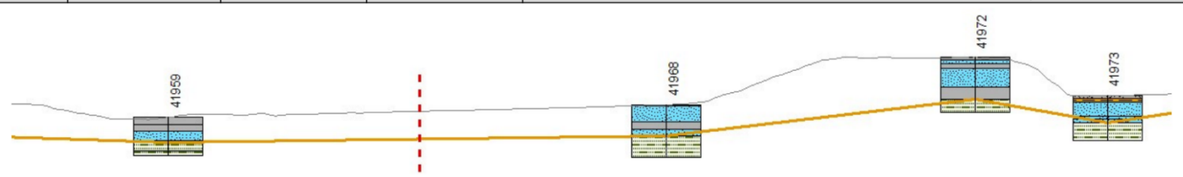							
28	EROSION	DOWN TO NORTH	41958	-	77.47	-	-	-	-	B 2-2'. POTENTIAL LANDSLIDE OR OLD RAVINE.
			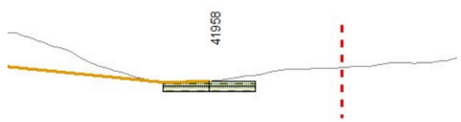							
28	EROSION	DOWN TO NORTH	14193	41964	40.93	105.24	64.30	80.78	38.52	B 3-3'. POTENTIAL LANDSLIDE OR OLD RAVINE.
			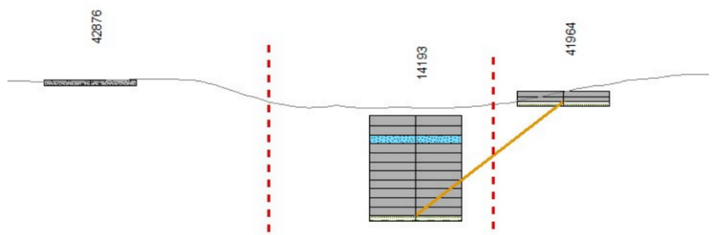							

28	EROSION	DOWN TO NORTH	72803	2511	66.30	145.05	78.75	340.12	13.04	B 4-4'. POTENTIAL LANDSLIDE OR OLD RAVINE.
			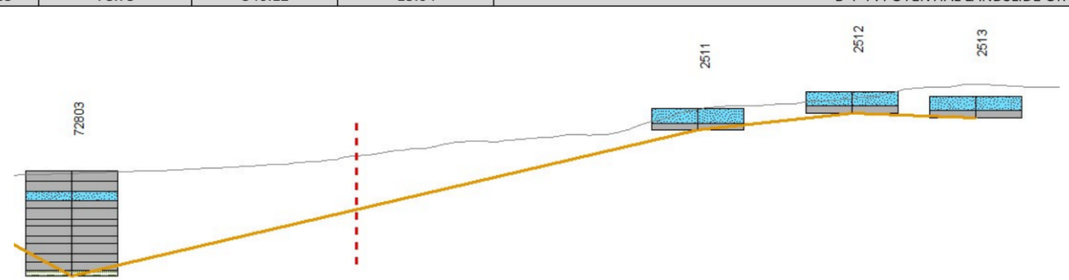							
29	FAULT	DOWN TO NORTH	41968	41972	57.85	111.23	53.38	223.16	13.45	B 1-1'
			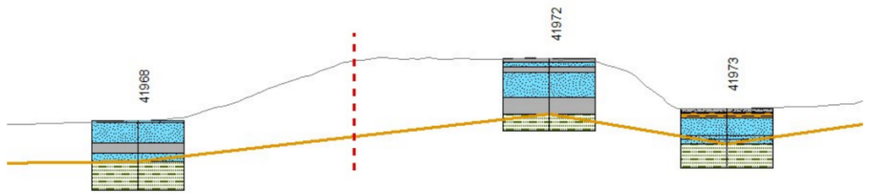							
29	FAULT	DOWN TO NORTH	41176	43208	110.96	120.06	9.10	120.91	4.31	D 18-18'
			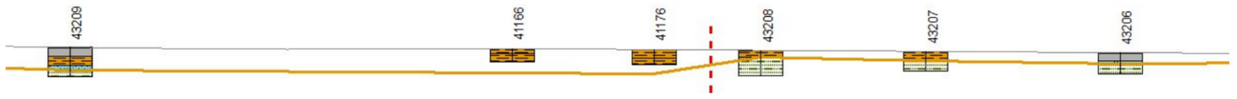							
30	FAULT	UP TO NORTH	59693	5507	33.54	11.36	22.18	342.11	3.71	E 10-10'
			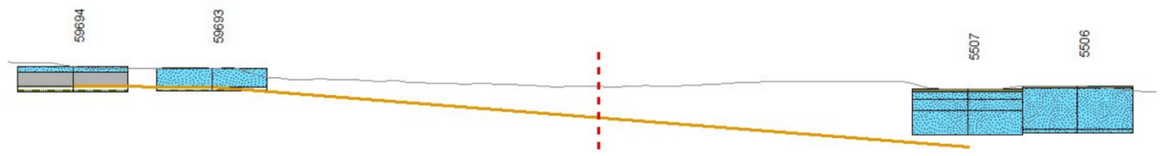							
30	FAULT	UP TO NORTH	59693	5509	33.54	17.09	16.44	346.68	2.72	E 11-11'
			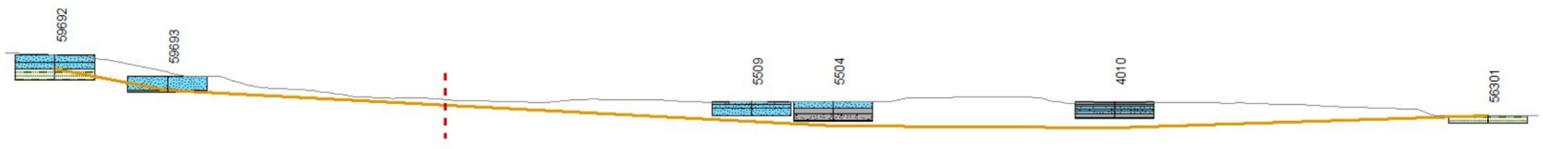							

31	ANTHROPOGENIC ALTERATION	UP TO NORTH	41972	41973	111.23	67.66	43.57	96.07	24.40	B 1-1'
32	FAULT	DOWN TO NORTH	41973	41974	67.66	86.26	18.60	122.53	8.63	B 1-1'
33	FAULT	UP TO NORTH	41974	41975	86.26	79.06	7.19	40.70	10.02	B 1-1'

34	FAULT	DOWN TO NORTH	41975	41977	79.06	86.75	7.69	35.73	12.14	B 1-1'
			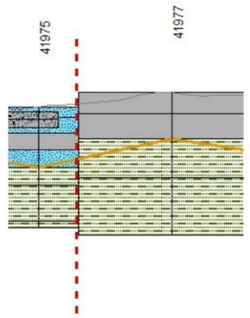							
35	FAULT	UP TO NORTH	41977	42863	86.75	78.58	8.16	56.74	8.19	B 1-1'
			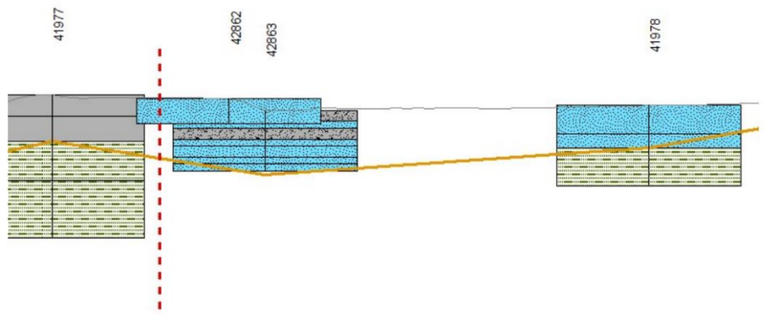							
36	FAULT	DOWN TO NORTH	41978	42864	84.79	99.21	14.42	78.58	10.40	B 1-1'
			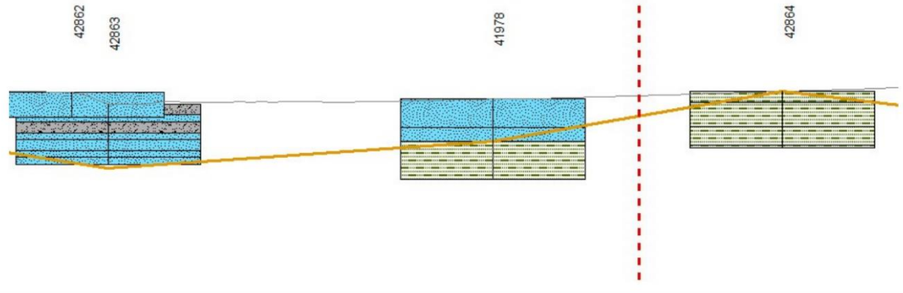							

37	FAULT	UP TO NORTH	42864	41979	99.21	93.53	5.68	73.82	4.40	B 1-1'
			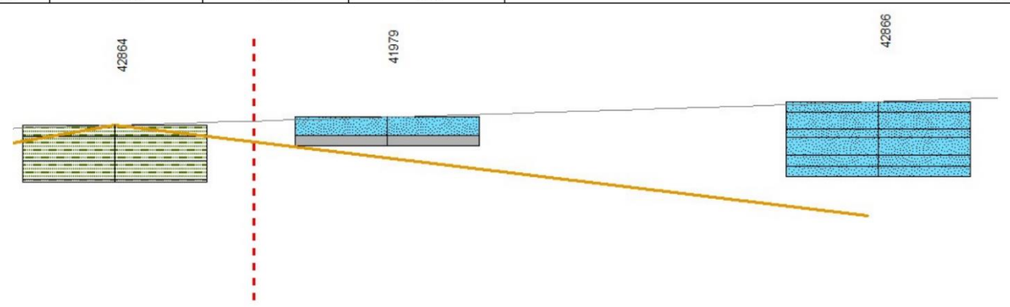							
38	ANTHROPOGENIC ALTERATION	DOWN TO NORTH	33263	33262	163.14	177.21	14.07	46.20	16.94	A 24-24'. POTENTIAL ANTHROPOGENIC ROAD GRADE.
			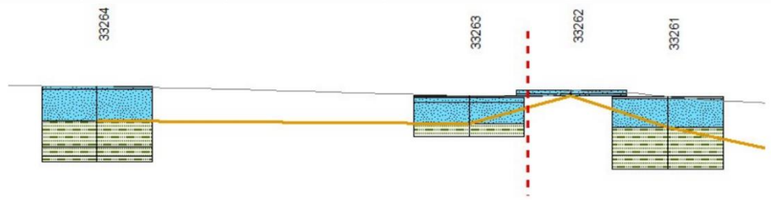							
39	ANTHROPOGENIC ALTERATION	UP TO NORTH	33261	33253	175.89	134.95	40.94	120.75	18.73	A 24-24'. POTENTIAL ANTHROPOGENIC ROAD GRADE.
			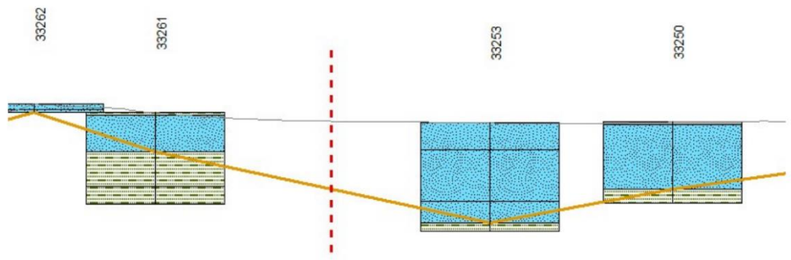							
40	ANTHROPOGENIC ALTERATION	DOWN TO NORTH	33254	33245	131.94	160.57	28.63	424.48	3.86	A 2-2'. POTENTIAL ANTHROPOGENIC ROAD GRADE.
			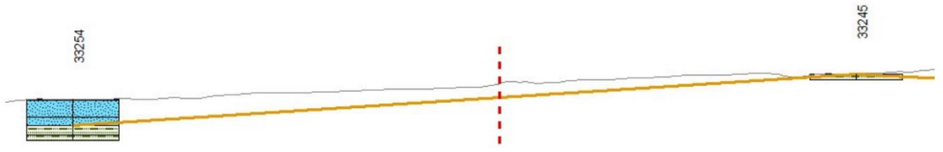							

40	ANTHROPOGENIC ALTERATION	DOWN TO NORTH	33250	33249	147.41	172.21	24.80	173.41	8.14	A 24-24'. POTENTIAL ANTHROPOGENIC ROAD GRADE.
			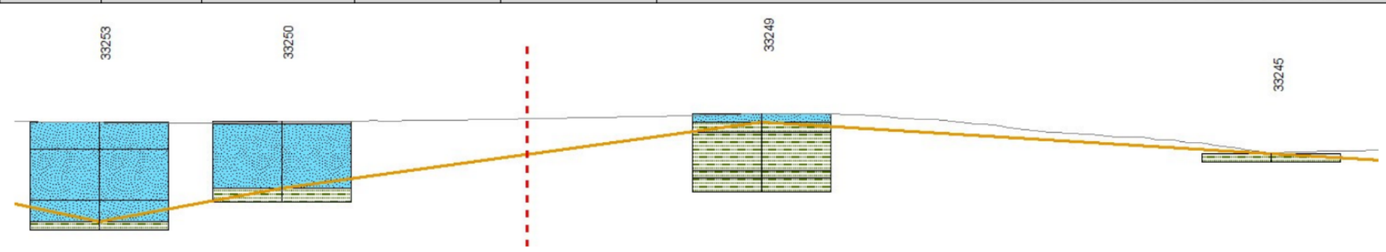							
41	ANTHROPOGENIC ALTERATION	UP TO NORTH	43205	41167	115.85	111.08	4.77	35.23	7.71	D 18-18'. POTENTIAL ANTHROPOGENIC ROAD GRADE.
			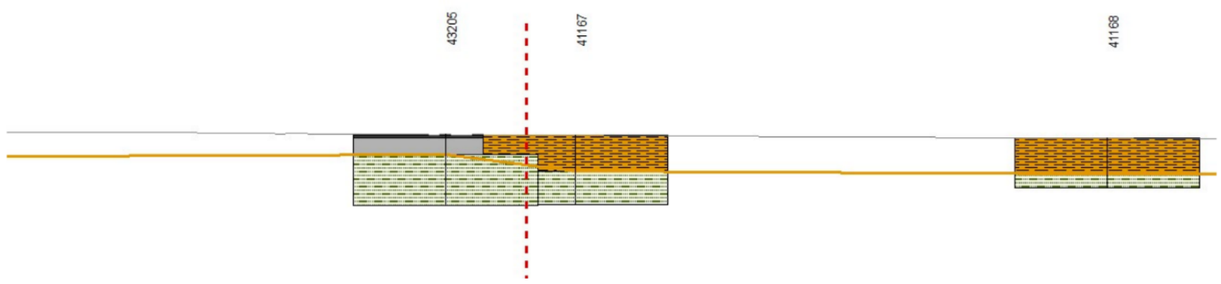							
42	ANTHROPOGENIC ALTERATION	DOWN TO NORTH	3919	3937	173.26	192.86	19.60	119.83	9.29	D 5-5'. POTENTIAL ANTHROPOGENIC ROAD GRADE. NO NEIGHBORING CROSS SECTIONS VERIFY CONTINUOUS ANOMALIES.
			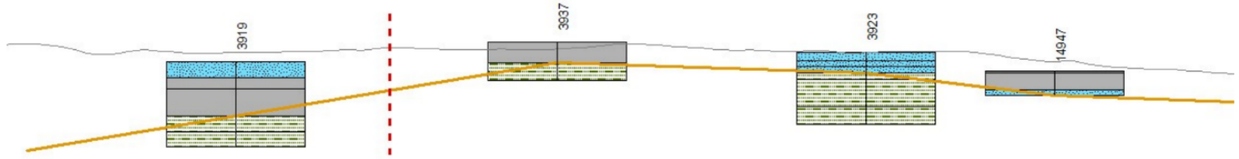							
43	COMPRESSION FOLD	UP TO NORTH	41170	43204	112.94	108.03	4.91	117.86	2.39	D 18-18'. POTENTIAL COMPRESSION FEATURE.
										
44	FAULT	DOWN TO NORTH	43204	43217	108.03	122.50	14.46	554.79	1.49	D 18-18'
										
45	ANTHROPOGENIC ALTERATION	DOWN TO NORTH	56232	56495	73.94	100.93	26.99	1301.10	1.19	E 3-3'. POTENTIAL ANTHROPOGENIC ROAD GRADE.
										

45	ANTHROPOGENIC ALTERATION	DOWN TO NORTH	56619	30176	58.31	104.80	46.50	357.29	7.41	E 17-17'. POTENTIAL ANTHROPOGENIC ROAD GRADE.
			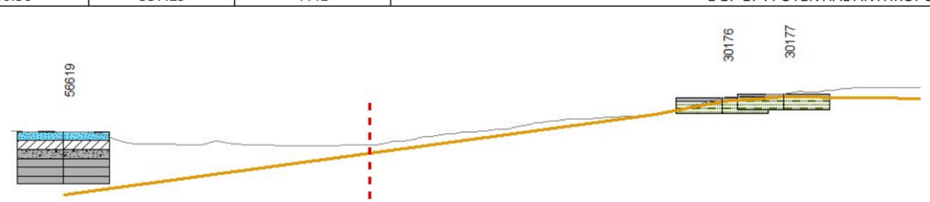							
46	ANTHROPOGENIC ALTERATION	UP TO WEST	3941	56498	114.39	101.86	12.53	75.44	9.43	D 13-13'. POTENTIAL ANTHROPOGENIC.
			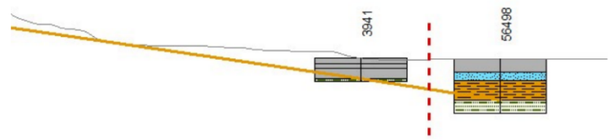							
46	ANTHROPOGENIC ALTERATION	UP TO WEST	3942	3943	127.35	114.06	13.29	309.21	2.46	D 12-12'. POTENTIAL ANTHROPOGENIC.
										
46	ANTHROPOGENIC ALTERATION	UP TO WEST	3929	30738	124.80	111.51	13.29	125.76	6.03	D 11-11'. POTENTIAL ANTHROPOGENIC.
			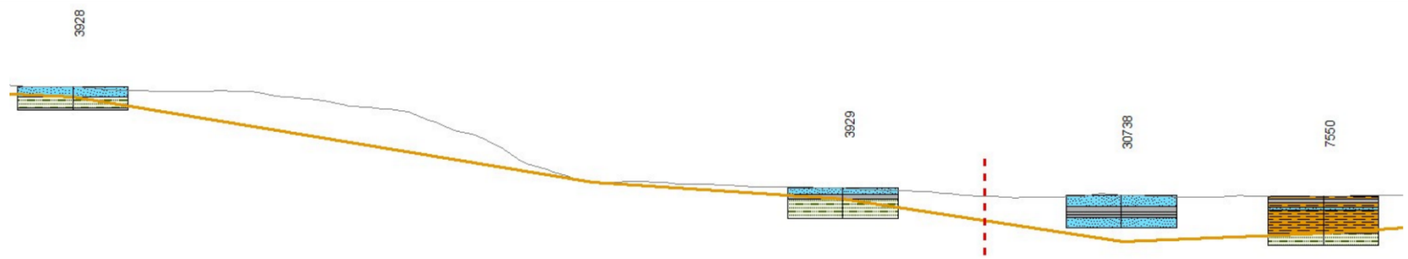							
46	ANTHROPOGENIC ALTERATION	UP TO WEST	3929	56497	124.80	104.94	19.86	201.26	5.63	D 6-6'. POTENTIAL ANTHROPOGENIC.
			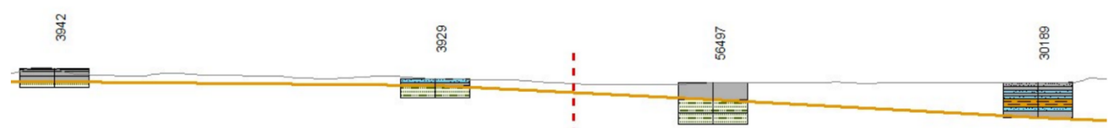							

46	ANTHROPOGENIC ALTERATION	UP TO WEST	3932	30189	138.14	101.82	36.32	329.45	6.29	D 10-10'. POTENTIAL ANTHROPOGENIC.
			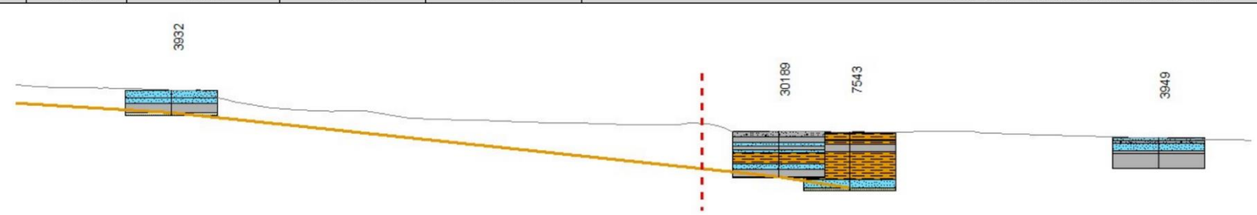							
46	ANTHROPOGENIC ALTERATION	UP TO WEST	3932	7542	138.14	94.23	43.91	405.62	6.18	D 17-17'. POTENTIAL ANTHROPOGENIC. ANOMALY 46 PASSES NORTH OF ANOMALY 50.
										
46	ANTHROPOGENIC ALTERATION	UP TO WEST	14925	3934	137.65	108.79	28.86	233.16	7.06	D 16-16'. POTENTIAL ANTHROPOGENIC.
			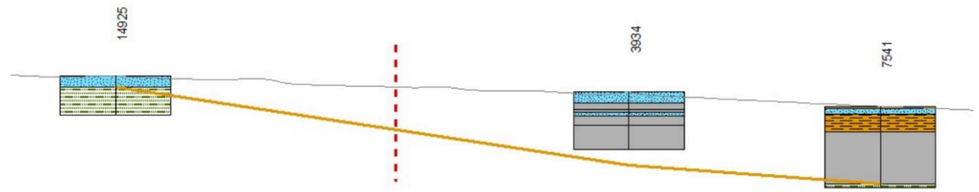							
46	ANTHROPOGENIC ALTERATION	UP TO WEST	3932	-	138.14	-	-	-	-	D 4-4'. POTENTIAL ANTHROPOGENIC. ANOMALY 46 PASSES SOUTH OF ANOMALY 50.
			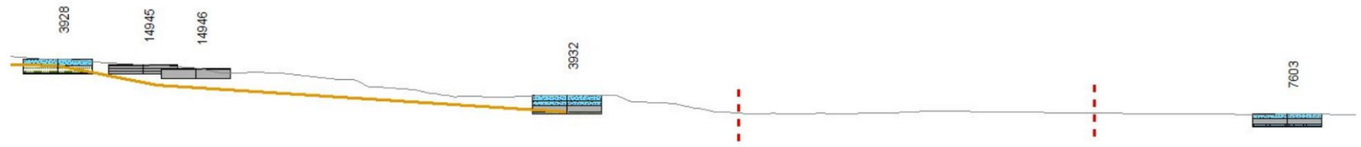							
47	EROSION	UP TO WEST	1728	4076	26.12	9.51	16.61	247.25	3.84	E 16-16'. POTENTIAL EROSION - LANDSLIDE.
			1745	1746	14.68	25.07	10.39	25.07	22.51	
			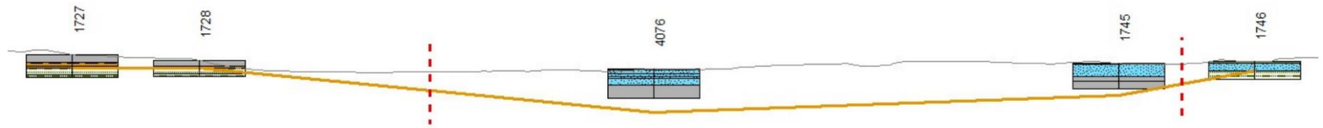							

48	FAULT	DOWN TO NORTH	57729	100038	72.38	76.34	3.96	21.54	10.42	A 7-7'
			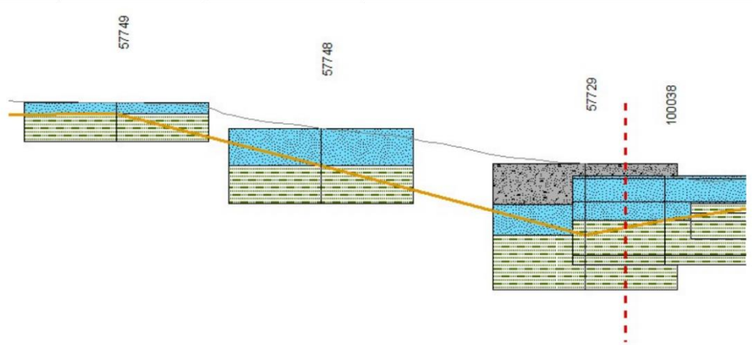							
48	FAULT	DOWN TO NORTH	57730	57729	86.24	72.38	13.86	16.13	40.68	A 15-15'
			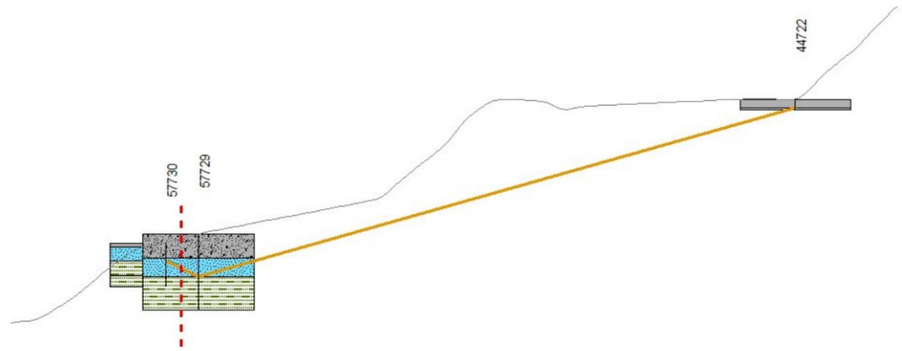							
49	FAULT	DOWN TO NORTH	70080	41367	115.74	123.29	7.55	19.06	21.60	D 18-18'
			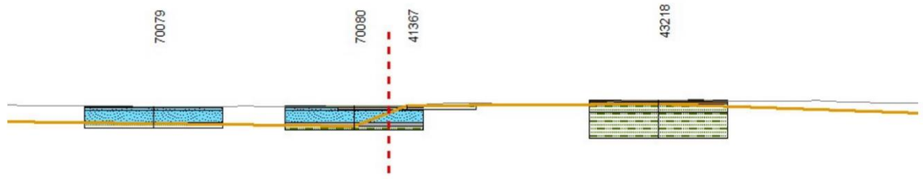							
49	FAULT	DOWN TO NORTH	70081	41358	116.41	119.55	3.14	14.26	12.43	D 23-23'
			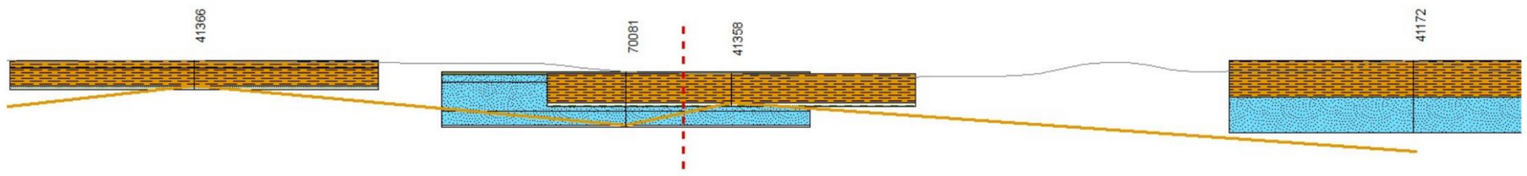							

49	FAULT	DOWN TO NORTH	41367	70080	123.29	115.74	7.55	19.06	21.60	D 9-9'
			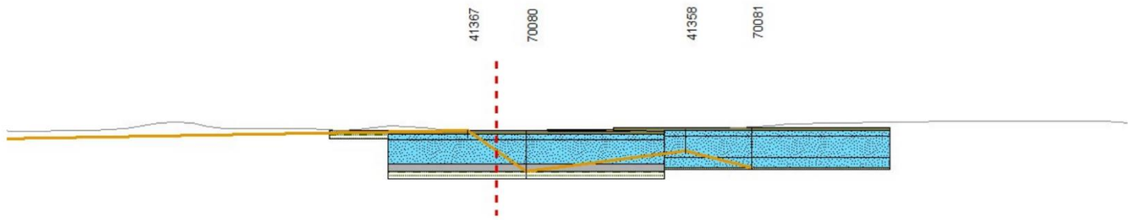							
50	FAULT	UP TO NORTH	100037	100036	81.44	61.50	19.94	40.84	26.02	A 7-7'
			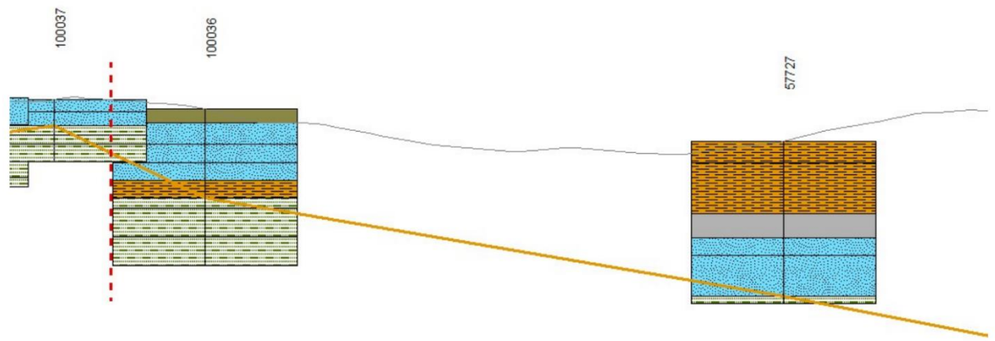							
50	FAULT	UP TO NORTH	44725	100035	108.68	86.95	21.73	277.67	4.47	A 3-3'
			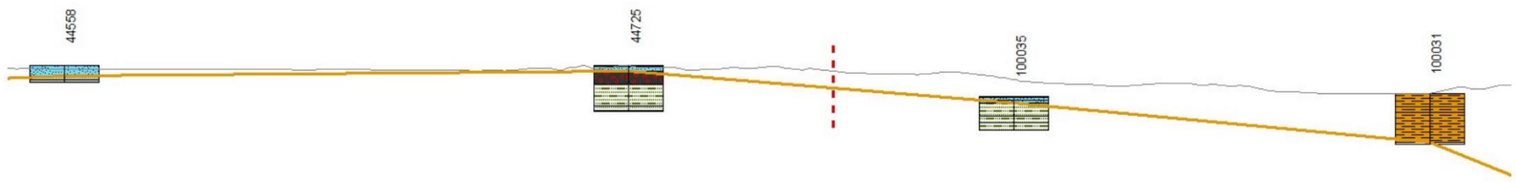							

50	FAULT	UP TO NORTH	100036	100035	61.50	86.95	25.45	22.79	48.16	A 16-16'
			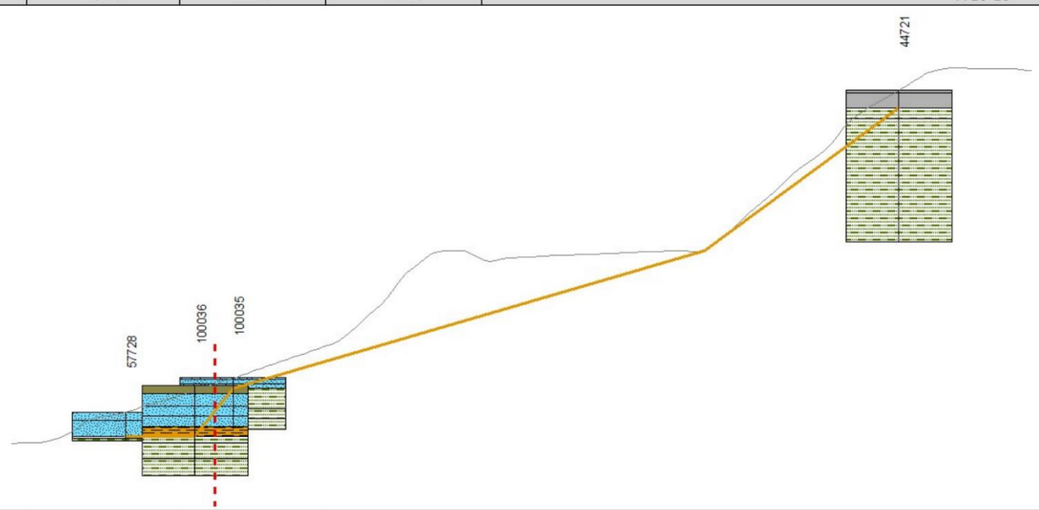							
50	FAULT	-	-	-	-	-	-	-	-	A 2-2'. LIMITED DATA.
										
50	FAULT	UP TO NORTH	44561	57695	224.09	210.16	13.92	86.95	9.10	A 24-24'
			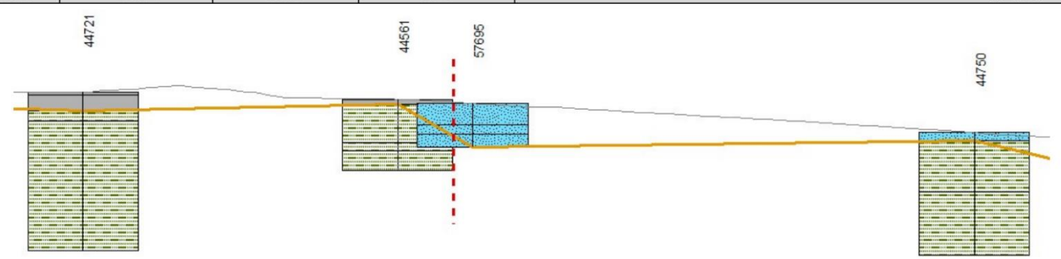							
50	FAULT	UP TO NORTH	58756	-	160.51	-	-	-	-	D 1-1'
			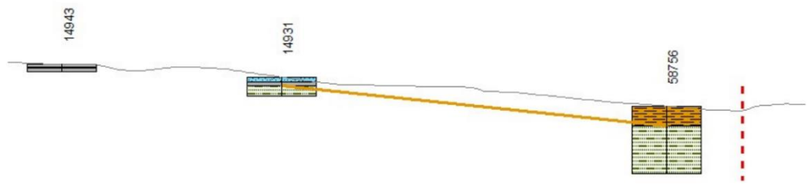							

50	FAULT	UP TO NORTH	33014	-	167.70	-	-	-	-	D 2-2'
			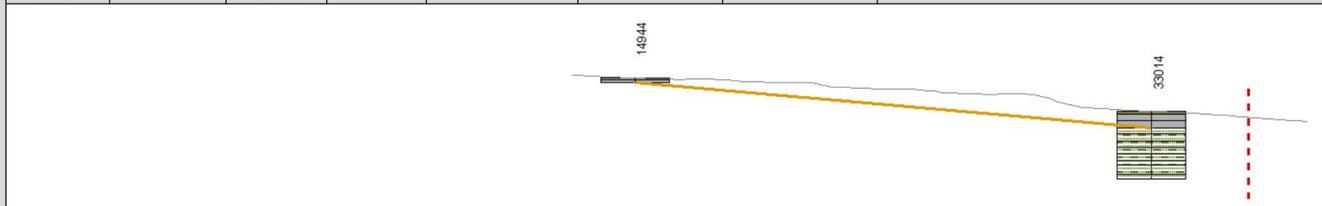							
50	FAULT	UP TO NORTH	3931	3933	167.54	124.71	42.83	378.01	6.46	D 3-3'. 14925 ENDS IN WEATHERED BLAKELEY FORMATION.
			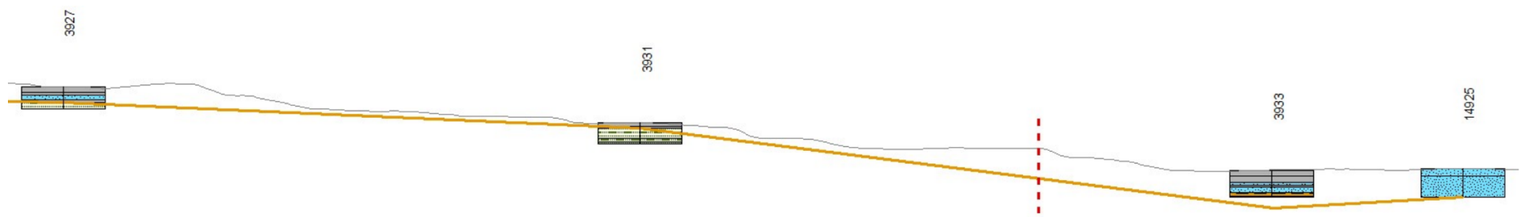							
50	FAULT	UP TO NORTH	3932	3933	138.14	124.71	13.42	201.11	3.82	D 5-5'. 14925 ENDS IN WEATHERED BLAKELEY FORMATION.
			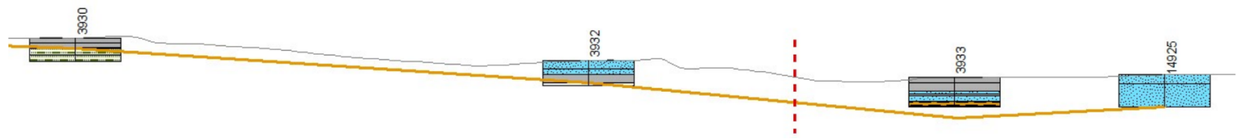							
50	FAULT	UP TO NORTH	3932	-	138.14	-	-	-	-	D 4-4'. ANOMALY 50 PASSES NORTH OF ANOMALY 46.
			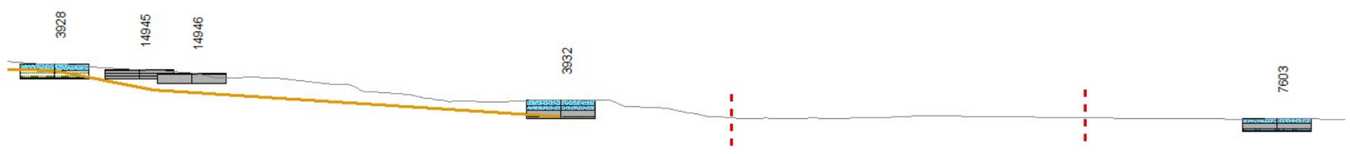							
50	FAULT	UP TO NORTH	3932	7542	138.14	94.23	43.91	405.62	6.18	D 17-17'. ANOMALY 50 PASSES SOUTH OF ANOMALY 46.
			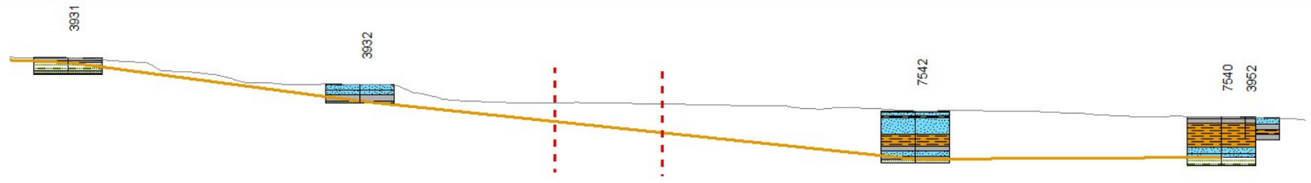							
50	FAULT	UP TO NORTH	30189	7542	101.82	94.23	7.59	158.14	2.75	D 6-6'
										

50	FAULT	UP TO NORTH	30191	7544	105.62	84.86	20.75	251.42	4.72	D 8-8'
			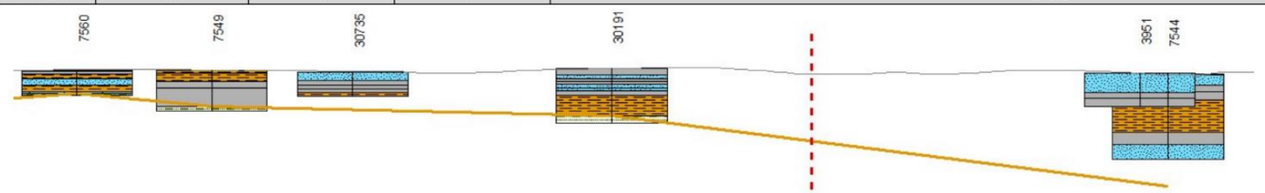							
50	FAULT	UP TO NORTH	7545	7544	108.39	84.86	23.53	159.33	8.40	D 7-7'
			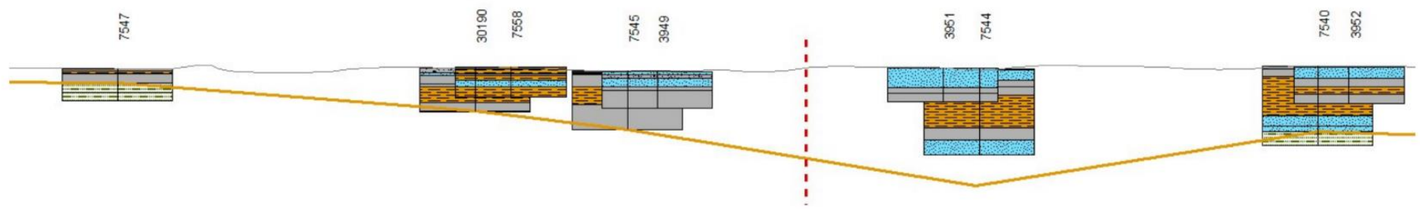							
50	FAULT	UP TO NORTH	43218	43219	123.96	114.51	9.45	254.62	2.13	D 18-18'
										
51	ANTHROPOGENIC ALTERATION	UP TO NORTH	43219	41174	114.51	107.56	6.96	34.52	11.39	D 18-18'. POTENTIAL ANTHROPOGENIC.
			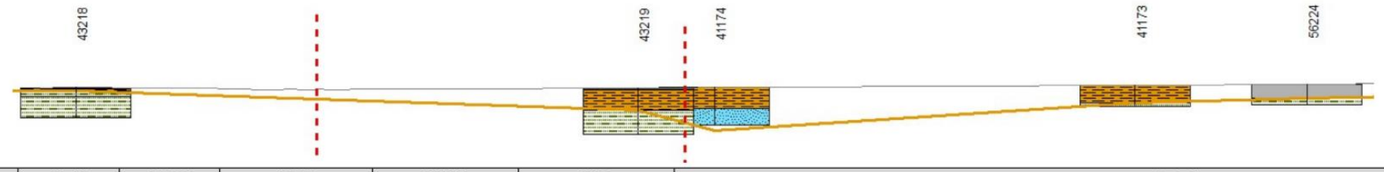							
52	FAULT	DOWN TO NORTH	7539	55900	91.77	108.97	17.20	166.71	5.89	D 6-6'
			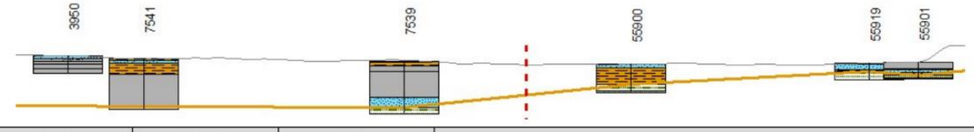							
52	FAULT	DOWN TO NORTH	5813	55904	110.38	116.62	6.23	189.50	1.88	D 22-22'
			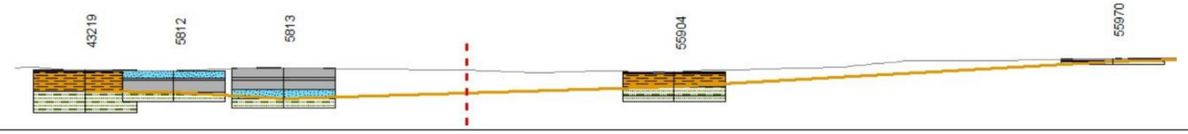							

52	FAULT	DOWN TO NORTH	41174	41173	107.56	118.31	10.75	190.38	3.23	D 18-18'
			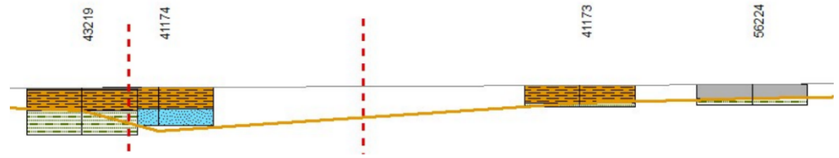							
53	FAULT	UP TO NORTH	100031	100026	55.86	-47.14	103.00	248.42	22.52	A 3-3'. ANOMALY 53 PASSES NORTH OF ANOMALY 56.
			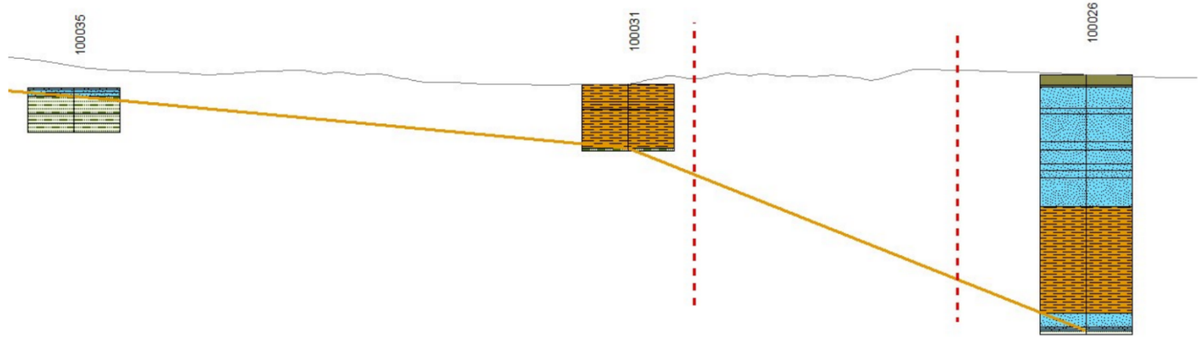							
53	FAULT	UP TO NORTH	44750	57694	207.24	188.84	18.40	93.40	11.15	A 6-6'. ANOMALY 53 PASSES NORTH OF ANOMALY 56.
			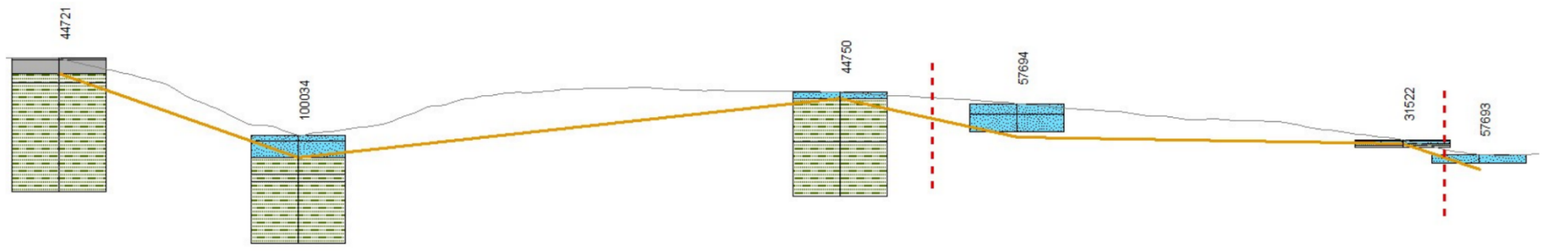							
53	FAULT	UP TO NORTH	44750	57694	207.24	188.84	18.40	93.40	11.15	A 24-24'. ANOMALY 53 PASSES SOUTH OF ANOMALY 50.
			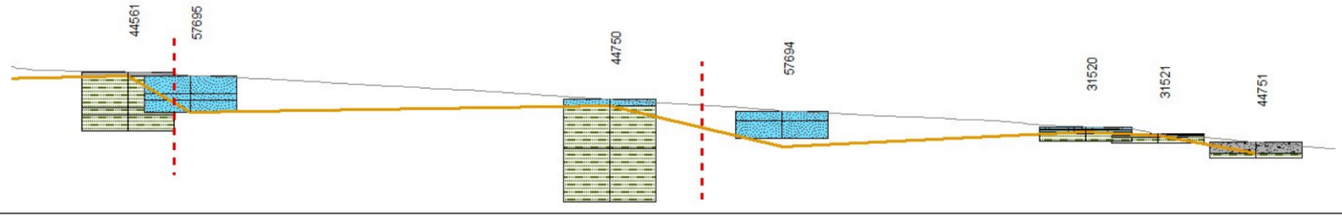							

54	FAULT/ ANTHROPOGENIC ALTERATION	DOWN TO NORTH	100028	44753	50.30	119.99	69.69	30.86	66.12	A 22-22'. POSSIBLY MATERIAL REMOVED OR EXTREME BUTTRESS UNCONFORMITY.
			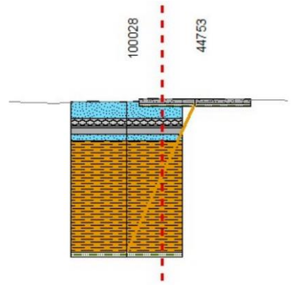							
55	FAULT	UP TO NORTH	43220	41175	123.96	112.40	11.56	142.14	4.65	D 18-18'
			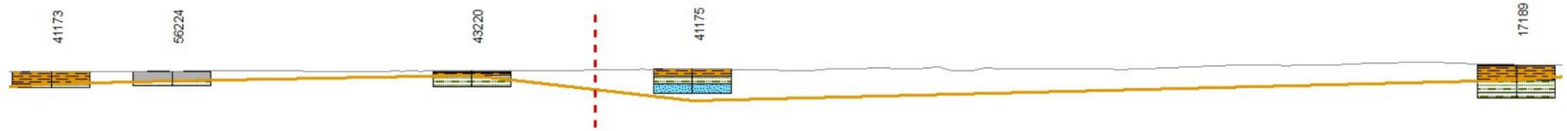							
56	FAULT	UP TO NORTH	100027	57726	-28.12	-34.21	6.09	13.20	24.78	A 7-7'
			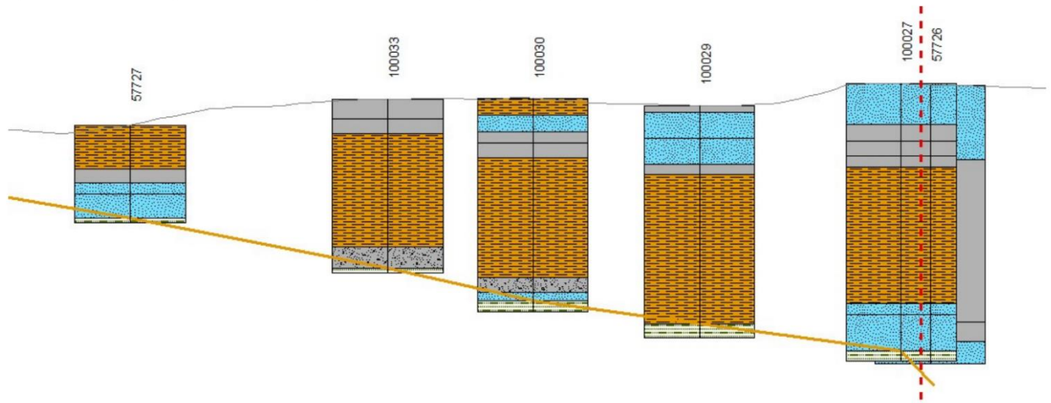							

56	FAULT	UP TO NORTH	100031	100026	55.86	-47.14	103.00	248.42	22.52	A 3-3'. ANOMALY 56 PASSES SOUTH OF ANOMALY 53.
			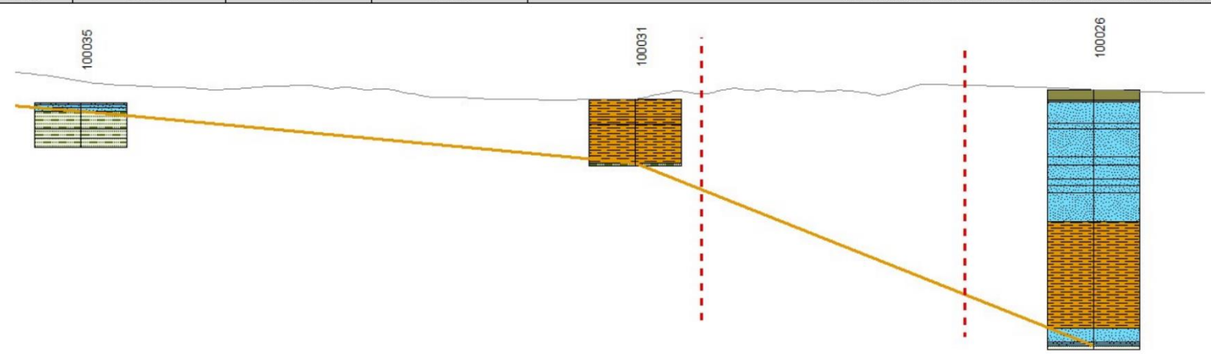							
56	FAULT	UP TO NORTH	31522	57693	182.54	171.88	10.65	40.29	14.81	A 6-6'. ANOMALY 56 PASSES SOUTH OF ANOMALY 53.
			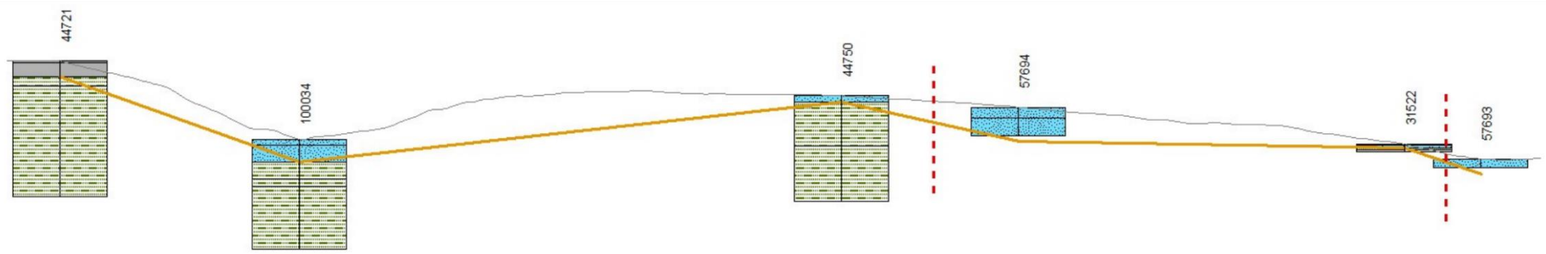							
56	FAULT	UP TO NORTH	17189	17168	121.07	128.91	7.84	109.56	4.10	D 18-18'
										
56	FAULT	UP TO NORTH	56242	-	90.47	-		-	-	E 3-3'. NO BEDROCK SOUTH OF 56242.
										
56	FAULT	UP TO NORTH	56241	-	90.66	-		-	-	E 17-17'. NO BEDROCK SOUTH OF 56241.
										

57	FAULT	DOWN TO NORTH	78655	78664	-146.54	-11.25	135.29	1625.24	4.76
			G 1-1'						
			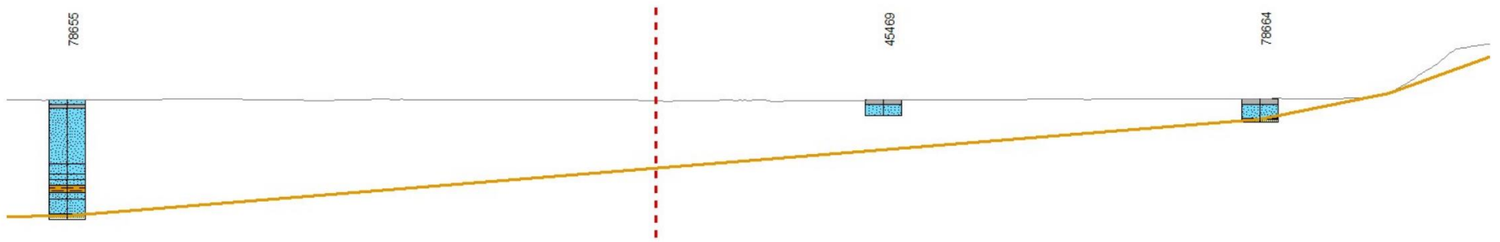						
58	FAULT	DOWN TO NORTH	31615	31618	-12.81	7.68	20.49	410.43	2.86
			F 2-2'						
			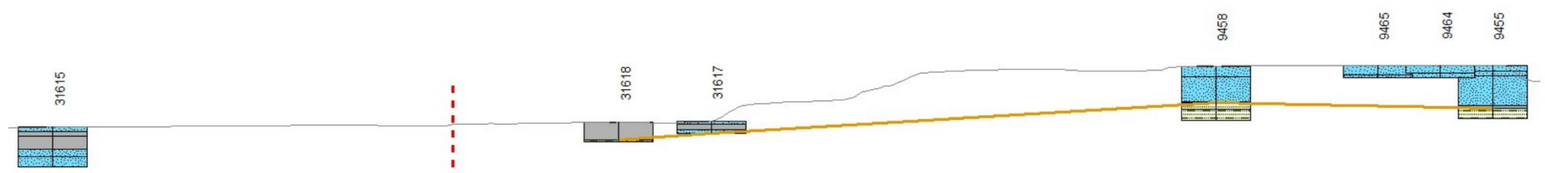						
58	FAULT	DOWN TO NORTH	58098	58097	-21.85	4.24	26.09	226.21	6.58
			F 3-3'						
			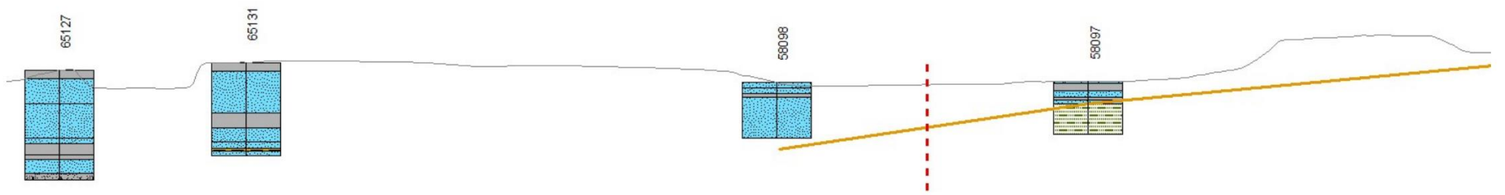						
58	FAULT	DOWN TO NORTH	78664	31800	-11.25	56.70	67.95	310.14	12.36
			F 1-1'						
			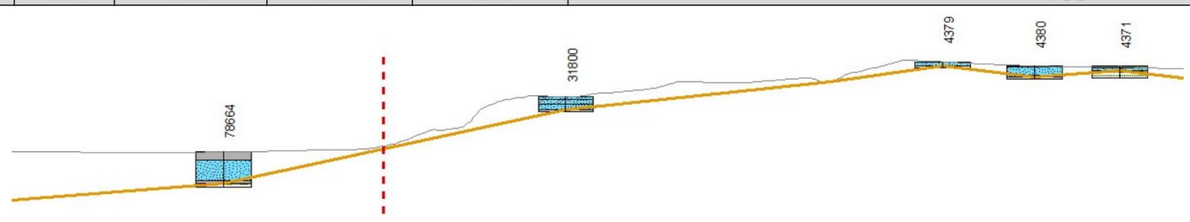						
58	FAULT	DOWN TO NORTH	78664	31807	-11.25	96.63	107.88	364.08	16.51
			G 1-1'						
			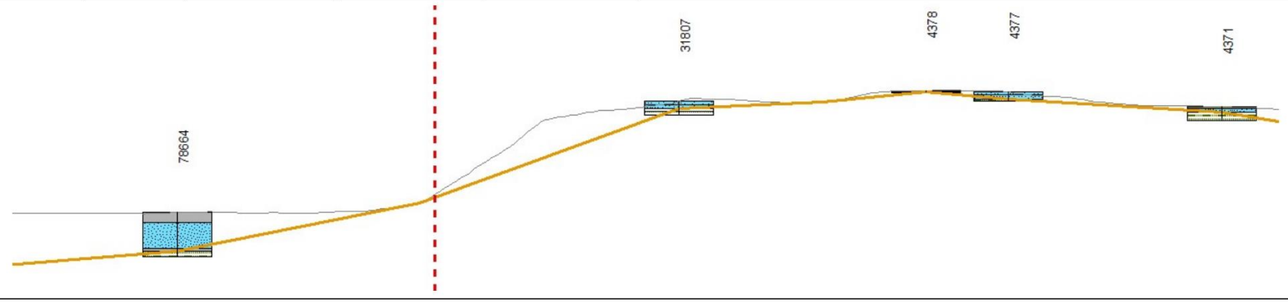						

58	FAULT	DOWN TO NORTH	78657	2961	-76.64	99.78	176.41	953.79	10.48	F 4-4'
										
58	FAULT	DOWN TO NORTH	3743	2403	-3.28	9.04	12.32	362.95	1.94	F 5-5'
			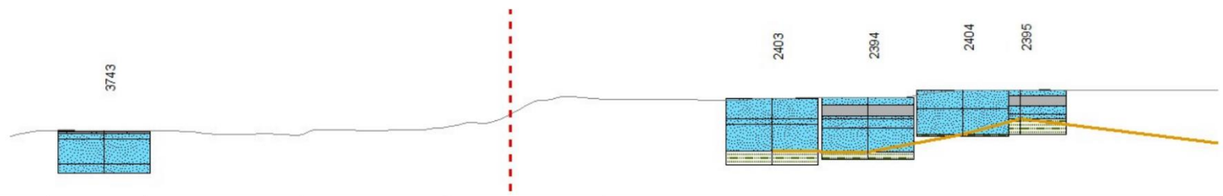							
59	ANTHROPOGENIC ALTERATION	DOWN TO WEST	31806	31800	-6.17	56.70	62.87	501.20	7.15	F 6-6'. POTENTIAL ANTHROPOGENIC.
			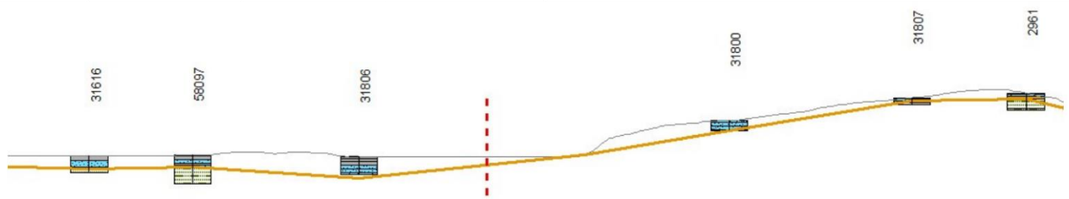							
59	ANTHROPOGENIC ALTERATION	DOWN TO WEST	9453	4380	44.16	87.38	43.23	1038.78	2.38	F 7-7'. POTENTIAL ANTHROPOGENIC.
										
60	ANTHROPOGENIC ALTERATION	UP TO WEST	2961	58659	99.78	1.03	98.75	982.98	5.74	F 6-6'. POTENTIAL ANTHROPOGENIC. ANOMALY 60 PASSES NORTH OF ANOMALY 61.
			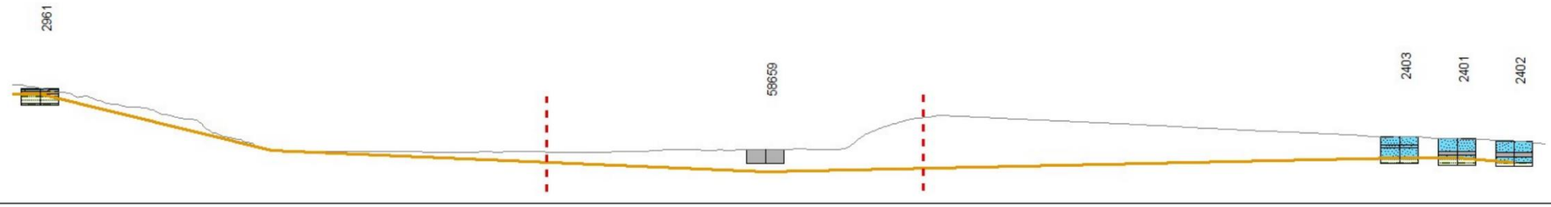							

60	ANTHROPOGENIC ALTERATION	UP TO WEST	4372	59815	95.51	-12.12	107.63	699.03	8.75	F 7-7'. POTENTIAL ANTHROPOGENIC.
			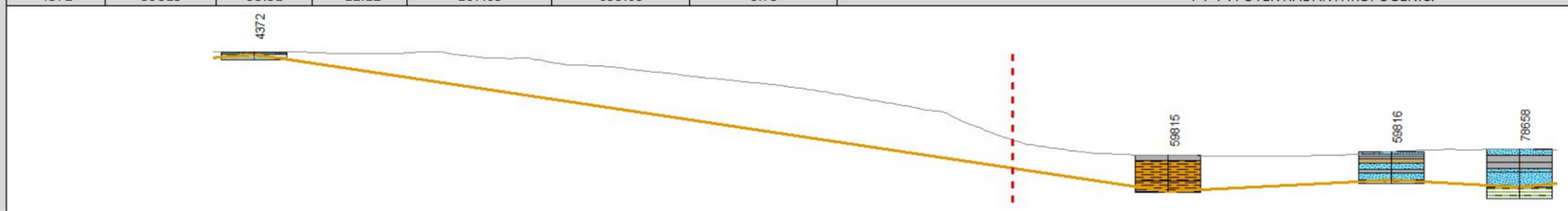							
61	ANTHROPOGENIC ALTERATION	DOWN TO WEST	58659	2403	1.03	9.04	8.01	859.14	0.53	F 6-6'. POTENTIAL ANTHROPOGENIC. ANOMALY 61 PASSES SOUTH OF ANOMALY 60.
			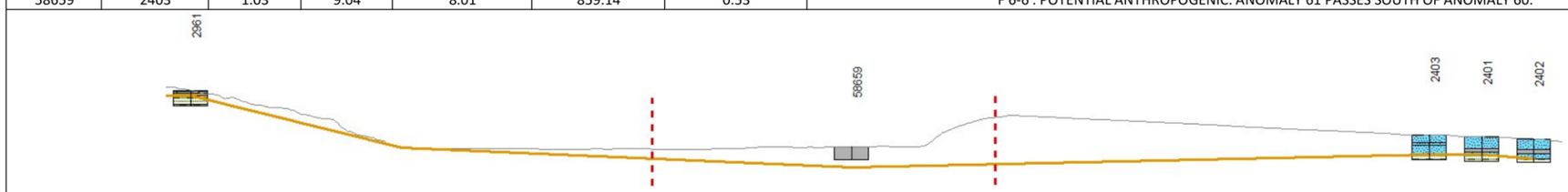							
61	ANTHROPOGENIC ALTERATION	DOWN TO WEST	78658	2397	-8.91	55.20	64.10	638.06	5.74	F 7-7'. POTENTIAL ANTHROPOGENIC.
			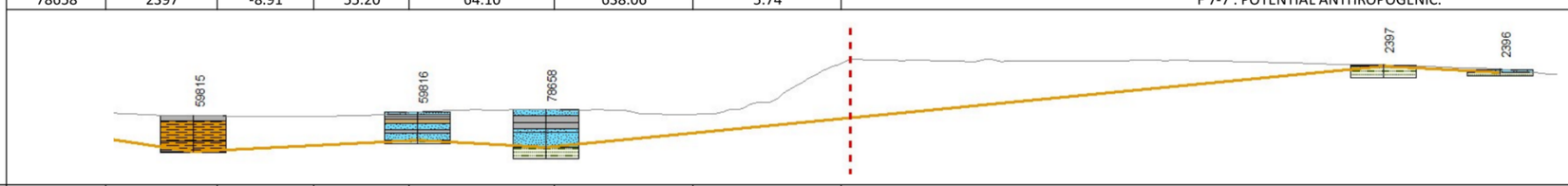							
62	ANTHROPOGENIC ALTERATION	UP TO NORTH	2395	5659	27.04	-65.68	92.72	22.12	76.58	F 5-5'. POTENTIAL ANTHROPOGENIC FOR THE CONSTRUCTION OF BOEING SOUTH PARK.
			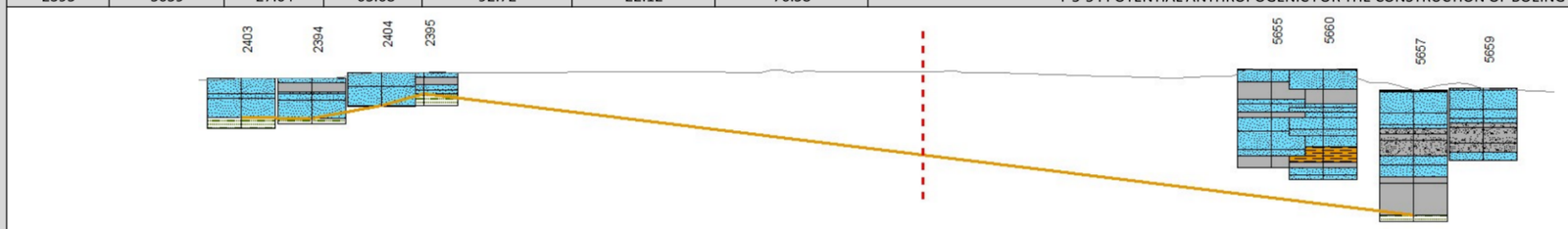							
63	ANTHROPOGENIC ALTERATION	UP TO NORTH	4371	60343	93.17	-29.20	122.37	1068.88	6.53	F 1-1'. POTENTIAL ANTHROPOGENIC.
			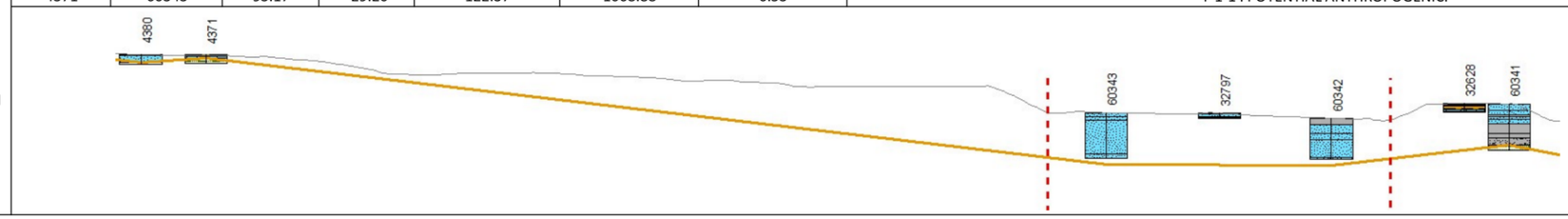							

64	ANTHROPOGENIC ALTERATION	DOWN TO NORTH	60342	60341	-30.62	-13.16	17.46	210.68	4.74	F 1-1'. POTENTIAL ANTHROPOGENIC ROAD GRADE FOR DES MOINES MEMEORIAL DRIVE BRIDE OVER HWY 99.
			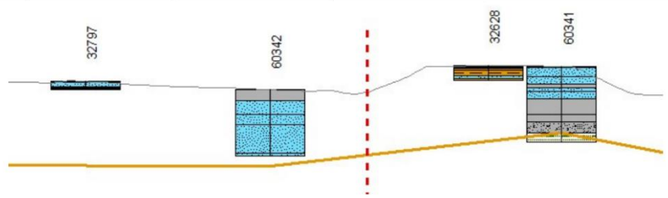							
65	ANTHROPOGENIC ALTERATION	UP TO NORTH	60341	60339	-13.16	-56.73	43.58	277.33	8.93	F 1-1'.POTENTIAL ANTHROPOGENIC ROAD GRADE FOR DES MOINES MEMEORIAL DRIVE BRIDE OVER HWY 99.
										
66	EROSION	DOWN TO WEST	10729	33278	-291.1	-5.1	286.0	3564.1	4.59	G 2-2'. DUWAMISH EROSION.
			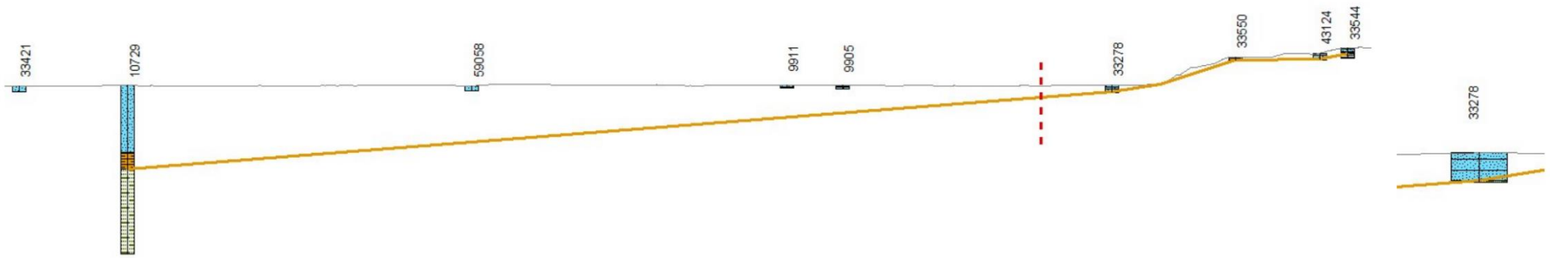							
66	EROSION	DOWN TO NORTH	-	33272	-	-6.91	-	-	-	C 24-24'. LACK OF DATA TO CONFIRM OR DENY ANOMALY 66 CROSSES C 24-24'.